UNIVERSITY OF PADOVA

MSc Level Degree in Environmental Engineering
ICEA Department

Master Thesis
Silvia Di Bona

MODELING OF COASTAL EVOLUTION: LONG TERM SIMULATION IN THE VAGUEIRA REGION (PORTUGAL)

Supervisors
Prof. Antònio Trigo Teixeira
Prof. Piero Ruol

ACADEMIC YEAR 2012-2013

Abstract

The Portuguese west coast faces the Atlantic Ocean and is exposed to a very severe wave climate. Part of that coast is quite recent in geologic terms and is of a sandy nature and very low lying. The area south of the Aveiro Lagoon is one of the most vulnerable area of the coast: Coastal erosion is particularly pronounced in correspondence of the Vagueira village. This study provides an important contribution to the design of a shore protection works for the Vagueira region on the Portuguese west coast using mathematical modelling of coastal evolution. The model used is the GENESIS model, present in NEMOS set of codes, within CEDAS (Coastal Engineering Design and Analysis System) package. The model was first calibrated to the reference situation and then used to investigate future scenarios: the *do nothing scenario* and a *detached breakwaters protected scenario*. Original wave climate data were directly provided by the *Hydrographic Institute of Portugal*, and used as the forcing input for the shoreline evolution modelling. The results confirm the presence of a strong eroding trend in the project area, worsened by the fact that the equilibrium position has still to be reached. The model predicts that the equilibrium position will be reached in 2026. If nothing is done, Vagueira village and most of its coastal area will disappear. The results of the *detached breakwater protected scenario* provide for a valid alternative to reverse the present eroding phase and preserve this coastal area from complete erosion. The detached breakwaters (length, orientation and position), were designed to reach the *tombolo* configuration, and will effectively control the coastline evolution starting a new accreting trend. This lays the foundations for further studies and the fine-tuning of this defence coastal scheme, as a serious option to protect the Vagueira coast in the near future. The impact of the coastal defence scheme on the down drift coast, up to cape Mondego should be further investigated. One option to minimize the impact of the coastal defence scheme is to promote *tombolo* formation using material from the maintenance dredging of the Port of Aveiro navigation channel. Maintenance dredging is estimated to be of the order of 400000 m^3/yr.

Index

Introduction

The Portuguese west coast faces the Atlantic Ocean and it is exposed to a very severe wave climate. Part of that coast is quite recent in geologic terms and is of a sandy nature and very low lying. The area south of the Aveiro Lagoon is one of the most vulnerable of the coast. Coastal erosion is particularly pronounced in correspondence to the Vagueira village. The aim of this study is to provide an important contribution to the design of a shore protection works for the Vagueira region on the Portuguese west coast using mathematical modelling of coastal evolution. The model is calibrated and used to investigate the shoreline future behaviour in two different scenarios: the *do-nothing* scenario and the *detached breakwaters protected* scenario. The *shoreline equilibrium position* and the time needed to reach it are considered as targets for both simulations. The *do-nothing* scenario shows how the shoreline will evolve in near future, if no additional interventions were carried out in the coastal stretch. The *detached breakwaters protected* scenario is presented as an alternative solution. The results should be interpreted in the perspective of a feasibility study. This lays the foundations for further studies and the fine-tuning of this defence coastal scheme, as a serious option to protect the Vagueira coast in the near future. Chapter 1 presents a comprehensive description of the project area and the software used to set up the model. A brief historical description of the project area seeks to contextualize the present severe erosion. The NEMOS software composition is presented. Codes are listed following the data processing flow order. References about their main features and function are reported. In this context, the goal of the study is clarified. Chapter 2 deals with the core of mathematical modelling: input data analysis and preparation. Original input data (bathymetry, topography and wave climate) are presented as they were first derived by the data source. Chapter 3 enters the first phase of the modelling study. The grids creation of the two main models (STWAVE and GENESIS) is presented. Details are provided about their extension, spacing and the way information is passed from one to the other. When the two grids are ready, the modelling can start. Waves are first propagated in STWAVE model, from the offshore boundary to a specified *near shore reference line*. This is presented with detail in Chapter 4. Wave data propagation results are stored at the *near shore reference line* and are ready to be input in GENESIS. Chapter 5 deals with the setup and calibration of GENESIS model. Once the model is calibrated, it is used to study shoreline evolution under different scenarios. Chapter 6 presents the *do-nothing* scenario and the *detached breakwater protected* scenario simulations of shoreline evolution. Several detached breakwaters configurations are tested in terms of structures position and orientation. The section ends with the best spatial configuration for the detached breakwaters i.e a defence costal scheme that if constructed will be able to compensate the present erosion and start a new accreting trend in the entire costal stretch.

Chapter 1

Objectives of the study

This chapter presents the goal of the study, starting with a comprehensive description of the area of interest. A brief history of the coastal stretch of interest, presents the events that have contributed to make the project area exposed at such high risk. The second part of the chapter focuses on the software, which has been used to simulate coastal evolution. The last part gives a comprehensive overview of all the steps that have been done in order to adequately respond to the erosion that is threatening the project area.

1.1 The project area

The area of interest is located on the North West coast of Portugal, near the *Aveiro* lagoon. Coastal sediments are mainly driven by strong swells from north-westerly directions, which finally result in a North-South net littoral sediment transport, Figure 1.1.

Vagueira coastal stretch is located on a sand spit, which separates the *Aveiro* lagoon from the Atlantic Ocean. As recent study confirm (Talbi *et al*, 2008) the sand spit grew from North to South, starting from *Espinho* and fed by the sediments coming from the watershed of river *Douro*. When the sand spit reached *Cape Mondego* it caused the closure of the gulf, forming the present coastal lagoon. In 1808 an artificial inlet was opened to restore the access to the ocean, Figure 1.2.
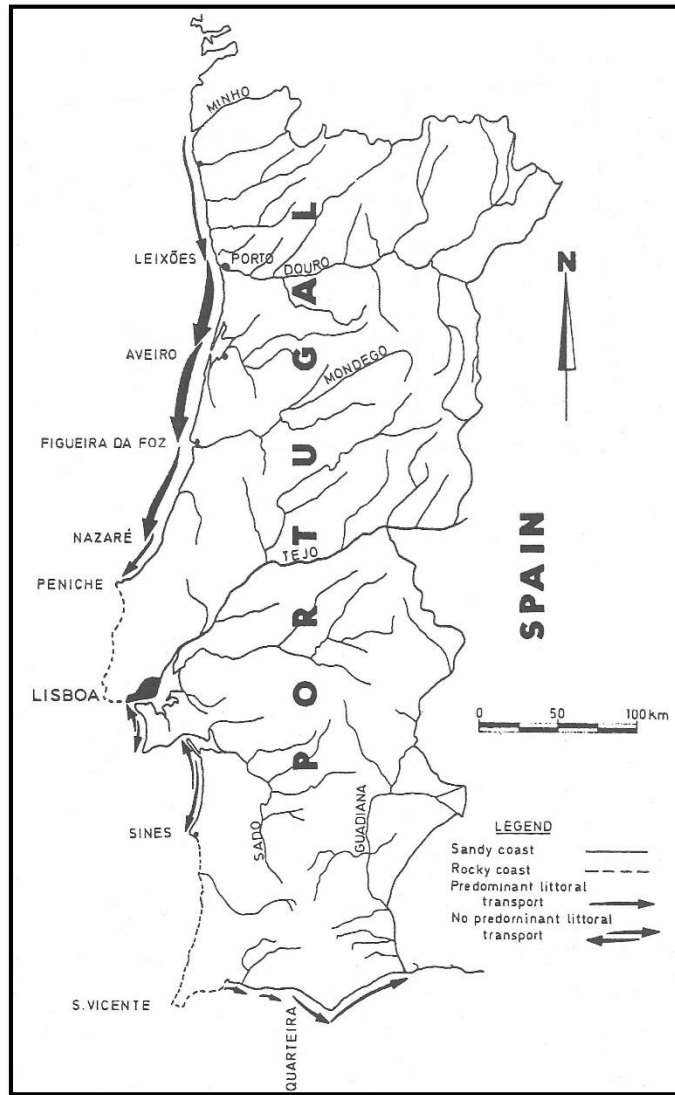
Figure 1.1.*The Portuguese coast and net littoral sediment transport (Gomes et al.1981).*
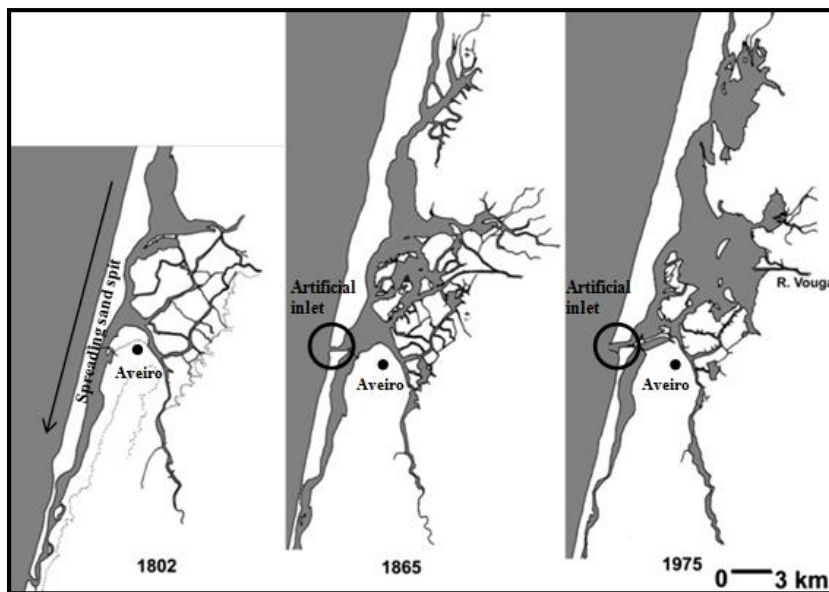

Figure 1.2.*Morphological and artificial changes affecting Aveiro region.*

The inlet was first controlled with interior corrective measures (1935-1940) and then it was finally fixed with two long jetties, constructed during years 1950-1956. Figure 1.3 illustrates the different phases of the inlet opening and the training works construction.

1808 - opening and securing works for the inlet;

1939 - interior corrective works;

1958 - conclusion of the two jetties construction.
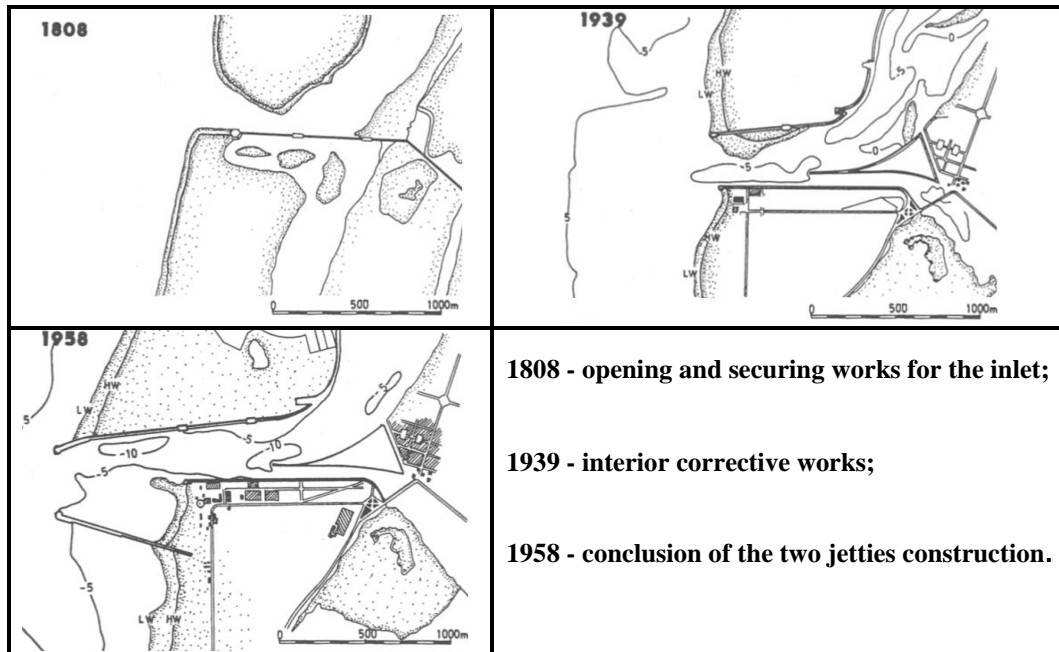
Figure 1.3. *Inlet opening phases (Gomes et al.1981).*

Past studies (Gomes *et al.*1981) show that the opening of the inlet had immediate worsening effects on a coast which was already affected by a general erosion problem. The construction of the two long jetties, in particular the one at the up drift side, had significant impact on the North-to-South littoral sediment transport. The extension of the northern jetty was such (200 m) that it interrupted the flow of sediments coming from the North, since the initial phase of the jetties' construction. To worsen the situation, important control works in the river *Douro* basin reduced the capacity of the river to act as source of sediments. Surveys done in the past (Gomes *et al.*1981) show that sediments have problems in naturally bypassing the jetties and the ones that manage to pass, settle down immediately down drift the channel.

Since the construction of the two jetties the coastal stretch south of Aveiro lagoon inlet started to be affected by a strong erosion trend (Gomes et al.1981) leading to a progressive reduction of the width of the sand spit.
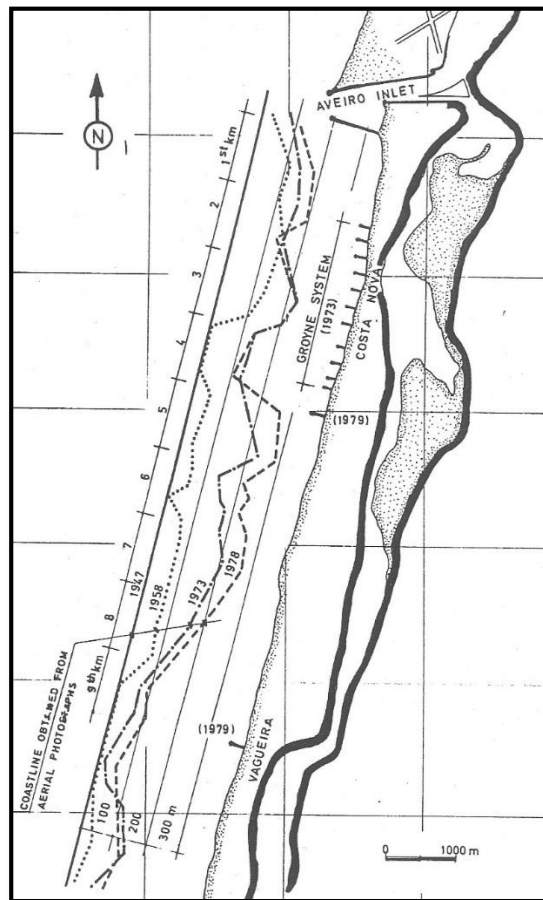
Figure 1.4. *Coast evolution south of Aveiro inlet (Gomes et al.1981).*

In this 9 km stretch of coast, the mean recession of the beach during the period between 1954 and 1978 was of about 150 m (Gomes *et al.*1981), Figure 1.4.

At present, there is an area where the erosion is more evident than in all other parts. This area is located South of *Costa Nova* village: it approximately starts in correspondence of the groin built in 1979, south of the *Costa Nova* groin field, and extends southwards. The reason why this area is of such concern is related to the distance from the inlet. In fact, even during the construction phase of the jetties, the natural bypassing has never been totally interrupted (Gomes *et al.*1981). A small amount of the littoral sediment transport was still able to go through the artificial channel and settle down immediately after the artificial structure. Consequently, the strongly eroded stretch starts south of *Costa Nova* village.

In 1973, a groin field with eleven groins was constructed in order to protect *Costa Nova* village. This local solution worsened the situation down drift. Between 1976 and 1978, the recession of the coastline south of the groin field was continuing at a rate of 20 m/year (Gomes *et al.*1981). In order to face this strong erosion other local interventions were carried

out in the following years. In 1979, two groins were built: one immediately south of the *Costa Nova* groin field, and the other in *Vagueira* village.

In spite of all these erosion-containing efforts, the area of *Vagueira* is still eroding and at risk. One of the latest events is the breaching of the coastline in *Labrego beach* on the 3rd of November 2011, during a storm. The ocean was able to overtop the dunes, flood the agricultural fields behind, cut the road and reach the lagoon, Figure 1.5.

Figure 1.5. *Labrego beach: breaching on the 3rd of November, 2011.*

The last strong coastal defensive work, which was introduced recently, is the *Vagueira* seawall. This long construction has been erected close and parallel to the houses and it was built to stop erosion that was already threatening buildings at Vagueira sea front, Figure 1.6.

Figure 1.6. *Vagueira: the huge seawall prevents the ocean view from the houses. Site visit on October, 2012.*

In the 2004 a curved groin was built in *Praia do Areão* further south of the Vagueria village. This structure represents the end point of the coastal stretch, which will be modelled in this study.

The coastal stretch of interest for this study is defined in Figure 1.7.

Figure 1.7. *Area of the study: most eroded coastal stretch south of Aveiro artificial inlet.*

1.2 ICZM and aim of the study

This section presents the goal of the study in the wider perspective of the integrated coastal zone management. Figure 1.8 shows the process of design, execution and evaluation, which is followed when engineering works must be planned against beach erosion.
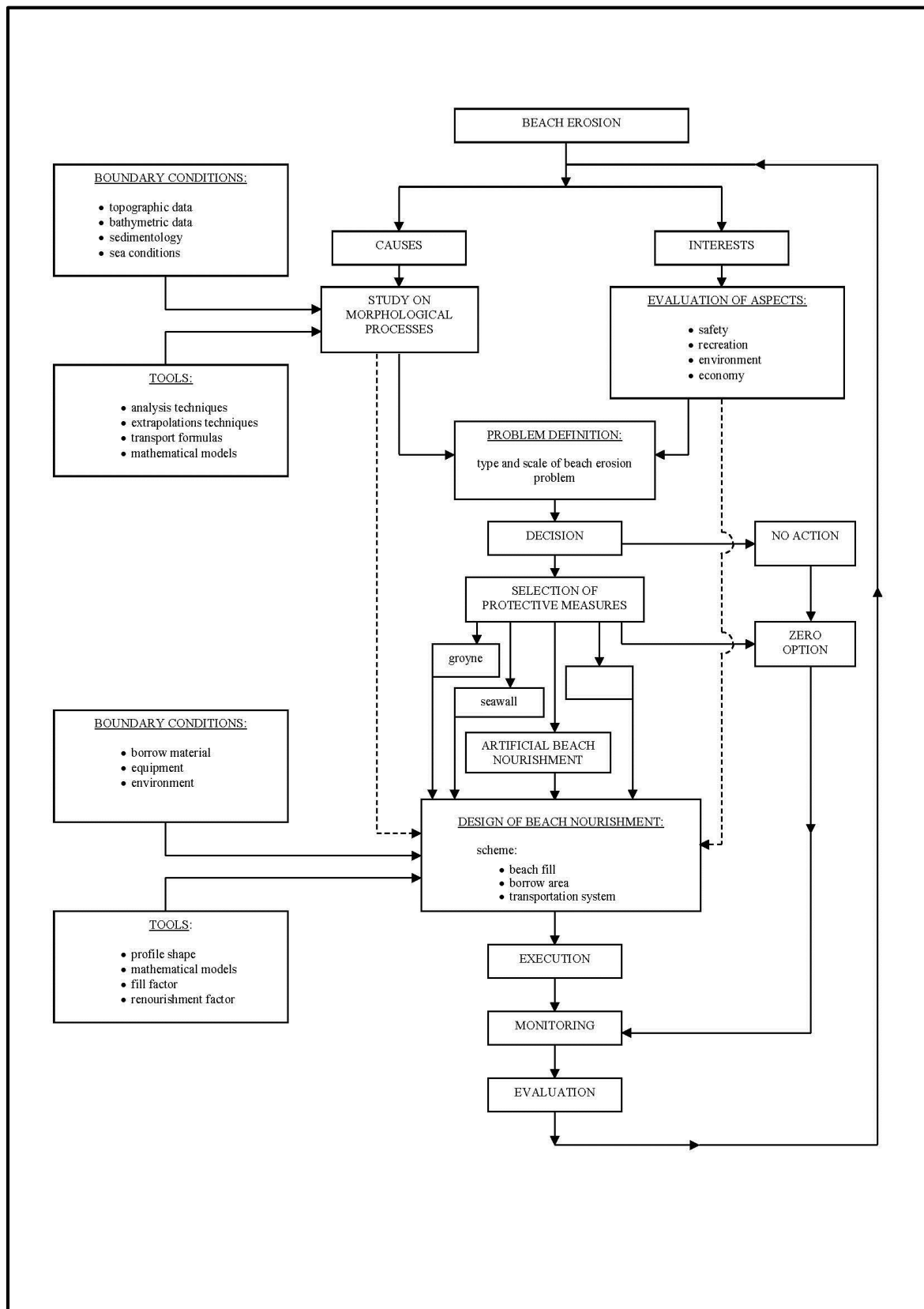
Figure 1.8. *Process of design, execution and evaluation (ICCE 1992).*

The beach erosion process has already been presented with detail (§1.1). The aim of this study is to provide an important contribution at the decision stage, in order to find the best

protective measure for this area. The goal is to mathematically model the evolution of this coastal stretch. After the model calibration, a new large-scale coastal protection scheme is investigated at a feasibility study level. Two possible protective measures were considered: the *do-nothing* (*zero-option*) option and a *detached breakwaters protected* option. The *do-nothing* solution was investigated because it provides important indications about what could be the future scenario in Vagueira region, if no interventions were carried out. The best alternative to the *do-nothing* scenario was chosen among all the options available, considering the peculiarities of the project area. Groins and seawall constructions could improve the situation, but only at local and temporary scale. Beach nourishment would result ineffective, considering the severe incoming wave climate and the related high erosion rate. Consequently, the *detached breakwater protected* scenario was chosen as the best option to stop and reverse the present eroding trend. This option is based on a similar solution used on the same coast. Actually as shown in Figure 1.9 a detached breakwater constructed in *Praia da Aguda* was able to promote quickly a tombolo formation and accumulate several millions of cubic meters of sand. The *tombolo* formation was thus a target for simulations, as it is expected to increase the sand spit width along the entire stretch. Besides, this defence scheme has the property to protect a very long stretch of coast with a very small footprint. The long-term evolution of the stretch is simulated in both the *do-nothing scenario* and in the *detached breakwaters protected scenario*. Results are provided in terms of *equilibrium position* and the time needed to reach it.
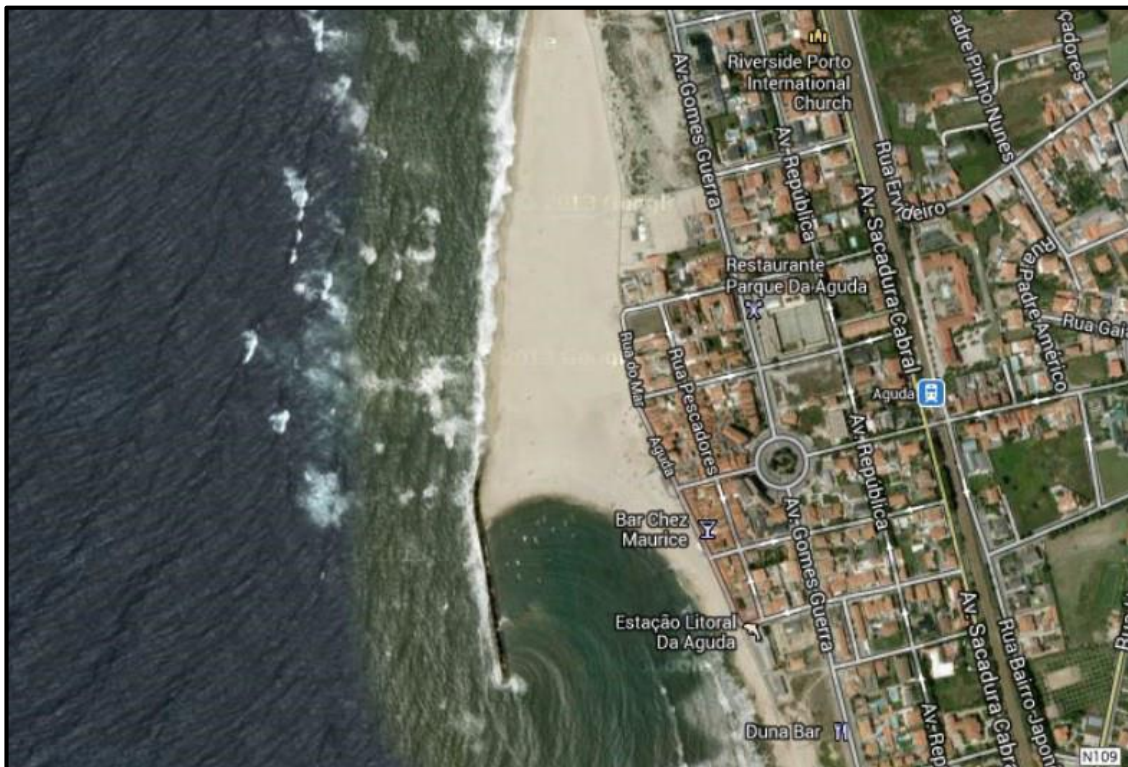
Figure 1.9. *Detached breakwater with tombolo formation in Praia da Aguda, Portuguese west coast.*

1.3 NEMOS software

The mathematical model used is the GENESIS model. This model is implemented within the NEMOS (Nearshore Evolution MOdeling System) model. NEMOS is a set of codes that operates as a cascade system to simulate the long-term evolution of the beach in response to imposed wave conditions, coastal structures, and other engineering activity (e.g., beach nourishment). NEMOS is part of the wider collection of coastal engineering models, CEDAS (Coastal Engineering Design and Analysis System) provided by the Veri-Tech company (http://www.veritechinc.com).

The model has been set up following the NEMOS processing cascade pattern. Each code present within NEMOS serves a specific function. There are two main types of codes within NEMOS: *auxiliary* codes and *key* codes. The first type refers to quite simple, but still essential codes that are designated to data preparation, elaboration and visualization. The key codes instead, are more elaborated as they implement the two main mathematical models used in NEMOS: STWAVE wave propagation model and GENESIS model. Next section provides a brief description of each code according to the abovementioned distinction. At the end, a comprehensive description of NEMOS data flow process is provided.

1.2.1 NEMOS auxiliary and key codes

Here a list of NEMOS *auxiliary codes* follows.

- *Grid Generator* (**GRIDGEN**): this is a code to create uniform grids at arbitrary orientations from random bathymetry/topography data. This code allows the user for the construction of both the wave model grid (STWAVE grid) and GENESIS grid.

- *WWWL* (**Waves, Winds, WaterLevels**): this code is an editor used for specifying and editing a variety of record-oriented data types. Common data sources include WWWL databases, analysed gage data, statistically derived datasets, theoretical cases, and data derived from other model simulations.

- *WSAV* (**Wave Station Analysis and Visualization**): this code is used to perform statistical analysis of series of wave events, graphically displaying the results of these analyses, and producing a representative group of wave events for use in simulations.

- *SPECGEN* (**Spectrum Generator**): this code represents a very useful helper application used to import, create, or visualize directional spectra for use in STWAVE. It can be run as a standalone application, or invoked within CEDAS when working on data that should be go as input for STWAVE.

- *WMV* (**Wave Model Visualization**): this is an application for performing graphical analysis from the various uniform rectilinear grid models within CEDAS. It displays data produced by wave model simulations solved on uniform rectilinear grids. The various plan views of scalar and vector data is overlaid for simultaneous viewing. In 3-D views, several planes of plan views can be stacked above one 3-D surface.

Here NEMOS *key codes* are listed along with their main features.

- **STWAVE (STeady State spectral WAVE)**: this is a 2-D finite-difference representation of a simplified form of the spectral balance equation to simulate near-coast, time-independent spectral wave energy propagation. This model relies on two main assumption; the first is that only wave energy directed into the computational grid is significant, i.e., wave energy not directed into the grid is neglected. The second assumption states that wave conditions should vary slowly enough that the variation of waves at a given point over time may be neglected relative to the time required for

waves to pass across the computational grid. STWAVE is based on a simplified form of the spectral balance equation. The model has also the capability of using tidal currents, nested grids, and a variable ocean boundary condition.

- **GENESIS (GENEralized Model for SImulating Shoreline Change)** is a model for calculating shoreline change caused primarily by wave action and can be applied to a diverse variety of situations involving almost arbitrary numbers, locations, and combinations of groins, jetties, detached breakwaters, seawalls, and beach fills. The system is based on one-line theory, whereby it is assumed the beach profile remains unchanged permitting beach change to be described uniquely in terms of the shoreline position. The program can be applied to a diverse variety of situations involving also wave shoaling, refraction, and diffraction; sand passing through and around groins, and sources and sinks of sand. The GENESIS_T solution scheme is available when *tombolo* formations are supposed to occur.

1.2.2 NEMOS data processing flow

NEMOS operates as cascade system of different codes where the output of one code will be used as input for the next ones. This cascade process follows a rational leading principle whose ultimate target is to allow the user to perform the desired long-term simulations within the only GENESIS environment. The overall process flow can be thus divided in the following three main steps:

- Step 1: *spatial domain preparation*: definition of the project area boundaries and proper format acquisition of bathymetric information;

- Step 2: *wave model preparation*: elaboration of the forcing wave climate, which will cause the long-term shoreline plan form change;

- Step 3: *GENESIS configuration and simulations*: all external input data are ready for the user to be operative within GENESIS; the user configures GENESIS with the desired settings to perform the desired long-term simulations.

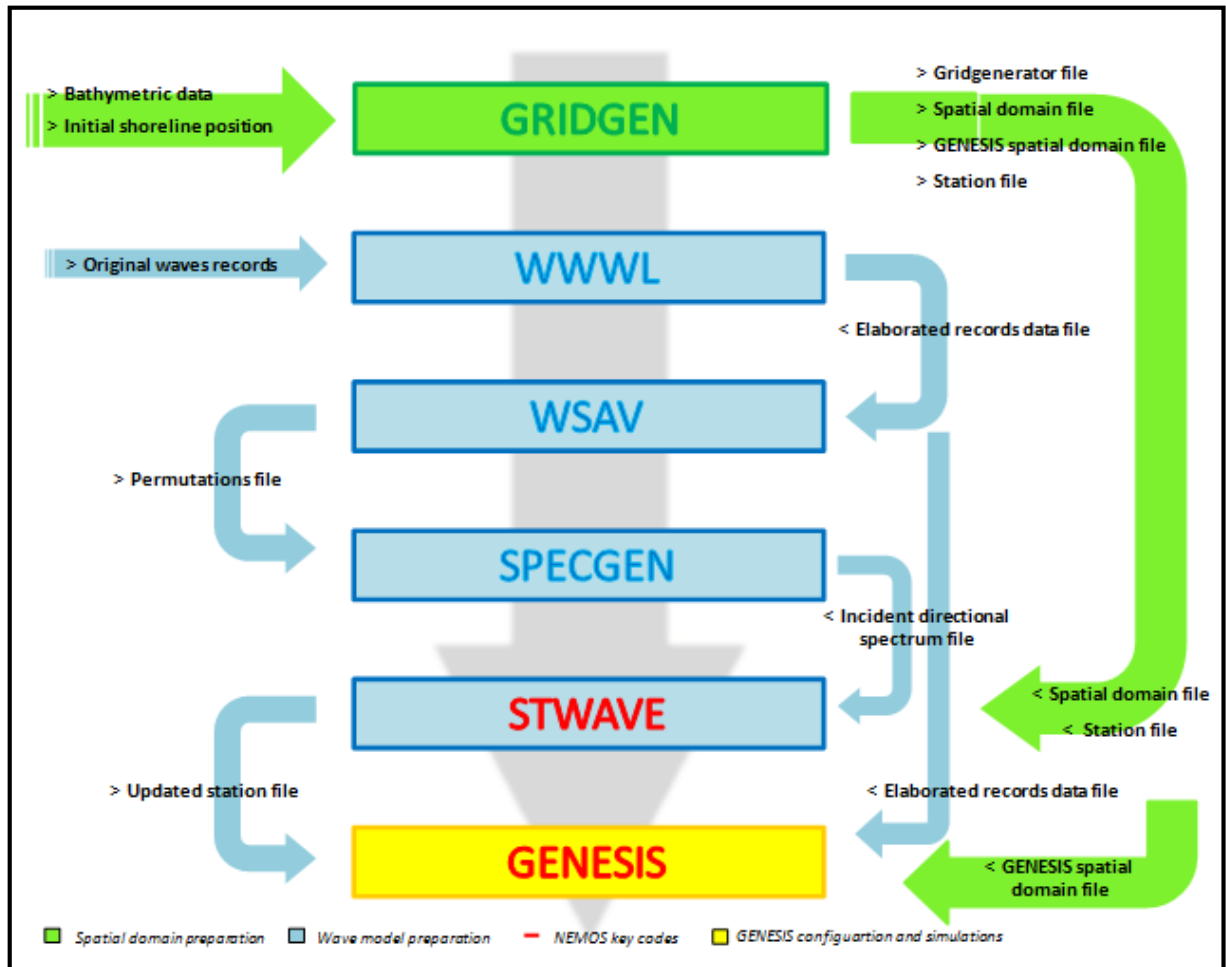These three basic requirements for GENESIS are represented in the flow chart of Figure 1.10.

Figure 1.10. *NEMOS data processing flow. Data are processed in cascade: the output of first phase is the input for the next step. The auxiliary codes provide input data for the key codes (STWAVE and GENESIS). Three main steps are represented: the spatial domain preparation, the wave model preparation and GENESIS configuration and simulation.*

Chapter 2

Data analysis and Preparation

In this chapter the model input data are presented. Three main input data are required by NEMOS. Wave data, which represents the driving agent of the shoreline evolution. The topographic and bathymetric datasets, used to create the model computational grids. Finally, the shoreline position in two distinct years, used to perform the model calibration. Data analysis and preparation always occupy a substantial part of coastline evolution studies. The available data are not always in the proper format to be readily processed or even worse, they are not available at all. In the following subsections, the original available input data are presented. The last section describes the elaboration process that has been carried out to make input data meet the model requirements.

2.1 Original input data

In this section the original input data are presented as they were first provided by the data source. Data type, dataset extension (in both time and space) and data reliability are specified for each input dataset.

2.1.1 Wave input data

Wave data represent the agent that drives the sediments transport and thus the shoreline evolution.

Original wave input data were directly provided by the *Hydrographic Institute of Portugal*. The location of the recording buoy and wave series specifications are summarized in the following picture.
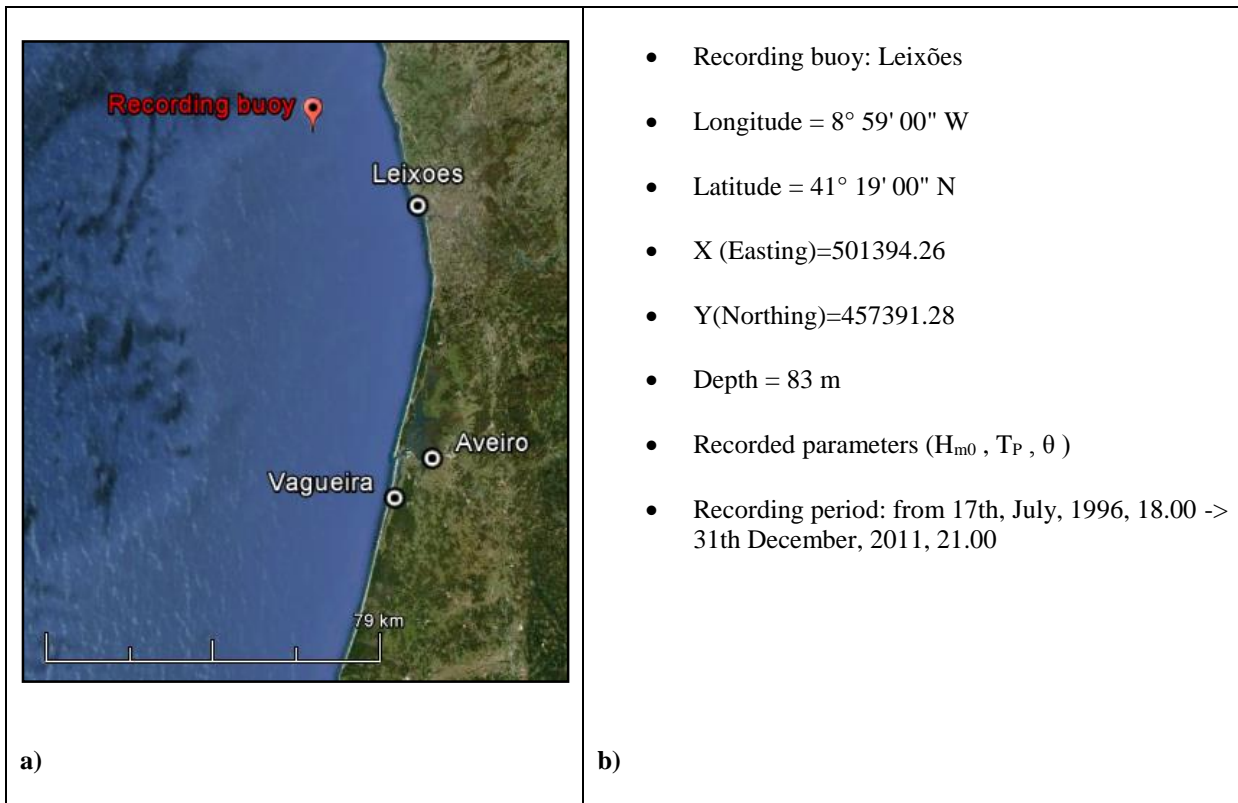
Figure 2.1. *Recording buoy position (a), original wave series specifications (b).*

The buoy provides wave parameters in terms of *significant wave height* (H_{m0}), *wave peak period* (T_P) and *wave mean direction* associated to the peak period ($\theta°$) calculated respect to the True North. The *wave peak period* (T_P) and *wave mean direction* associated to the peak period ($\theta°$) will be hereafter referred as *wave direction* and *wave period* for simplicity.

The buoy records start on the 17th of July 1996 at 18.00 and end on the 31th of December 2011 at 21.00. Each record is identified by hour, minutes, day, month and year specification. The *original wave series* consists of records given every 3 hours starting from 18.00 of the 17th of July, 1996. Consequently, the records were provided at hours (hh) which are multiple of 3 and 00 (mm) minutes. Due to technical problems in the recording wave device, some records were missing or provided at different times (irregular time step). The *original wave series* was thus not continuous and it was not given at regular intervals.

If the data were recorded at every 3h and 00min time step, a *continuous wave series* of 45162 total records, regular in time, would be available. This is not the case: in the *original wave series* 11838 records (3h00min) are missing. The pie chart, Figure 2.2, specifies the portion of missing records (3h00min) in the *original wave series*.
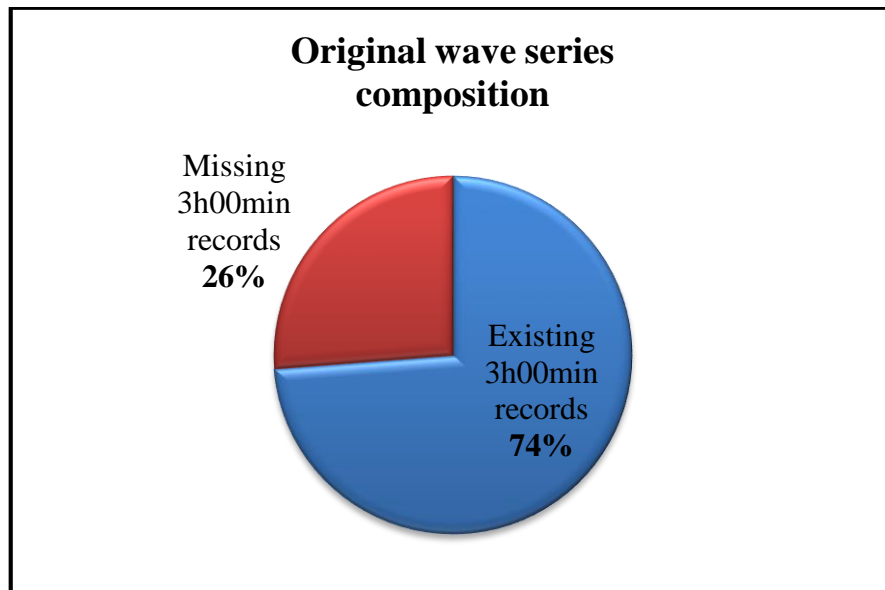
Figure 2.2. *Original wave series composition.*

2.1.2 Bathymetric input data

Bathymetric data, along with topographic data, are required to create the model computational grid, on which calculations are performed. Within this study, bathymetric data were provided as a composite pattern of data coming from different surveys. Datasets, coming from different surveys were assembled in a unique coverage. Figure 2.3 gives an idea of the extension and type of each bathymetric input dataset, which forms the total coverage available.
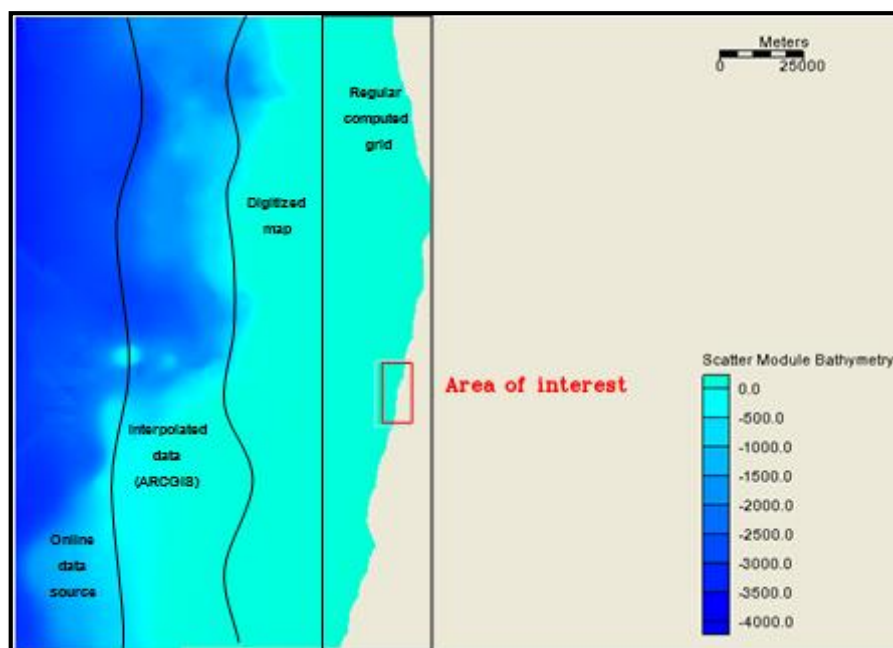

Figure 2.3. *Bathymetric input datasets forming the total coverage available.*

The furthest offshore dataset was derived from an online database. Moving shoreward there is

a dataset which was derived by using ARGIS software. What follows is a dataset derived by digitizing a hydrographic chart. The dataset closest to land was derived by performing an interpolation of known values at base points. The final result is a regularly spaced grid dataset. It is worth stressing that the regularly spaced pattern is not suitable to describe the intertidal zone, especially at the closest landward side. The reason is that the intertidal zone morphology is in continuous evolution.

2.1.3 Topographic input data

Topographic data, along with bathymetric data, are required to create the model computational grids.

Topographic input data derived from aereophotogrammetic surveys were provided in the *.dwg* format for both years 1996 and 2001. Table 2.1 summarizes the main features of these datasets.

DATASET	SOURCE	DATE	MAIN FEATURES
Vagueira 1996	"ESTEREOFOTO, Levantamentos Aerocartograficos, Lda"	4th of October 1996	- aereophotogrammetic survey; - geo referenced data; - reference system: rectangular coordinates, HAYFORD GAUSS DATUM 1973 (HGD73); - tide gauge: Cascais;
Vagueira 2001	"ARTOP Aero topografica, Lda"	September 2001	- aereophotogrammetic survey; - geo referenced data; - reference system: rectangular coordinates, HAYFORD GAUSS DATUM 1973 (HGD73); - tide gauge: Cascais;

Table 2.1. *Topographic datasets specifications*.

2.1.4 Shoreline position input data

GENESIS model requires the shoreline position in two different years to be calibrated. The wider the time interval between the two shoreline positions, the more reliable the calibration is. In this study the time span between 1996 and 2001 has been considered to perform the calibration. With reference to this, the shoreline position in 1996 will be hereafter referred as *initial shoreline* position, while the one in 2001 as *target shoreline position*. This convention reflects the calibration process: the model is set up for the *initial shoreline position* and it is run and calibrated in order to meet the *target shoreline* profile.

The derivation of the shoreline positions in 1996 and 2001 might seem a straightforward task, as topographic data were available in these years. Actually, the shoreline position derivation occupied a substantial part of the whole study. The reason is that the two shorelines (*initial* and *target*) were indeed not available. Aereophotogrammetic surveys are affected by the tidal range variation, because they just cover the land that is on the dry when the photographs are made, and in high tide they do not provide shoreline position, which is defined as the intersection of MSL-Mean Sea Level with the coast. Thus, they could not be used to directly derive the shoreline position either for 1996, or for 2001.

2.2 Input data preparation: meeting NEMOS requirements

The previous section contains a comprehensive description of all original input data available. Their reliability has been discussed and some datasets were finally revealed not to be completely suitable for model input. In this paragraph, properly devised methods, tailored to the original wave data availability and to the input data model requirements, are presented.

2.2.1 Wave input data preparation

It has already been pointed out that the *original wave series* was not continuous, neither regular in time. The major part of the *original wave series* consist of wave records every 3 hours and at 00 minutes. 74% of them were already present, but 26% were missing (see Figure 2.2, § 2.2). Furthermore, in the *original wave series* there are additional records, provided at different times in terms of hours, minutes or both of them. In order to get the complete record type composition of the *original wave series* a detailed investigation has been carried out. The results are displayed in the following table and reveal a great variety of record types.

Record Type	Record type description	N° of records
TYPE A	Data recorded every three hours starting from the 00h 00min of the current day (03h 00min)	33324
TYPE B	Data recorded every three hours, but at different minutes (03h min);	2514
TYPE C	Data recorded at different hours, but at zero minutes (hh 00min);	281
TYPE D	Data recorded at different hours and different minutes (hh min);	3072
TYPE E	No data recorded every 3h 00min	11838

Table 2.2. *Original wave series record type composition.*

TYPE A and TYPE E records are those records that summed up together form the complete 03h 00min series (74% and 26% respectively). The other three types of records (B, C, and D) represent the additional records provided at different times in terms of hours, minutes or both of them.

The idea was to create the 26% of missing records (TYPE E), by *recycling* the TYPE B, C, D records available. This *recycling* or *filling* procedure was carried out month by month.

Semptember 1998 is here given as an example. Its record type composition is summarized in the table below.

Month	Year	Record type	N° of records
September	1998	TYPE A	153
		TYPE B	14
		TYPE C	0
		TYPE D	13
		TYPE E	87

Table 2.3. *September 1998: record type composition.*

Type A and E records together give the total number of theoretical records for this month (records every 3h 00min means that there are 8 records per day, multiplied by 30 day gives 240 records). The 87 TYPE E records are created by using TYPE B, C and D records. The

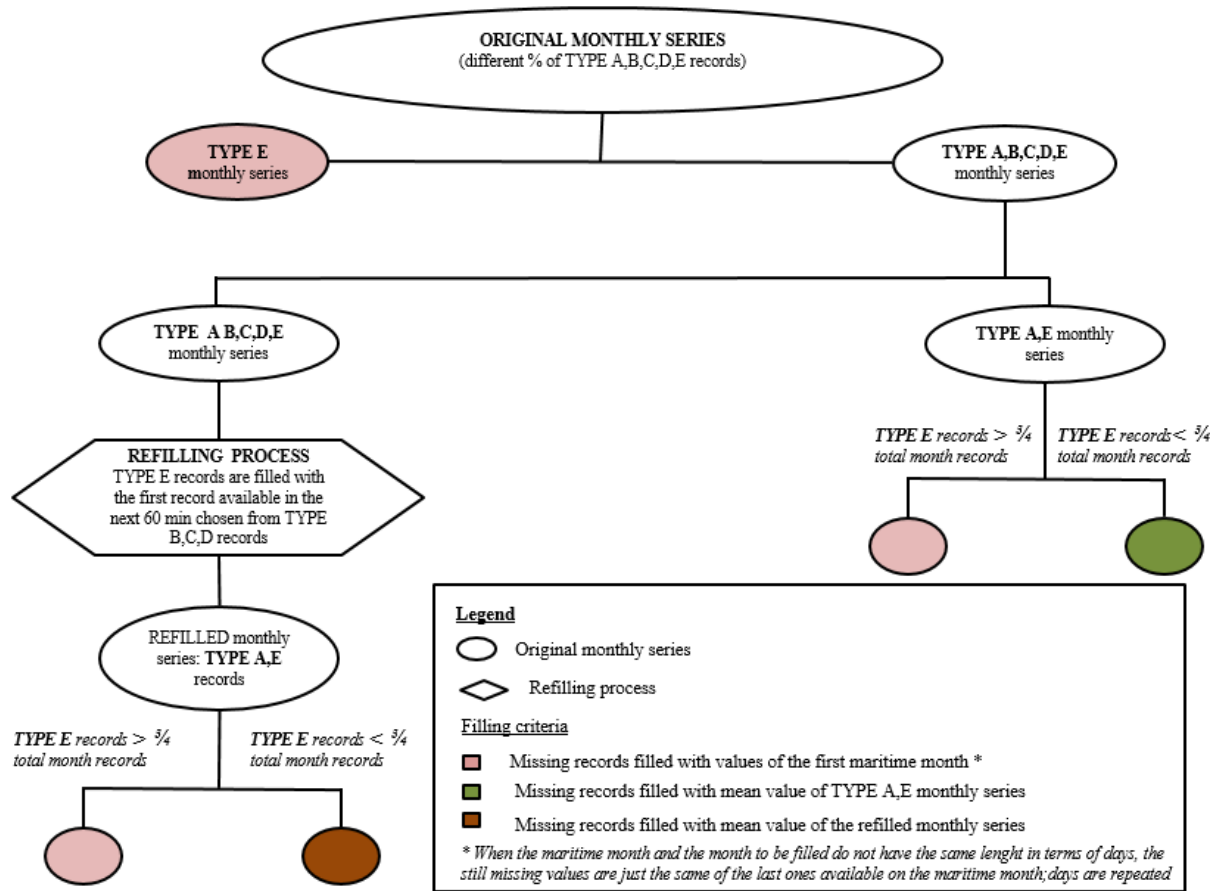following flow chart provides a comprehensive view of the *filling* procedure.

Figure 2.4. *Original wave series filling procedure.*

The leading principle is to classify each month based on its record type composition and then fill the missing records with a suitable criterion.

The first distinction separates months with no record inside (all TYPE E records) from months that have some records inside (TYPE A, B, C, D, E). The *original wave* series contains 19 months with only TYPE E records i.e there are 19 entire months with no records inside.

TYPE A, B, C, D, E monthly series are in turn subdivided according to the presence of mixed records (TYPE A, B, C, D, E). The months that have a mixed composition (TYPE A, B, C, D, E) can undergo the *refilling process* where the TYPE B, C, D records are *recycled* to recover the missing records (TYPE E). The criterion is to fill each missing record with the first TYPE B, C, D record available within 60 minutes. This *time recycling interval* allows to recover the highest possible number of missing records and to create TYPE A, E monthly series.

When all monthly series have been transformed into TYPE A, E series, the filling criterion is chosen on the basis of the amount of records which is still missing (TYPE E):

- if the missing records are less than the ¾ of the total month records, they are filled with the mean value of the TYPE A, E monthly series (*green filling criterion*) or with the mean value of the *refilled* monthly series (*brown filling criterion*);

- if the missing records are still more than the ¾ of the total month records the entire monthly series is *substituted* with the first monthly series available within the same *maritime season*.

This last point is fundamental, as it ensures the consistency with the real wave climate i.e it considers that wave events in autumn/winter have different intensity from wave events that occur in spring/summer. Figure 2.5 specifies the sequence of winter and summer *maritime seasons* that has been considered to perform the substitution of the entire monthly series.
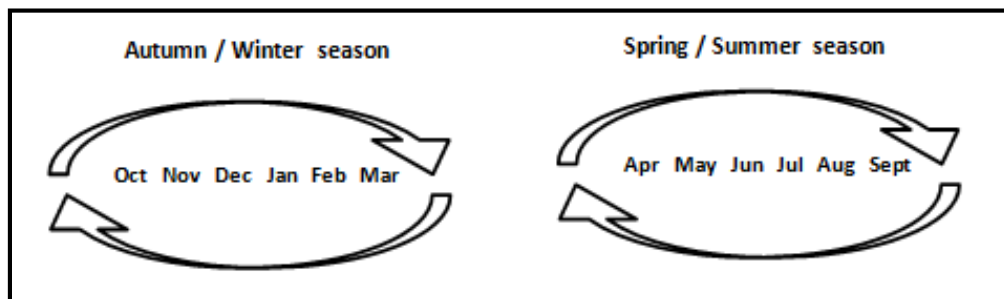
Figure 2.5. *Maritime seasons for monthly series substitution.*

The final result is the creation of a continuous and time regular wave series, which will be hereafter referred as *continuous wave series*. This series consists of 45162 records, at 3h 00min time step (TYPE A records).

Checks were performed on the filling method devised. The results proved that the *continuous wave series* is consistent with the *original wave series* . The graph of Figure 2.6 is a strong evidence of this consistency.
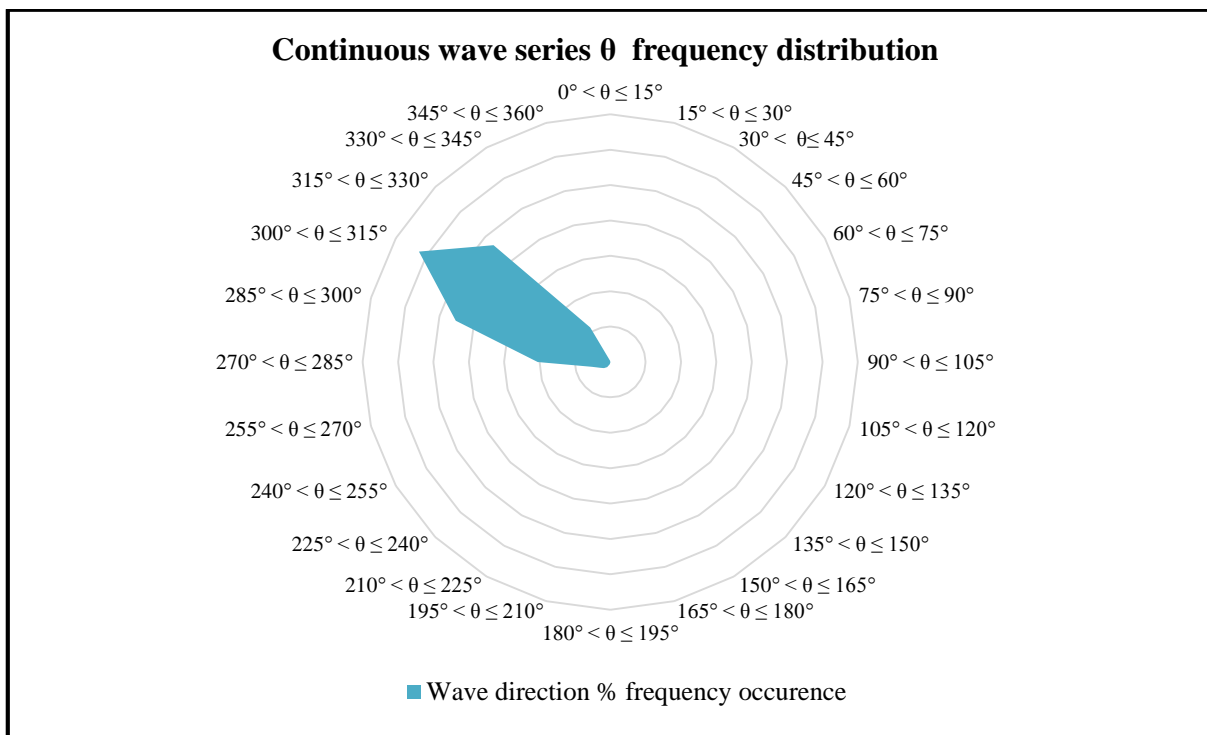
Figure 2.6. *Continuous wave series, wave direction frequency distribution.*

The wave climate resulting from the *continuous wave series* is evidently North-Westerly directed. This is consistent with the real wave climate information contained in the *original wave series.*

2.2.2 Bathymetric input data preparation

Bathymetric input data were provided as a composite pattern of several datasets coming from past studies. The resulting dataset extension is very large in both long shore and cross-shore directions. Data were available offshore from the -4000m water depth contour up to 0m value inland.

This extension is much wider than the one needed to setup the model for this study. Furthermore, landward data are not reliable, as they are provided in a regular grid pattern, which is not suitable to describe the strong irregularities of the intertidal zone.

All these things considered, the original bathymetric dataset was cut, in order to get the exact coverage extension for the study. Figure 2.7 provides a graphical representation of the selection performed.
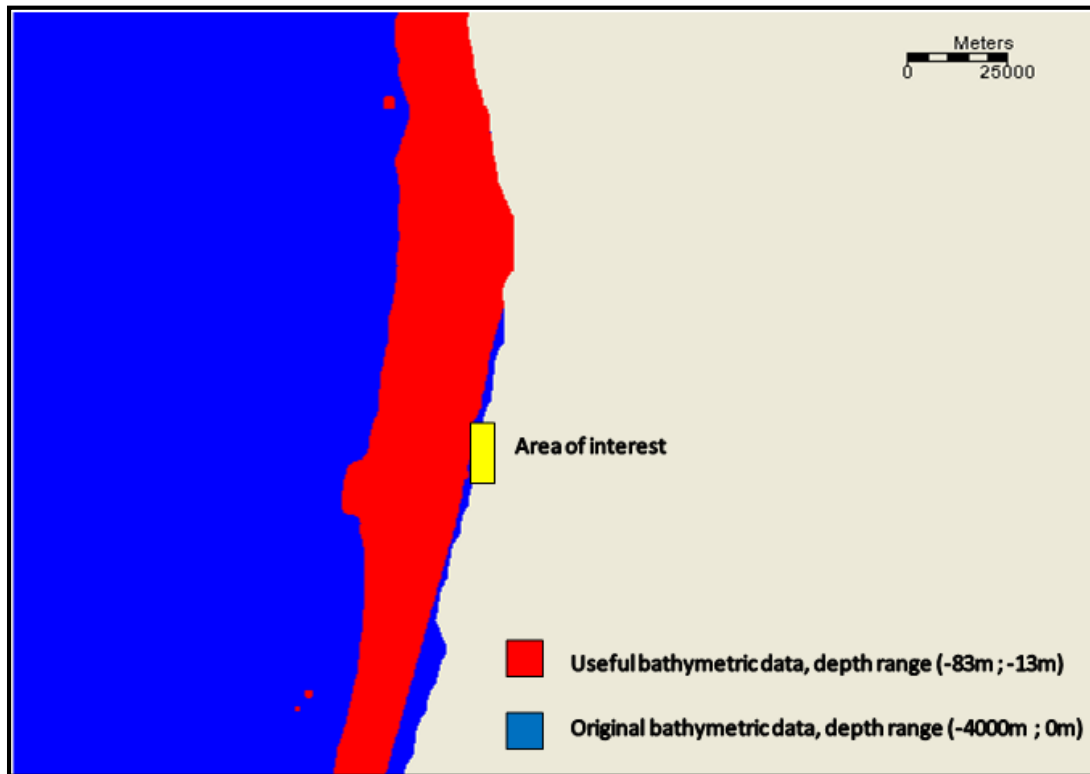
Figure 2.7. *Bathymetric data selection.*

The original bathymetric dataset was cut offshore at the -83m depth contour, and at the -13m contour at the landward side. The offshore contour limit value (-83m) corresponds to the recording buoy depth. The other contour limit (-13m) represents the first contour depth closest to the land in the vicinity of the depth of closure.

The reliability of the intertidal zone data was verified by comparing the dataset with an hydrographic chart. With the support of *SMS* software (http://www.aquaveo.com/sms), the original dataset layer was mounted on top of the digitalized hydrographic chart. In this way, it was possible to verify that the original bathymetric data were consistent with the contours present in the map.

The *bathymetric input dataset* will hereafter indicate the bathymetric dataset cut according to the abovementioned specifications.

2.2.3 Topographic input data preparation

Topographic data were provided for both 1996 and 2001 as *dwg* sheets. Each sheet covers an extension of 1600m x 1000m. Therefore, the first step was to join all the sheets in a unique *Autocad* file, to cover the desired area.

The following step was to extract inland points coordinates from the *dwg* file using ARCGIS support. As the coordinates refer to the local Portuguese reference system (HAYFORD GAUSS DATUM 1973) they were converted into the Global Reference System (WGS84).

The final result was a raw data file (ASCII x,y,z format) for both 1996 and 2001, containing the inland points coordinates in both years 1996 and 2001. These two datasets will be hereafter referred to as *topographic input dataset* of 1996 and 2001, respectively.

To help in the data visualization the ASCII files were imported in SMS workspace. The following picture gives an idea of how data were transformed and finally visualized. Data are those of 1996.
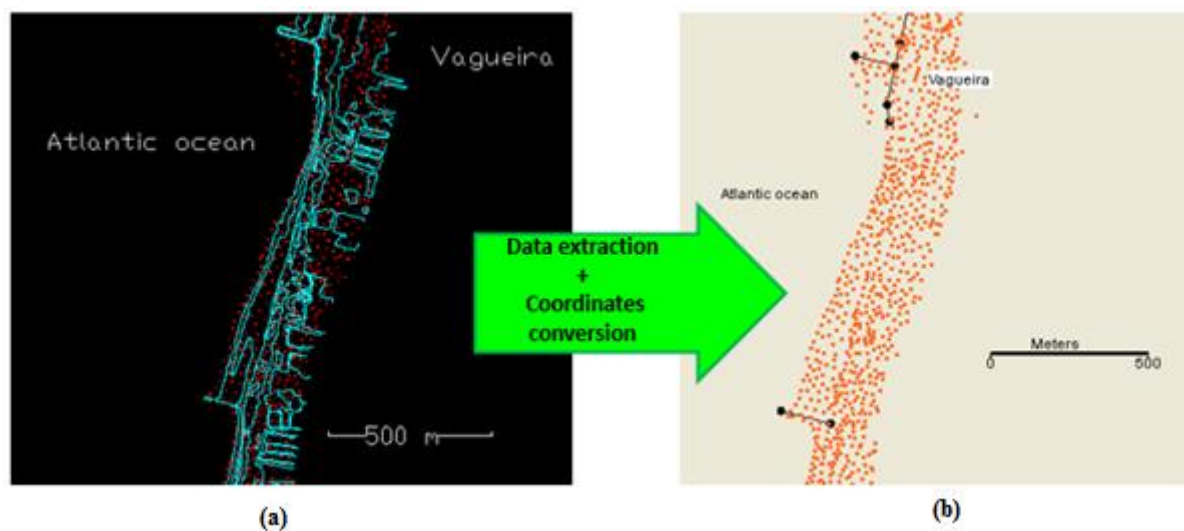
Figure 2.8. *Topographic dataset 1996: original dwg file (a) and final data visualization (b).*

It must be stressed that the line that separates water from dry land at the time the photograph was made (*Linha d'agua*) was not considered as reliable datum for the shoreline positions of both 1996 and 2001. The reason is that it is affected by the tidal range variation, which in this region is around 4m. This gives an idea of error that would be committed if this datum was taken as reliable.

2.2.4 Getting shoreline positions input data

Getting shoreline positions in 1996 and 2001, has been one of the biggest issue of this study. An empirical method was devised, tailored to data available at this stage.

The following datasets were available at the current stage:

- *bathymetric input dataset*: offshore points from -83m up to -13 m depth contour (for further details see § 2.2.2);

- *topographic input dataset of 1996*: land points excluding the 0m contour line, (for further details see §2.2.3);

- *topographic input dataset of 2001*: land points excluding the 0m contour line, (for further details see §2.2.3);

With the help of SMS software two *linear interpolations* were performed: one between the bathymetric dataset and the topographic dataset in 1996, and the other between the same bathymetric dataset and the topographic one in 2001. These two interpolations provided the 0m contour lines that were indicative of the shoreline position in 1996 and 2001, respectively. Figure 2.9 help in visualizing the interpolation process.
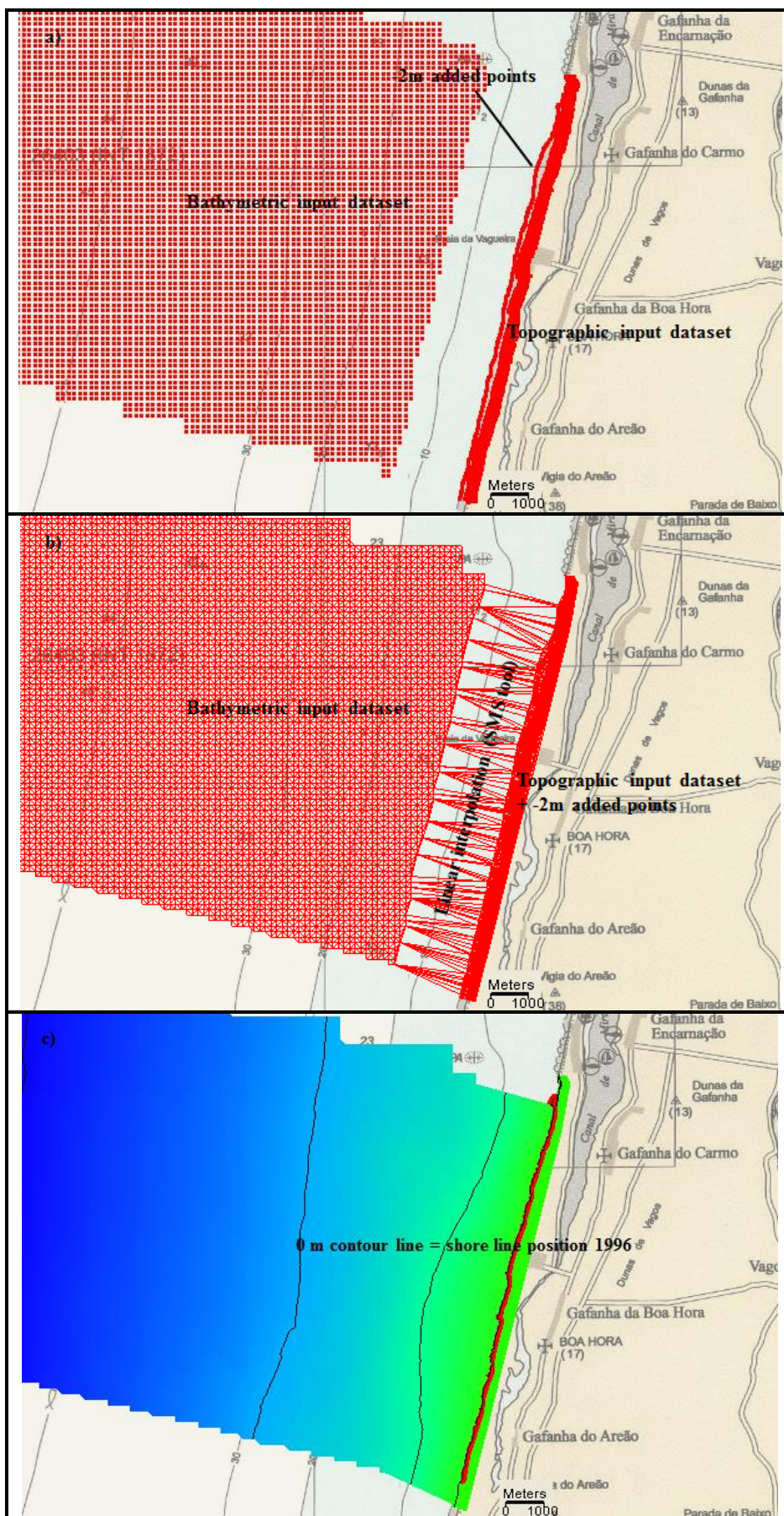
Figure 2.9. *SMS: getting shoreline position for year 1996.*

With reference to the interpolation process, some further considerations are needed. It is worth stressing that the same bathymetric dataset was used for both the interpolations (1996 and 2001). This is a reasonable approximation, as bathymetry does not change so much in time, especially in deep water. In addition, the interpolation was performed between the *bathymetric input* dataset and the two *topographic input datasets* (1996 and 2001), but some points derived from the underlying hydrographic chart were added. In particular, -2m water depth points were manually inserted; they were derived by tracing the -2m contour line present in the underlying hydrographic chart. This procedure was followed to represent better the cross-shore profile of the beach. The final results were consistent with the bathymetric contours contained in the hydrographic chart.

The very last verification has been performed recently when LIDAR data were made available for this coastal stretch. The shoreline positions of 1996 and 2001 obtained have been compared with the LIDAR dataset.
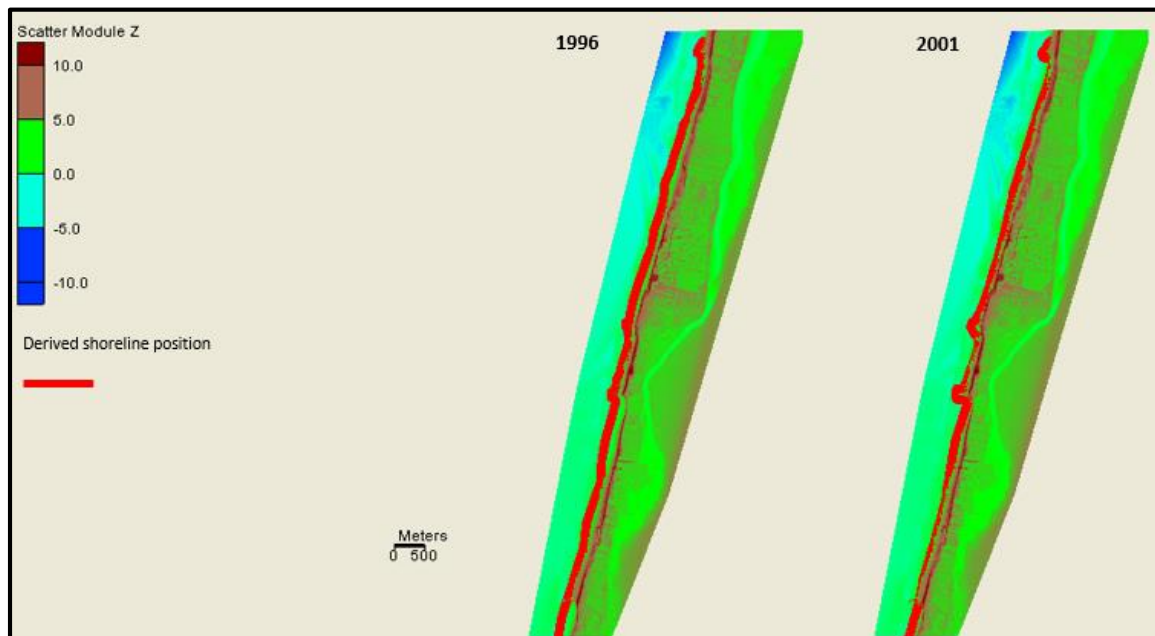
Figure 2.10. *SMS: comparison between LIDAR data and interpolation derived shorelines (1996 and 2001).*

LIDAR data refer 2012, but it is still possible to check the consistency between the two shoreline positions (1996 and 2001) and the remote sensing LIDAR data. From the picture it is evident and reasonable that the derived shoreline position in 1996 is shifted further offshore than the one in 2001. This makes sense as the shoreline is receding in this area.

The final results have been definitely proved to be consistent with the real bathymetric and

topographic pattern. From now on the two derived shoreline positions will be referred to as *input shoreline position (1996* or *2001* respectively) or they might be also referred to as *initial (2001)* and *target (2001)* shorelines.

Chapter 3

Model computational grids

This chapter introduces the two key models, STWAVE and GENESIS. The description focuses on the basic requirement for a mathematical model: the computational grid, set to cover the domain of interest. The bathymetric and shoreline information are interpolated to those grids. STWAVE wave model is presented first, as its results are input in GENESIS. The last section explains the interrelation between the two computational grids: the *near shore reference line* represents the link used to pass information from STWAVE to GENESIS model.

3.1 The STWAVE model grid

STWAVE is a steady-state finite difference 2D model based on the wave action balance equation. This model quantitatively calculates the change in wave parameters (wave height, period, direction) between the offshore boundary and a specified *near shore reference line*. The computational grid must be wide enough to allow for the wave propagation. The first of the following subsections (§ 3.1.1) provides details about the theoretical extension and numerical discretization of STWAVE model grid. §3.1.2 presents the model grid creation performed within NEMOS and provides more practical details and considerations.

3.1.1 STWAVE numerical discretization

STWAVE is formulated on a *Cartesian grid*, referred to a *local coordinate system*. The x-axis is oriented in the cross-shore direction and the y-axis is oriented alongshore, forming a right-handed coordinate system. The origin is placed offshore at the *model offshore boundary*.

The orientation of the x-axis ($\pm 87.5°$) defines the half plane that is represented in the model. The y-axis is typically aligned with the direction of the bottom contours (McKee *et al.*2001).

The lateral boundaries in the long shore direction are defined according to the long shore extension of the area of interest.

Grid cells are square ($\Delta x=\Delta y$) and the model allows for variable grid resolution obtained by

nesting model runs. Figure 3.1 provides a schematic view of STWAVE model calculation grid.
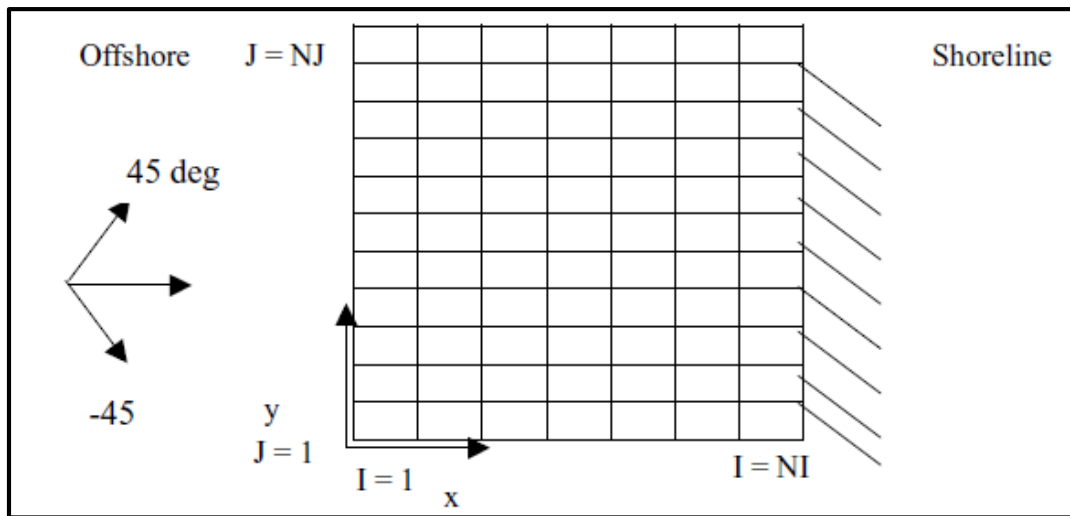
Figure 3.1. *Schematic of STWAVE model calculation grid (McKee et al.2001).*

3.1.2 Model grid definition

STWAVE calculation grid was created using the *GridGen* auxiliary code.

The *bathymetric dataset* was first imported as a set of discrete raw points. Then a linear interpolation was performed using the *Delaunay* triangulation. The interpolation is automatized within *GridGen* and it allows for the creation of a *continuous* bathymetric data set. Figure 3.2 shows the bathymetric dataset contours.
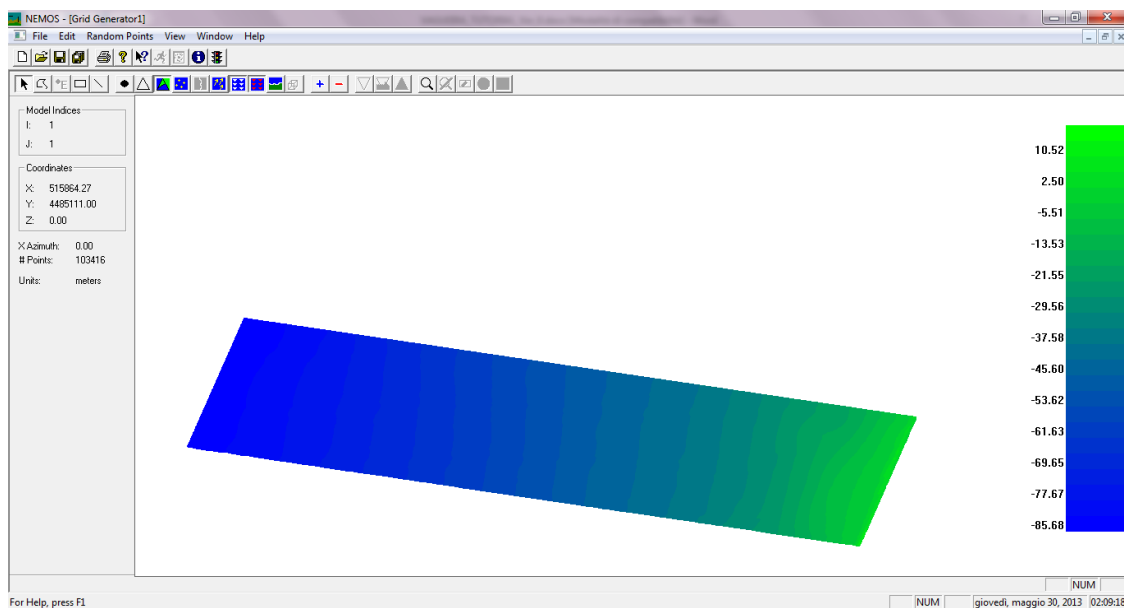
Figure 3.2. *GridGen: continuous bathymetric dataset, coloured contours.*

After this, the *initial shoreline position (1996)* was imported as x,y pairs. Figure 3.3 shows the *initial shoreline* points (white coloured) at the landward side of the bathymetric dataset.
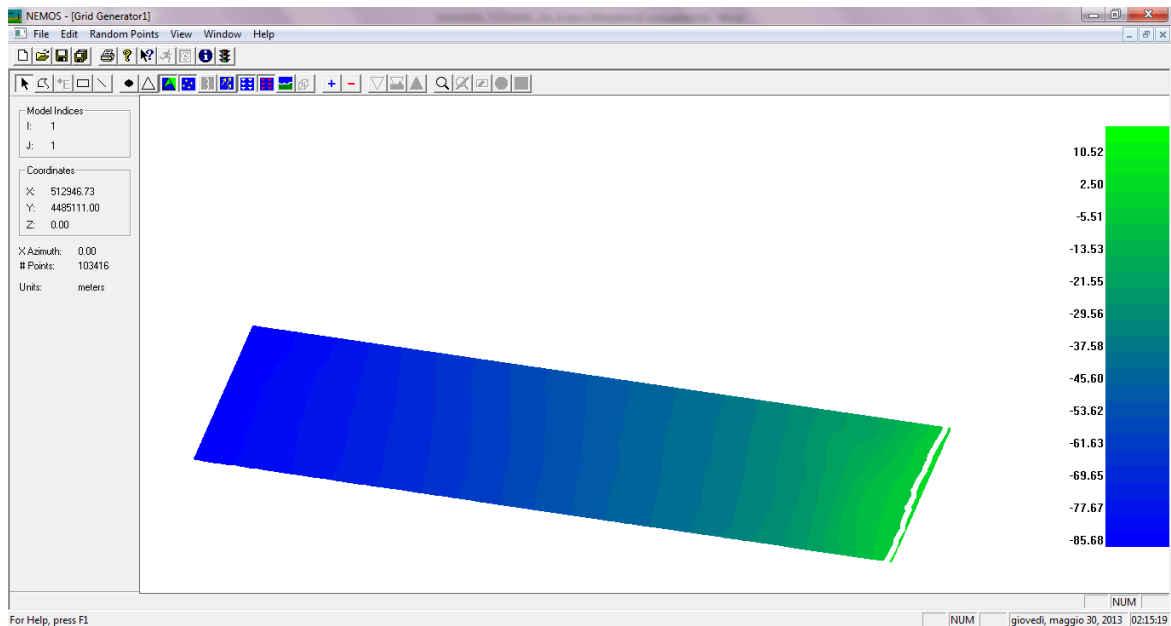
Figure 3.3. *GridGen: imported initial shoreline points (1996).*

The STWAVE model grid was finally created by providing specifications of Figure 3.4.
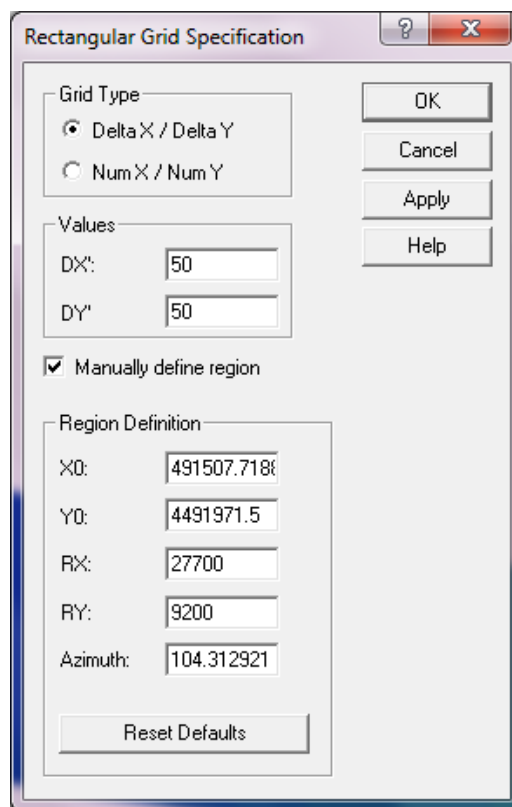
Figure 3.4. *GridGen: rectangular grid specifications for STWAVE grid.*

The grid cells are square (*DX=DY=50m*). This value was chosen as a compromise between the computational efforts and the detail of the model results (the smaller the grid cells, the more detailed the model results, but the more time consuming the calculations). The grid origin (X_0, Y_0) was placed at the *offshore boundary* which was fixed at the buoy water depth contour (-83 m). The cross-shore (RX) grid length is 27700 m, which corresponds to 555 grid cells (*columns*). The long shore model length (RY) is 9200m, which corresponds to the length of coastal stretch of interest. The coastal stretch is thus subdivided into 185 grid cells (*rows*) on the long shore direction. The grid azimuth (104.312921°) represents the orientation of the x-axis with respect to the North. Figure 3.5 shows the final layout.

Figure 3.5. *GridGen: STWAVE model grid. Grid cells are not displayed as they cannot be distinguished at this resolution. The origin and axis specifications were added for completeness.*

Before saving the grid as a *spatial domain file*, additional checks were made. The idea was to see how waves were propagating to the coast and verify the influence of the position of the lateral boundaries of STWAVE, on the results. In order to perform this verification STWAVE model was run externally within SMS (http://www.aquaveo.com/sms). Figure 3.6 shows the calculated wave direction for waves coming from north-westerly directions (which are the most frequent in this area).
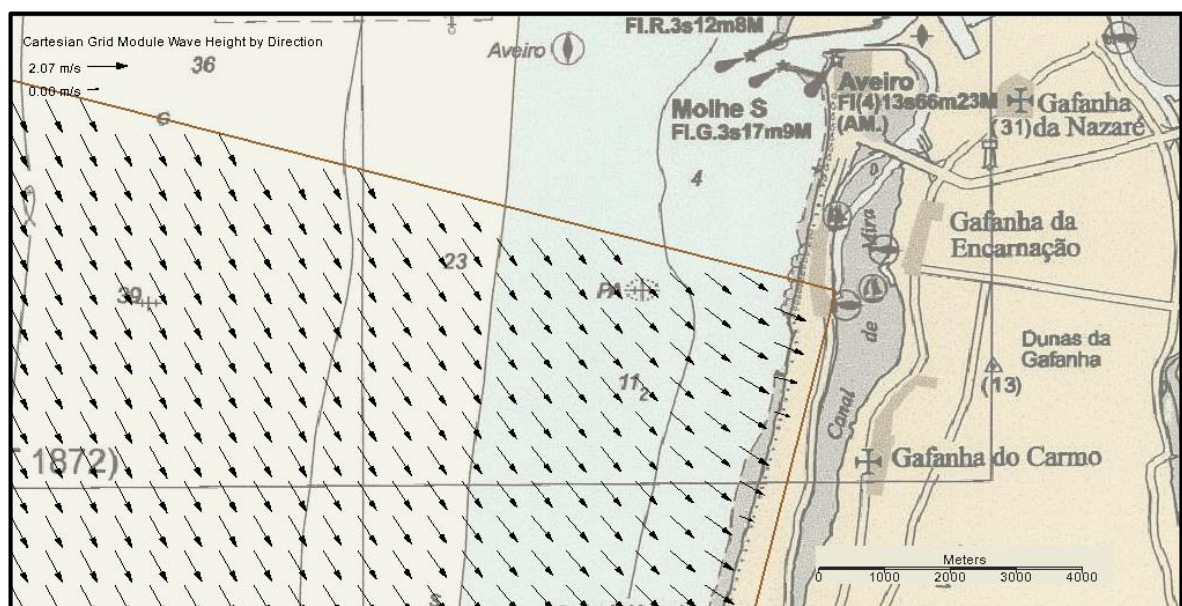
Figure 3.6. *SMS: testing the boundary effect at the northern model boundary.*

Figure 3.6 clearly shows how the wave is refracted and changes direction in the propagation towards the coast. It can be seen that waves arrive at the coast with an angle (they are not normal to the coastline) justifying the southward directed long shore sediment transport. The position of the STWAVE lateral boundary does not seem to have an effect on the model results. However, much larger domains can be modelled with STWAVE using the nested grid facility. This can be further investigated in future studies.

3.2 The GENESIS model grid

GENESIS is a one-line shoreline change model, which calculates shoreline change due to spatial and temporal differences in long shore transport as produced by breaking waves (US Army Corps of Engineers 2002). GENESIS computational grid thus accommodates both the shoreline position and the long shore sediment transport calculation. The first subsection (§ 3.2.1) provides details about the finite difference representation used in GENESIS. The last part (§3.2.2) presents more practical aspects about the creation of GENESIS grid.

3.2.1 Finite difference representation

GENESIS grid is a 1D finite difference grid, long shore directed. In GENESIS, calculated quantities along the shoreline are discretized on a staggered grid in which shoreline positions (y_i) are defined at the center of the grid cells ("*y-points*") and transport rates (Q_i) at the cell walls ("*Q-points*") (Hanson *et al.* 1991) as shown in Figure 3.7.
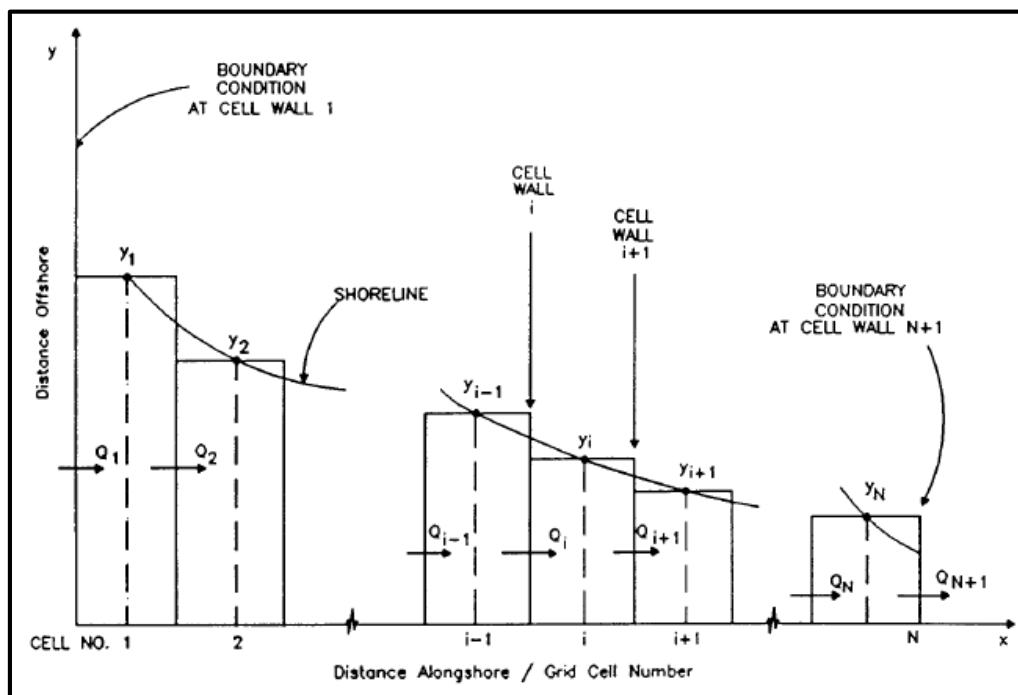
Figure 3.7. *GENESIS finite difference staggered grid (Hanson et al. 1991).*

GENESIS grid must meet the following requirements:

−   for each "*y-point*" an initial shoreline position value must be specified i.e the total length of GENESIS grid must be within the *initial shoreline* length;
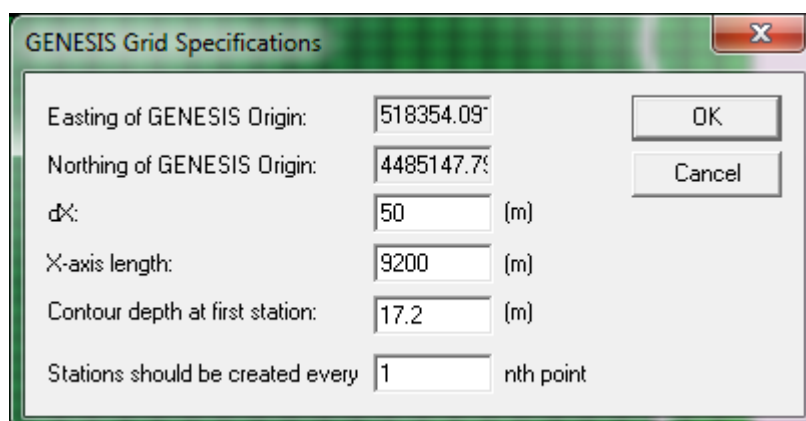
- its origin must be placed landward enough to allow for shoreline recession, if apparent;

- it must match the STWAVE grid (the GENESIS origin will lie ½ dx away from STWAVE cell walls i.e GENESIS cell walls will be placed at the center of STWAVE grid cells);

- the cell spacing (dx) must be equal or a multiple of the STWAVE cell spacing (DY) in the long shore direction;

- the cell spacing (dx) should account for the position of coastal structures (groins, seawalls, etc.) if present in the project area.

3.2.2 Model grid definition

GENESIS grid was created after the STWAVE grid, using the same *GridGen* auxiliary code.

It must be stressed that STWAVE grid (*spatial domain*) and GENESIS grid (hereafter referred to as *GENESIS spatial domain*) are two distinct calculations domains; nevertheless, they must match. Therefore, they are created within the same workspace (*GridGen*), but they are exported as two distinct files.

GENESIS grid definition is automatized within *GridGen*: the grid specifications are inserted in a dedicated window, as shown in Figure 3.8.

Figure 3.8. *GridGen: GENESIS grid specification window.*

The *Easting and Northing* of GENESIS origin, represents the x,y origin coordinates respect to the WGS84 Global Reference System. The origin was placed at the extreme landward lateral

boundary of the *spatial domain* in order to account for the presumed shoreline recession.

The *grid spacing* (*dx = 50m*) was set equal to the STWAVE cell spacing (*DX=DY=50m*). A previous study on paper on a topo/hydrographic chart was carried out in order to see where the coastal structures were located. The *50m* resulted to be the best value that allowed for the most realistic structure positioning.

The *X-axis length* corresponds to the length of the *initial shoreline,* as the model requires a specified *initial shoreline* position for each *y-point* of its grid.

The two last settings define the *near shore reference line*, which represents the link between STWAVE and GENESIS model.

Figure 3.9 shows the GENESIS grid placed within the STWAVE grid.
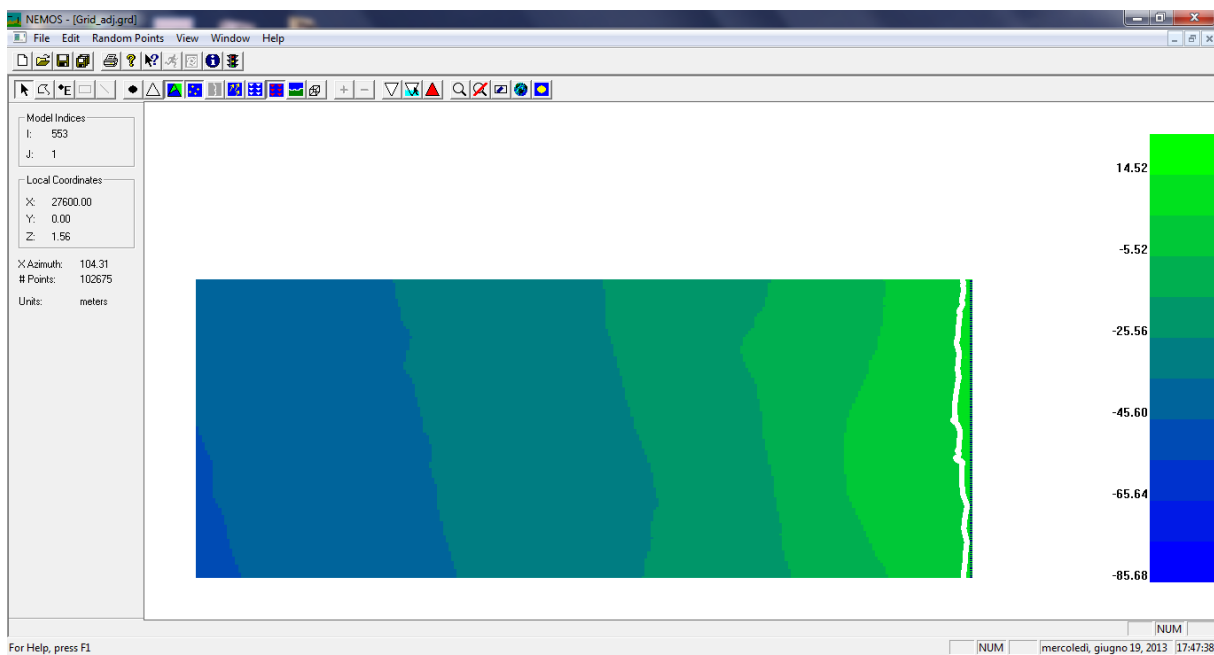
Figure 3.9. *GridGen: GENESIS model grid within STWAVE model grid (zoom). The black line at the landward extreme lateral boundary represents the GENESIS grid. The length of the GENESIS grid is within the initial shoreline length (white points).*

3.3 Connecting STWAVE and GENESIS grid: the near shore reference line

The *near shore reference line* represents the link through which STWAVE model information is passed into GENESIS environment.

The *near shore reference line* is an imagery boundary, placed *immediately before* the wave

breaking point, where wave propagation results (wave height, period, direction) coming from the *external wave model* (STWAVE) are stored. This information is then used by the *GENESIS internal wave transformation model* as input to calculate the wave parameters at the breaking point. Figure 3.10 illustrates the wave propagation performed by both the *external* (STWAVE) and *internal* (GENESIS) wave propagation models.
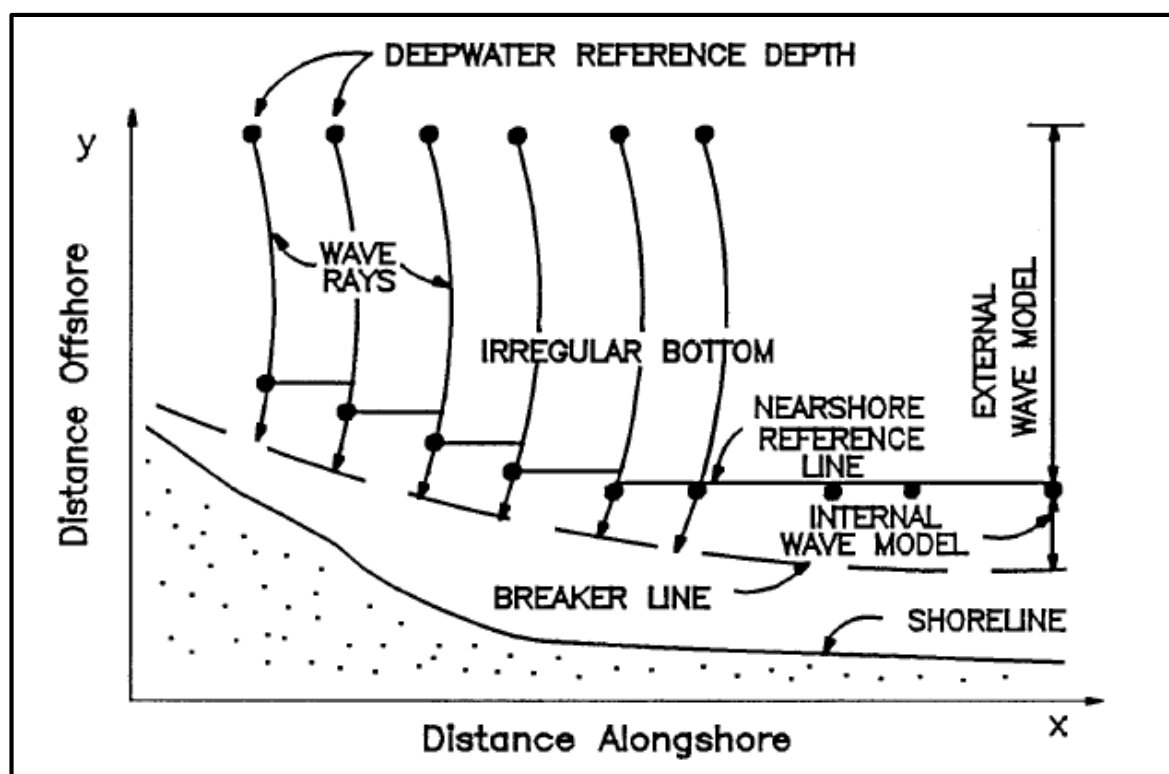
Figure 3.10. *Wave propagation by the external (STWAVE) and internal (GENESIS) wave models (Hanson et al.1991).*

From a practical point of view the *nearshore reference line* consists of a series of depth specified *stations* placed at each cell of the STWAVE grid, just before the wave breaking point. Each *station* is an *empty bin* where STWAVE model results (wave parameters) are stored after the model run. The matching between the STWAVE grid and the GENESIS grid ensures that these results are correctly passed to the *internal wave transformation model*, which finally brings waves to the breaking point.

The *stations* positions can be automatically set in *GridGen* by specifying the contour depth at which *stations* should be created. This is done while setting the GENESIS grid specifications, as Figure 3.11 shows.
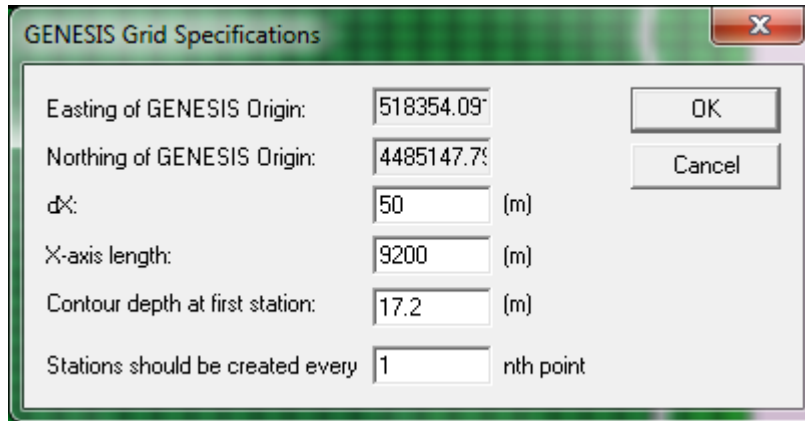
Figure 3.11. *GridGen: first attempt stations positions specifications, provided along with GENESIS grid specifications.*

In this study, stations were created at each model grid cell and they were placed at the *17.2m* water depth contour. This represents a *first attempt value*.
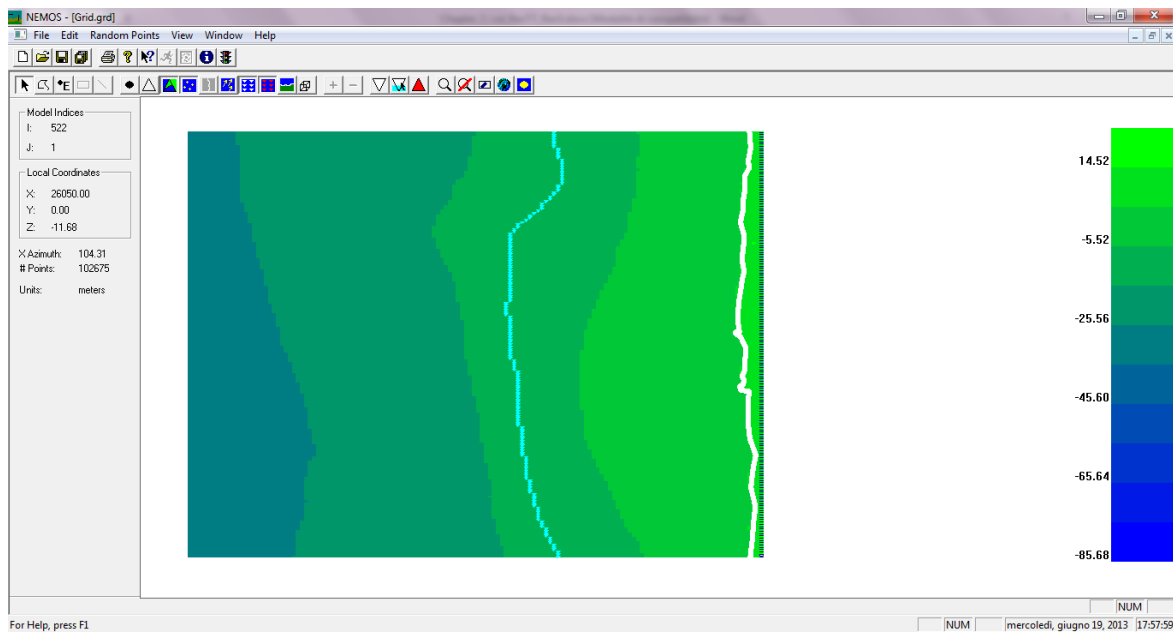
Figure 3.12. *GridGen: stations (light blue colored) located at the first attempt water depth contour value (17.2m).*

The *17.2m* contour depth was chosen as a *first attempt value* for the *nearshore reference line* definition. This value was derived considering the relationship between the wave height at breaking, H_{m0} (m) and the local depth, d (m) in the *saturated* breaking zone for irregular waves (US Army Corps of Engineers 2003).

$$H_{m0,b} = 0.6 \, d \tag{3.1}$$

An indicative water depth value was derived considering the most extreme wave event (H_{m0} = 9.7m; T_P = 16.7s; θ = 311°). This value was 16.2m, but in order to be absolutely sure that the *stations* where placed at the seaward side of the wave breaking point, a greater water depth value (17.2m) was assumed.

STWAVE was run up to the abovementioned specified *nearshore reference line*. The results of this first run provided the position of the wave breaking point at each wave model cell as reported in Figure 3.13.
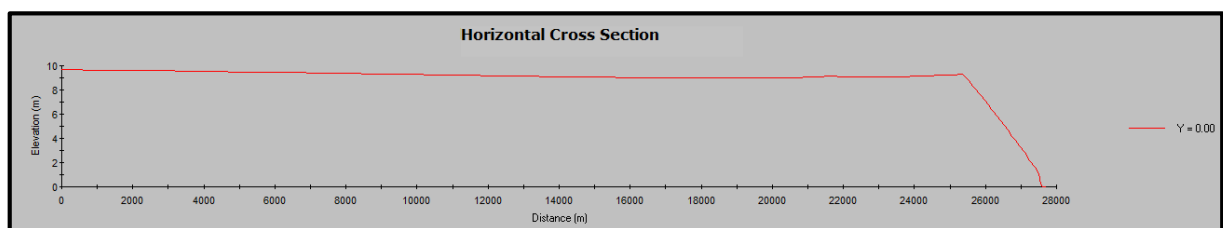
Figure 3.13. *WMV: STWAVE results visualization. Wave height cross sectional profile at the first wave model cell (Y=0).*

Figure 3.13 shows an example of the wave height cross sectional profile at the first STWAVE cell (Y=0) for the extreme wave event (H_{m0} = 9.7m; T_P = 16.7s; θ = 311°). The breaking point position is found at the wave height profile collapse point. The same plot was visualized for each one of the model grid cell in order to get the corresponding wave breaking point. Only the extreme event present in the wave record was considered. This ensured that the related wave breaking points serve for all wave events (the higher the wave height, the further offshore the wave breaking point will be).

The decision was to *adjust* the stations position and to place them two grid cells (100m) before the wave breaking point to account for uncertainties on the wave models. The *adjustment* consisted in dragging each *station* two grid cells further offshore in the *GridGen* workspace. The plot of Figure 3.14 shows the adjustment performed for *stations* placed at the Y STWAVE locations within [4950m; 6450m] interval.
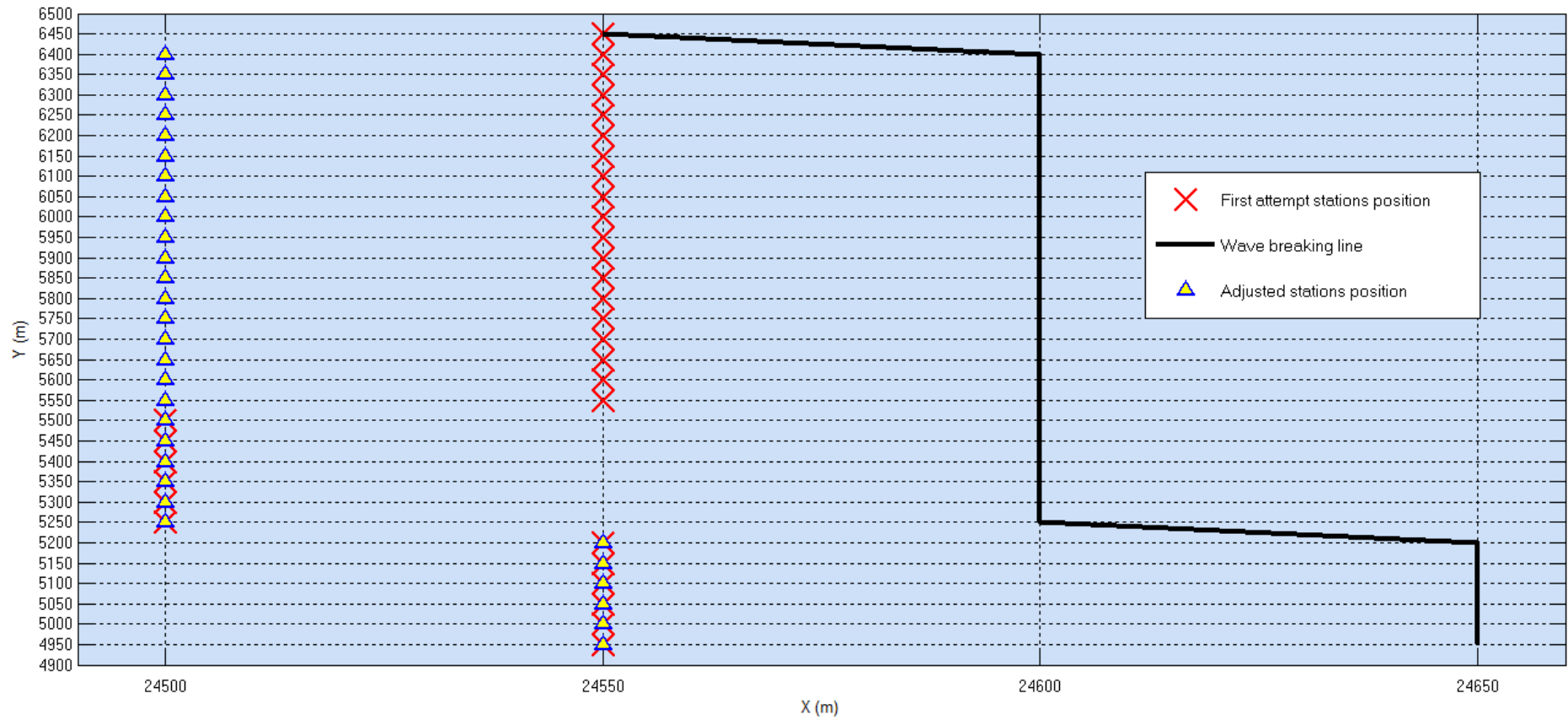
Figure 3.14. *Adjustment of stations position located within [4950m; 6450m] Y STWAVE coordinate. The X and Y axis represent the STWAVE model grid. The stations are moved two grid cells (100m) further offshore from the wave breaking point. This is the adjusted stations position.*

Figure 3.14 shows that the *first attempt near shore reference line* was almost complying with the model requirements, with the exception of *stations* placed within [5550m; 6450m] Y interval. These *stations* were thus adjusted and placed two grid cells (100m) further offshore from the wave breaking point.

The *adjusted near shore reference line* information was finally exported from *GridGen* as the *station file*. The simulations results finally confirmed that this was a reasonable and reliable reference position.

Chapter 4

Wave propagation

This chapter describes the wave propagation from the *offshore boundary* up to the *adjusted nearshore reference line*. STWAVE model is run as a standalone application and requires input wave data at the offshore boundary in the form of 2D directional spectra. SPECGEN code is used to create the spectra starting from integral wave parameters. WSAV code allows for the synthesis of wave information.

4.1 Synthesis of waves information

The *continuous wave series,* hereafter also referred to as *wave component*, must be organized in a more synthetized way in order to minimize computational efforts. The auxiliary code that serves this function is *WSAV* (*Wave Station Analysis and Visualization*). This code performs statistical analysis of the *wave component* and creates a representative group of wave events (*permutations*). A comprehensive description of WSAV processing is here reported. Section § 4.1.1 presents the statistical analysis of the *wave component* before being processed in WSAV. In the last section (§4.1.2) *permutation* results are presented and discussed.

4.1.1 Wave component statistics

These statistics refer to the *wave component* before being processed in WSAV. A statistical analysis was performed for each wave parameter.

− Significant wave height (H_{m0}) frequency distribution:
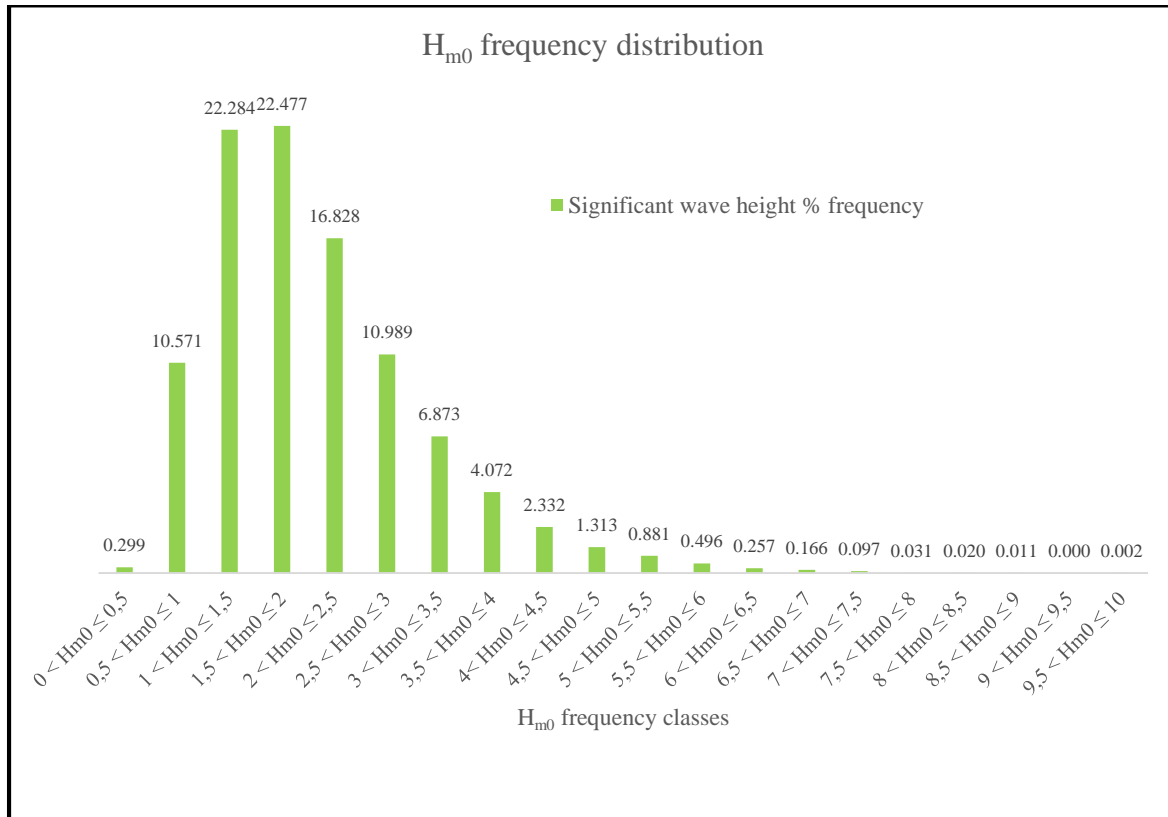
Figure 4.1. *Significant wave height frequency distribution.*

Figure 4.1 shows significant wave height distribution, organized in 20 *frequency classes* (*bands*). The highest frequencies are within the [1m; 2m] wave height interval. The mean wave height value is 2.09m. The minimum value ($H_{m0} = 0.35$m) and the maximum value ($H_{m0} = 9.7$m) are exceptional events that occur only twice and once respectively within the entire recording period. Nevertheless the maximum event ($H_{m0} = 9.7$m) must be taken into consideration, as the longitudinal sediment transport is proportional to the wave height at breaking at 5/2 power, according to the *CERC* formula (US Army Corps of Engineers 2002). This means that even a single wave event, characterized by a high value of H_{m0}, can theoretically move more sediments than a sequence of events with lower H_{m0}.

− <u>Wave peak period (T$_P$) frequency distribution:</u>
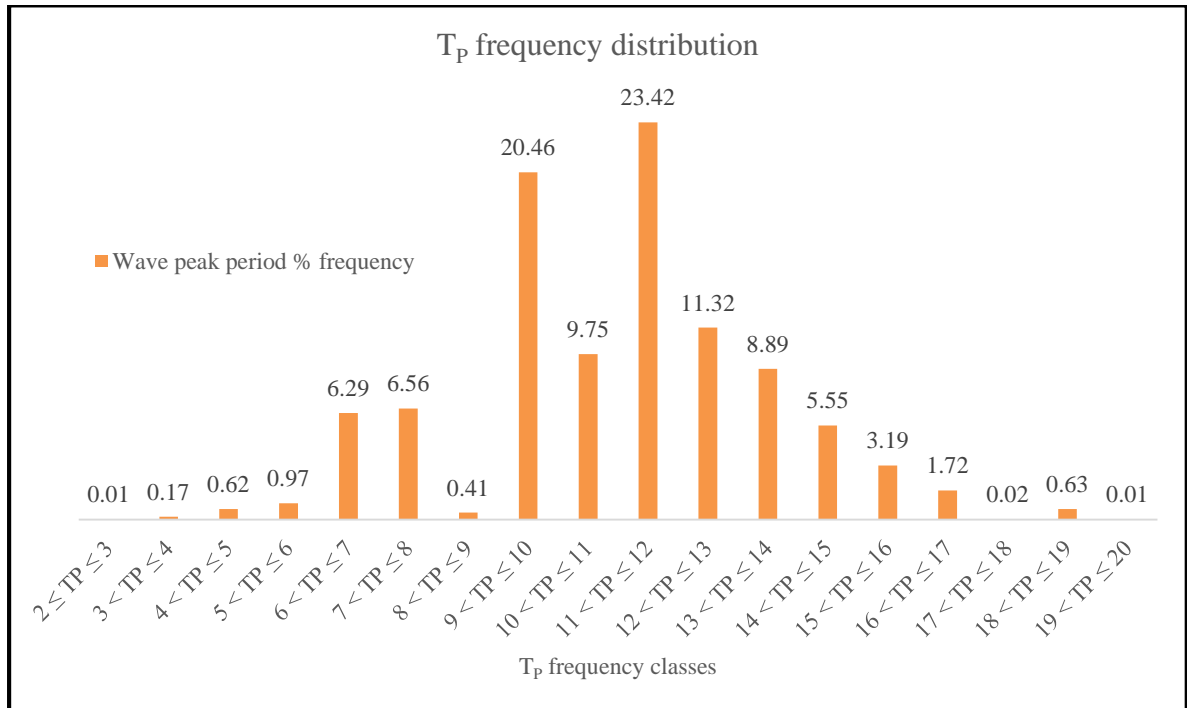
Figure4.2. *Wave peak period frequency distribution.*

Figure 4.2 illustrates the wave peak period distribution in 18 frequency classes (*bands*). The most frequent values fall within the [9s; 12s] interval and the mean value is 11.04s. These values are characteristic of *swells* in this region.

- Wave direction (θ) frequency distribution:
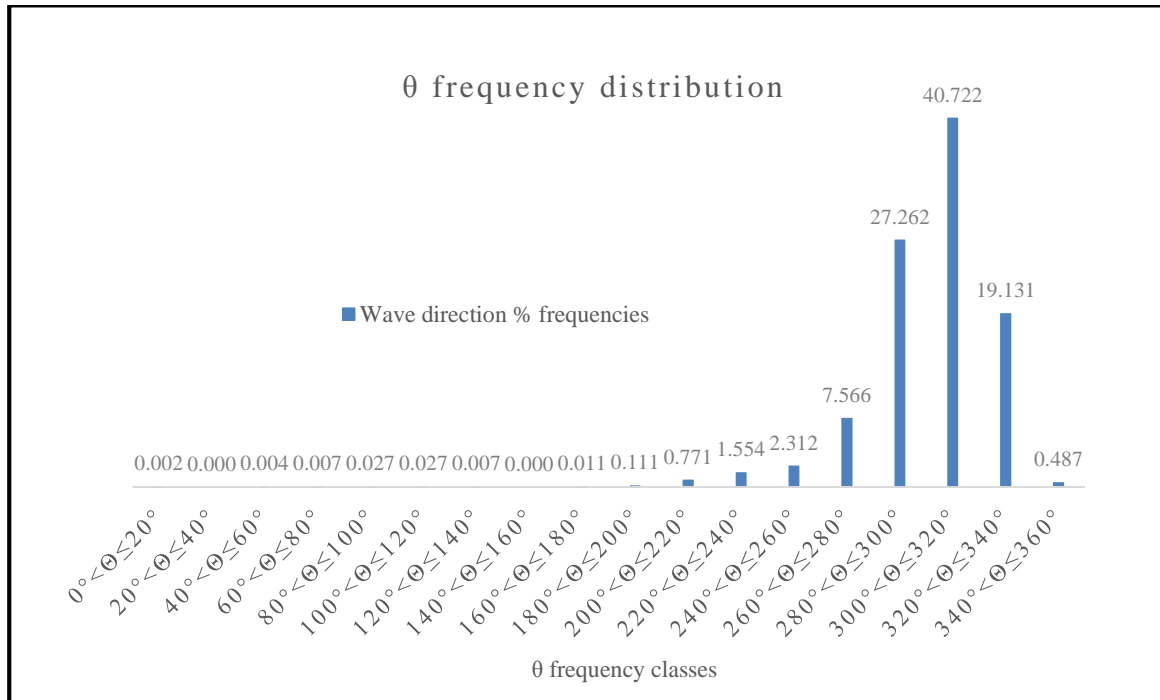
Figure 4.3. *Wave direction frequency distribution.*

Figure 4.3 shows wave direction distributed in 18 classes (*bands*). The most of events are within the [300°; 320°] direction interval. This is consistent with the real wave climate direction that is known to arrive from north-westerly direction.

4.1.2 WSAV: permutations results

WSAV requires *bands* specifications for each wave parameter. Table 4.1 summarizes the *bands* used for this study.

Band n°	H_{m0} (m)	T_P (s)	θ (°)
1	0÷1.5	2÷6	360÷340
2	1.5÷3	6÷9	340÷320
3	3÷4.5	9÷12	320÷300
4	4.5÷6	12÷15	300÷280
5	6÷7	15÷20	280÷260
6	7÷8	/	260÷220
7	8÷9	/	220÷200
8	9÷10	/	/

Table 4.1. *WSAV bands for wave parameters.*

*Bands w*ere derived taking care that the frequency classes with the highest frequency value were included. This is fundamental to get the most representative synthetic wave climate information.

WSAV performs a statistical analysis similar to the one presented in section §4.1.1. Figure 4.4 shows the results.
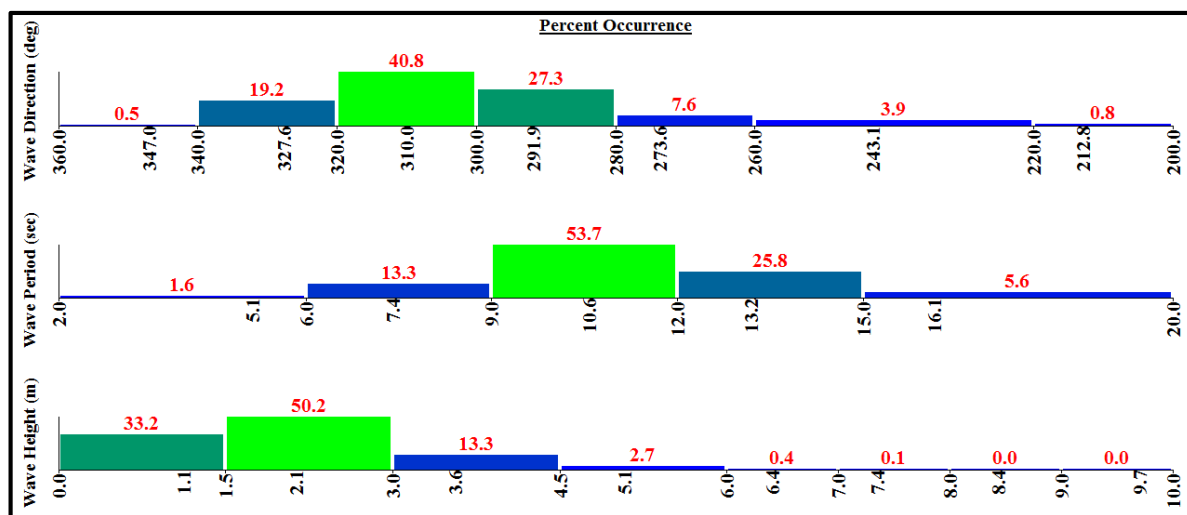
Figure 4.4. *WSAV: statistical analysis results. Mean values are reported as representative values of each band. Frequency distribution (% occurrence) is reported on top of each band column.*

Results can be also displayed in the wave rose plot. Figure 4.5 shows the results.
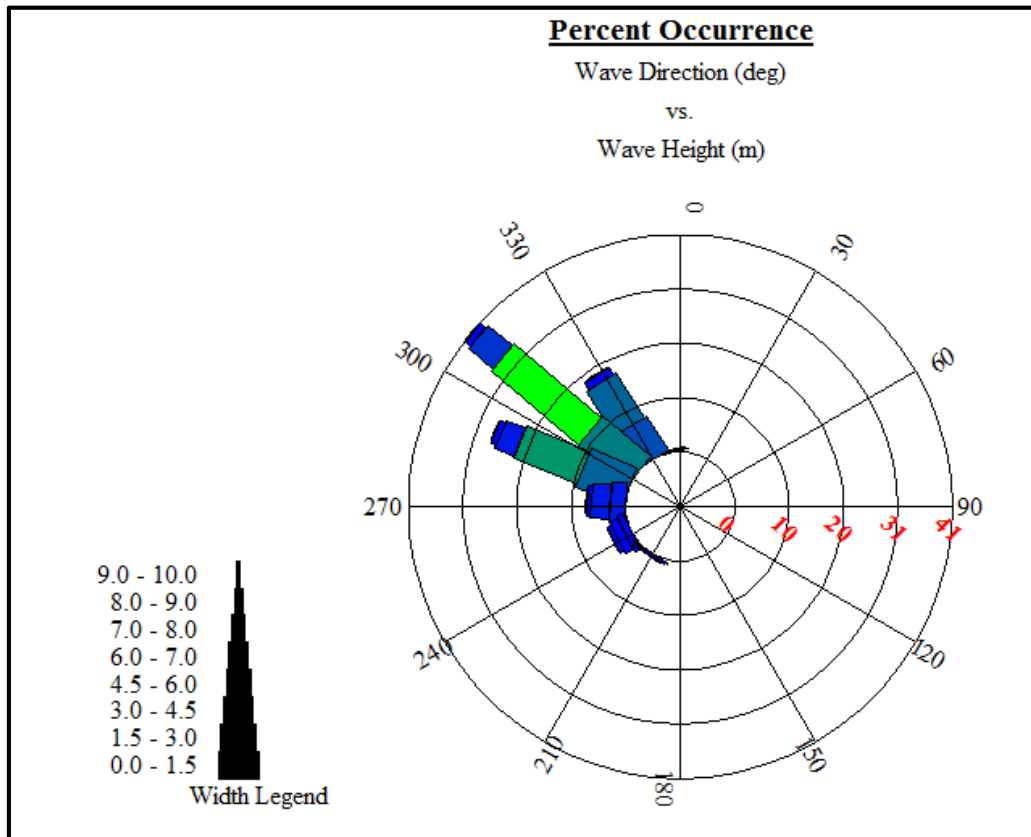
Figure 4.5. *WSAV: wave rose plot. Wave direction (°) vs wave height (m), % occurrence.*

Figure 4.5 confirms that *bands* were properly set: the main direction of real wave climate (NW) is well represented in the *synthetized wave information*.

WSAV session is completed when *permutations* are created. This term does not refer to the classic mathematical definition of permutations. In fact, in this context the term *permutations* indicates a combination of wave height, wave period and wave angle bands which have a relevant frequency of occurrences i.e which are sufficiently representative of the wave data series. To better explain: in this study wave parameters (H_{m0}, TP, θ) were divided in 8,5,7 *bands* respectively. The overall number of possible *permutations* should thus be 280 (8x5x7=280). This is not the case: only representative *permutations* will be selected by WSAV (138). This concept is further explained in §4.2.2.

4.2 Generation of 2D spectra

STWAVE requires wave information in the form of 2D spectra at the *offshore boundary*. Before presenting the directional spectra created with SPECGEN (§4.2.2) some references about the spectra generation performed by this code are provided (§4.2.1).

4.2.1 SPECGEN references

The wave spectrum is the most important form in which ocean waves are described ((Holthuijsen 2007).

A *parametric spectral shape* (*model*) together with a *directional spreading function* can be applied to specify and incident spectrum, knowing wave height, period and direction (McKee Smith *et al.*2001). SPECGEN generates 2D directional wave spectra using TMA (TEXEL storm, MARSEN and ARSLOE) *parametric spectrum model* combined with a cosine power *spreading function*.

The TMA spectrum was intended for wave hindcasting and forecasting in water of finite depth (…) and it is a modification of JONSWAP spectrum (US Army Corps of Engineers 2008). The *spreading function* reproduces the directional distribution of wave energy.

SPECCGEN requires two further parameters to generate the spectra: the *spectral peakness parameter* (γ) and the *directional spreading coefficient* (*nn*). The first parameter controls the peak of the frequency spectrum, while the second one is responsible for the spreading of the energy in the frequency spectrum. In this study these parameters are assumed with their default values (γ=3.3, nn=4).

4.2.2 Spectra generation

SPECGEN generates 2D directional spectra for each *permutation* (138) first created in WSAV. The *permutations* are hereafter also referred to as *events* or *bins*. This last term is revealing of how GENESIS will finally receive and process wave input data. For the time being the *permutations* (or *events,* or *bins*) are just representative *classes* of a wider wave climate information. The total number of *permutations* is 138.

As an example Figure 4.6 shows the directional 2D spectrum on a *Cartesian plot*, created for the *permutation* (*event*) with H_{m0}=1.12m, T_P=5.14s, θ= - 43.34°.
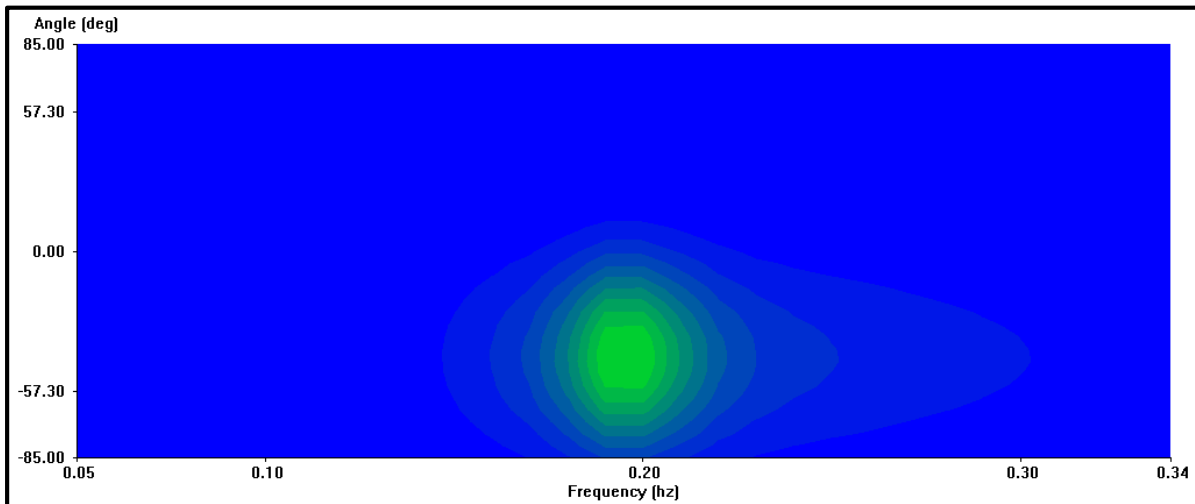
Figure 4.6. *SPECGEN: Cartesian plot type of the directional 2D spectrum for event H_{m0}=1.12m, T_P=5.14s, θ= -43.34°.*

Wave energy density (m²/Hz/deg) is calculated as a function of frequency and direction and it is represented by the coloured contours. The direction interval represent the half plane portion covered by STWAVE. Figure 4.7 shows the same spectrum plotted in *polar* coordinates.
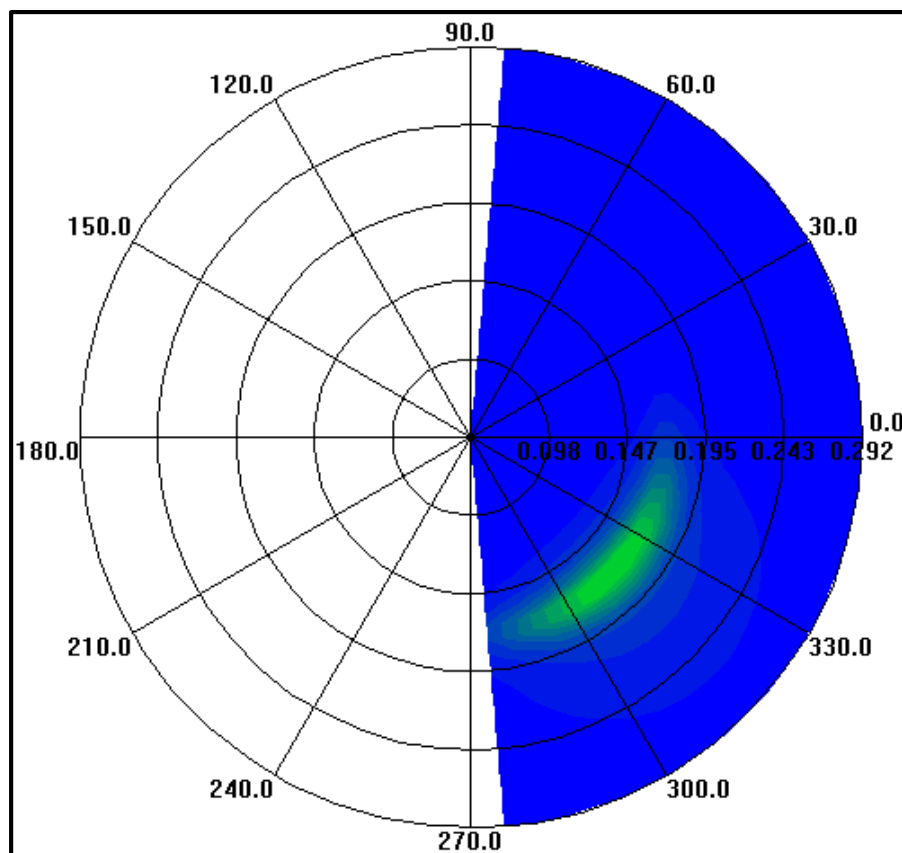
Figure 4.7. *SPECGEN: 2D directional spectrum plotted in polar coordinates for event H_{m0}=1.12m, T_P=5.14s, θ= - 43.34°.*

4.3 STWAVE wave propagation

In this section STWAVE (STeady-state spectral WAVE model) is presented, starting from its fundamentals. The model capabilities, assumptions and governing equations are fully described in the *STWAVE User's manual* (McKee Smith *et al.*2001). Some parts of it are reported in § 4.3.1 for sake of completeness. The last section (§4.3.2) shows the results of wave propagation for this case study.

4.3.1 STWAVE fundamentals

STWAVE is steady-state finite difference model based on the wave action balance equation. The model version implemented in CEDAS is version 3.0.

This model describes quantitatively the change in wave parameters (wave height, period, direction, and spectral shape) between the offshore and the near shore. In particular, it simulates depth-induced wave refraction and shoaling, current induced refraction and shoaling, depth- and steepness-induced wave breaking, diffraction, wind-wave growth, and wave-wave interaction and white capping that redistribute and dissipate energy in a growing wave field.

The model is based on the following assumptions:

– *Mild bottom slope and negligible wave reflection*. STWAVE is a half plane (±87.5°from the x-axis of the grid) model; this means that wave energy can propagate only from the offshore toward the nearshore. Waves reflected from the shoreline or from steep bottom features, travelling in directions outside this half plane are thus neglected. Waves reflected off a structure but travelling in the +x-direction, are also neglected.

– *Spatially homogeneous offshore wave conditions*. The input spectrum in STWAVE is constant along the offshore boundary. This is a reasonable assumption for domains on the order of tens of kilometres, as the variation in the wave spectrum along the offshore boundary is expected to be small.

– *Steady-state waves, currents, and winds*. STWAVE is formulated as a steady-state model. This assumption is appropriate for wave conditions that vary more slowly than the time it takes for waves to transit the computational grid.

— *Linear refraction and shoaling*. STWAVE incorporates only linear wave refraction and shoaling, thus does not represent wave asymmetry.

— *Depth-uniform current*. The wave-current interaction in the model is based on a current that is constant through the water column.

— *Bottom friction is neglected*.

— *Linear radiation stress.* Radiation stress is calculated based on linear wave theory.

The calculations start at the first grid column (*offshore boundary*) where the 2D directional spectra are set as input information. Each spectrum is related to a wave *event*. The model propagates each *spectrum* starting from the first column and proceeding in the landward direction.

The final output files available are:

—   wave directional spectra at the *nearshore reference line* (*stations*);

—   wave parameters (H_{m0},T_P,θ) at the *nearshore reference line* (*stations*);

—   *fields* of wave parameters (H_{m0},T_P,θ) over the entire model domain;

—   *fields* of breaker indices indicating active regions of breaking over the entire domain;

—   *fields* of radiation stress gradients over the entire domain.

4.3.2 STWAVE results

STWAVE was run two times in this study. The first run was done up to *a first attempt nearshore reference line* (*stations*). The results provided the exact wave breaking point positions required to perform the *station positions adjustment* (see Chapter 3, § 3.3).

The second run finally provided wave parameters at the correct *nearshore reference line* to be input in GENESIS.

WMV (Wave Model Visualization) code allows for the visualization of STWAVE results. Figure 4.8 shows a zoom in the *wave vectors field* on top of the bathymetric contours. *Event* is the same whose spectrum was visualized in § 4.2.2. The corresponding wave parameters are

$H_{m0}=1.12m$, $T_P=5.14s$, $\theta= - 43.34°$. *Stations* are in the *adjusted* position.
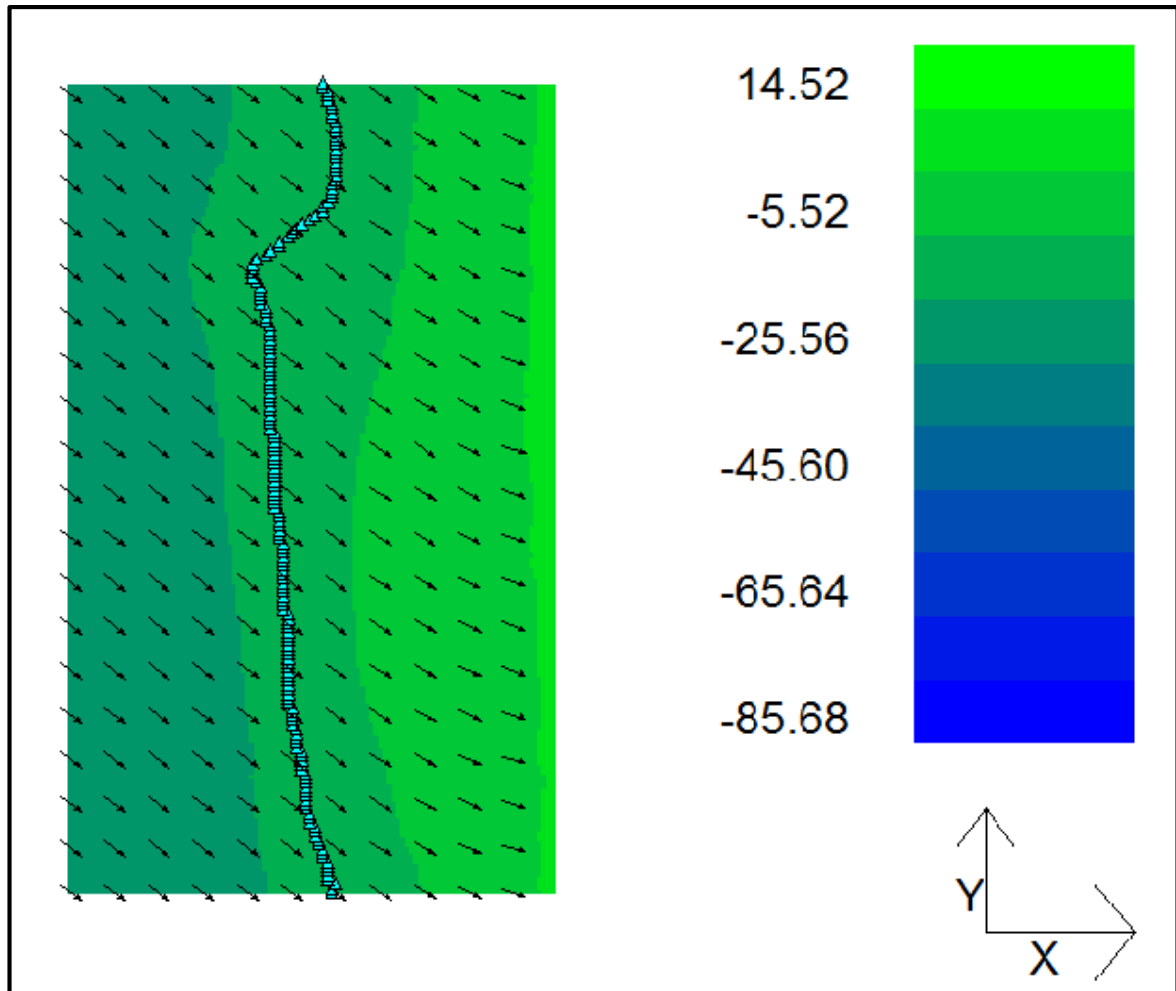
Figure 4.8. *WMV: zoom in the wave vectors field on to of bathymetric contours. Reference event: Hm0=1.12m, $T_P=5.14s$, $\theta= - 43.34°$.*

WMV allows for visualizing all types of information within the entire STWAVE domain. Nearshore results were checked and they resulted to be consistent with reality. The real wave climate direction (NW) was again used to double check the results.

Chapter 5

GENESIS model

This chapter provides a comprehensive description of GENESIS model. The first part (§5.1) presents the model fundamentals. Assumptions, limitations and governing equations are directly reported from *GENESIS Workbook* (Hanson *et al.*1991) and *GENESIS Technical Reference* (Hanson 1987). The second part of the chapter presents the model setup for this study: § 5.2 illustrates the spatial configuration of the project area and §5.3 provides information about the model calibration.

5.1 Fundamentals

GENESIS (GENEralized Model for SImulating Shoreline Change) calculates shoreline change due to spatial and temporal differences in long shore transport as produced by breaking waves (US Army Corps of Engineers 2002). The modelling system is generalized in that a wide variety of offshore wave inputs, initial beach plan shape configurations, coastal structures, and beach fills can be specified (Hanson *et al.*1991). The next sections provide information about the model assumptions and limitations (§5.1.1) and the governing equations (§5.1.2).

5.1.1 Model assumptions and limitations

The basic *assumptions* of the model are:

– *Constant beach profile shape.* The beach profile moves landward (erosion) and seaward (accretion) while retaining the same shape. The bottom profile does not change in time (see Figure 5.1).

– *Constant shoreward and seaward limits of the active profile*. Sand is transported alongshore between two well-defined limiting elevations on the profile. The shoreward limit (*berm height, D_B*) is located at the top of the active berm, and the seaward limit (*depth of closure*, D_C) is located where no significant depth changes occurs. These two limits define the active profile for long shore sediment transport.

−   *Wave breaking-induced long shore sediment transport*. Sand transport is caused by waves and waves-induced currents only. Long shore sediment transport is generated by wave height and wave direction at breaking respect to a specified long shore direction.

−   *Neglect of the near shore circulation*. The horizontal circulation in the near shore, which actually moves the sand, is not directly considered. One exception is the circulation pattern in the shadow region behind structure. The long shore gradient of in breaking wave height accounts for the description of this phenomenon.

−   *Long-term trend in shoreline evolution*. The model applies where there is a visible long-term trend in shoreline behaviour. This is to separate and predict a clear signal of shoreline change from cyclical and random movement in the beach system.
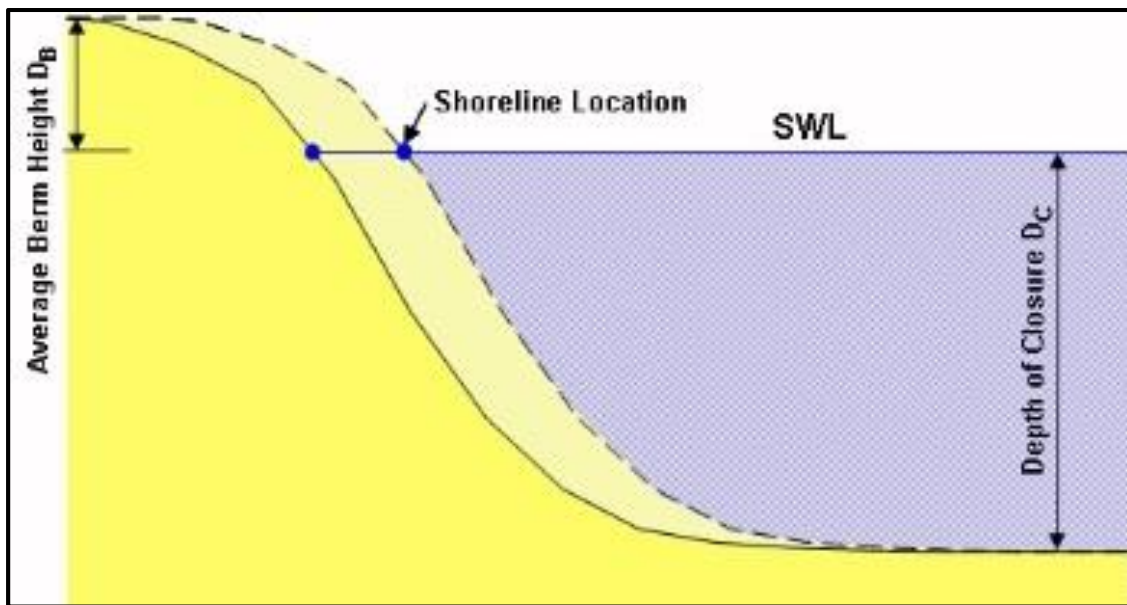
Figure 5.1. *Shoreline change and associated bottom profiles (http://www.vliz.be/wiki/Long-term_modelling_using_1-line_models_-GENESIS_and_new_extensions).*

The abovementioned assumptions have important implications in the model capabilities. The major *limitations* are:

−   *Neglect of cross-shore sediment transport*. Only long shore sediment transport is considered. In fact, imbalance in the long shore transport rates causes more gradual and permanent changes in the beach plan form. In this process, the beach profile can be assumed essentially unchanged. The same is not valid for the cross-shore sediment transport, which is related to short-term fluctuations of the beach profile.

- *Long term time scale.* The beach profile can be assumed to remain unchanged if the long shore sediment transport is the dominating process. The typical time scale is thus of the order of years.

- *Evident trend in beach profile.* The model does not apply to randomly fluctuating beach systems in which no trend in shoreline position is evident e.g beach change inside inlets or in areas dominated by tidal flow; beach change produced by wind-generated currents, storm-induced beach erosion in which cross-shore sediment transport processes are dominant and scour at structures.

- *Beach composition.* As the dominant process is long shore sediment transport, the coastal stretch must be composed of *transportable* material. The model best works for sandy beaches.

5.1.3 Model governing equations

The partial differential equation governing *shoreline change* is formulated by conservation of sand volume for an infinitely small length dx alongshore (Equation 5.1).

$$\frac{\partial y}{\partial t} + \frac{\left(\frac{\partial Q}{\partial x} + q\right)}{D_B + D_C} = 0 \tag{5.1}$$

The y quantity represents the *shoreline position* (m), x is the *long shore coordinate* (m), t is the time (s), D_B is the *average berm height* above the mean water level (m), D_C is the *depth of closure* (m), Q is the *long shore transport rate* (m³/s) and q represents *the line sources/sinks* along the coast (m³/s/m shoreline). Figure 5.1 provides a schematic of GENESIS shoreline position calculation.
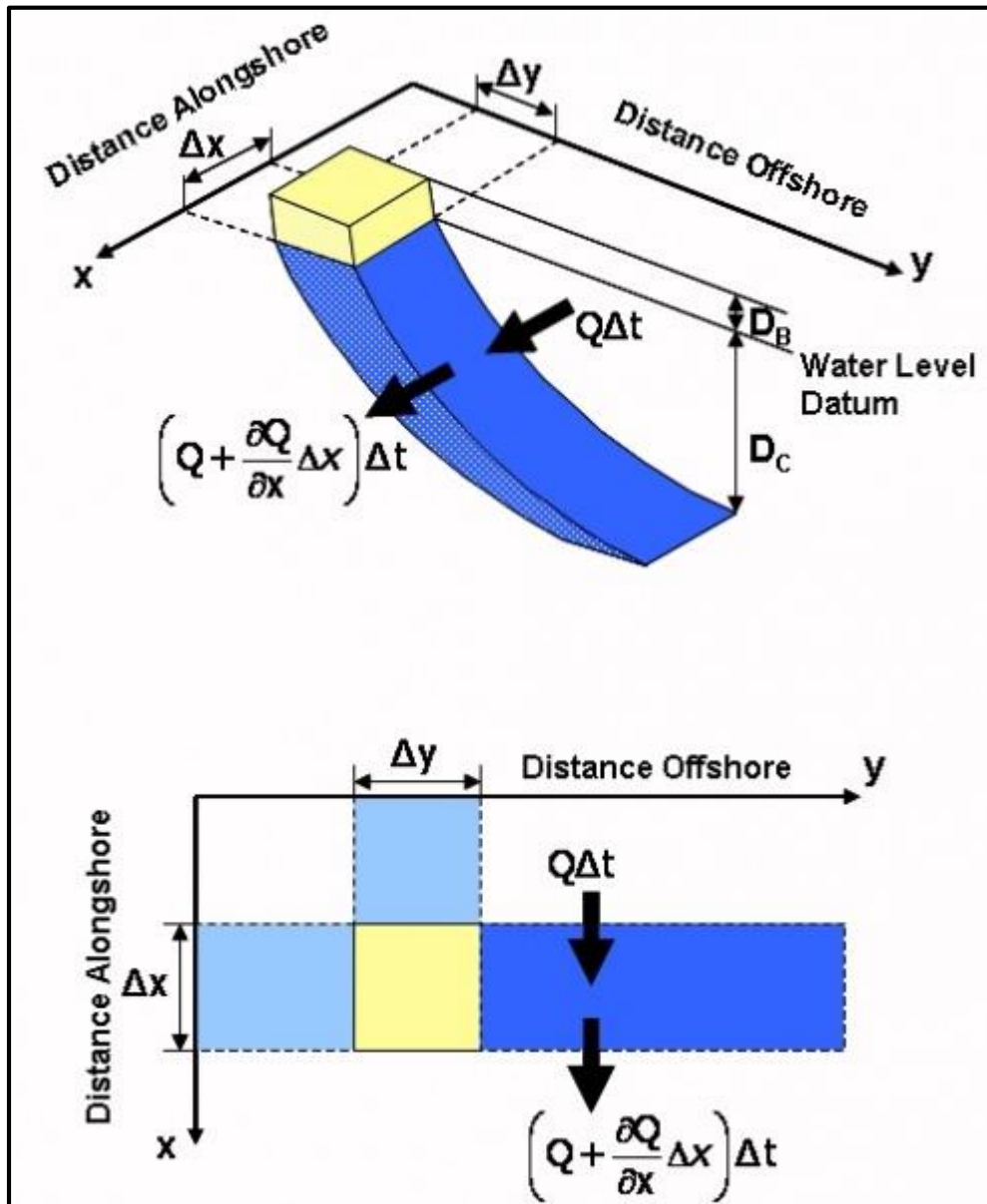
Figure 5.2. *Definition sketch for shoreline position calculation (http://www.vliz.be/wiki/Long-term_modelling_using_1-line_models_-GENESIS_and_new_extensions).*

In order to solve Equation 5.1 D_B, D_C, Q and q must be specified along with boundary conditions on each end of the beach, structures configuration and engineering activities present on the coast (beach fill, sand by passing, etc.).

The empirical predictive formula for the *long shore transport rate* used in GENESIS is (Equation 5.2):

$$Q = \left(H^2 C_g\right)_b \left(a_1 \sin 2\theta_{bs} - a_2 \cos \theta_{bs} \frac{\partial H}{\partial x}\right)_b \tag{5.2}$$

The C_g quantity represents wave group speed given by linear wave theory (m/s), the subscript *b* denotes wave breaking conditions, H (m) and θ (°) represent wave height and wave angle to the local shoreline direction at breaking, respectively. The non-dimensional parameters a_1 and a_2 are given by Equations 5.3, 5.4.

$$a_1 = \frac{K_1}{16(S-1)(1-p)(1.416)^{5/2}} \tag{5.3}$$

$$a_1 = \frac{K_2}{8(S-1)(1-p)\tan\beta\,(1.416)^{7/2}} \tag{5.4}$$

− K_1 and K_2 are empirical coefficients treated as a calibration parameters;

− $S = \rho_S/\rho$

− ρ_S is the density of sand (taken to be 2.65 10^3kg/m^3 for quartz sand);

− ρ is the density of water (1.03 10^3 kg/m^3 for sea water);

− p is the porosity of sand on the bed (taken to be 0.4);

− tanß is the average bottom slope from the shoreline to the depth of long shore transport;

− the factors 1.416 are used to convert from significant wave height H_{m0} (the statistical wave height required by GENESIS) to root-mean-square (H_{rms}) wave height.

The first term in Equation 5.2 corresponds to the "Coastal Engineering Research Center (CERC) formula" and accounts for long shore sand transport produced by obliquely incident breaking waves.

The second term in Equation 5.2 is not part of the CERC formula and describes the effect of another generating mechanism for long shore sand transport, the long shore gradient in breaking wave height *dHb/dx*. The contribution arising from the long shore gradient in wave height is usually much smaller than that from oblique wave incidence in an open-coast situation. However, in the vicinity of structures where diffraction produces a substantial

change in breaking wave height over a considerable length of beach, inclusion of the second term provides an improved modelling result.

Figure 5.2 illustrates a schematic view of the calculation procedure within the model.
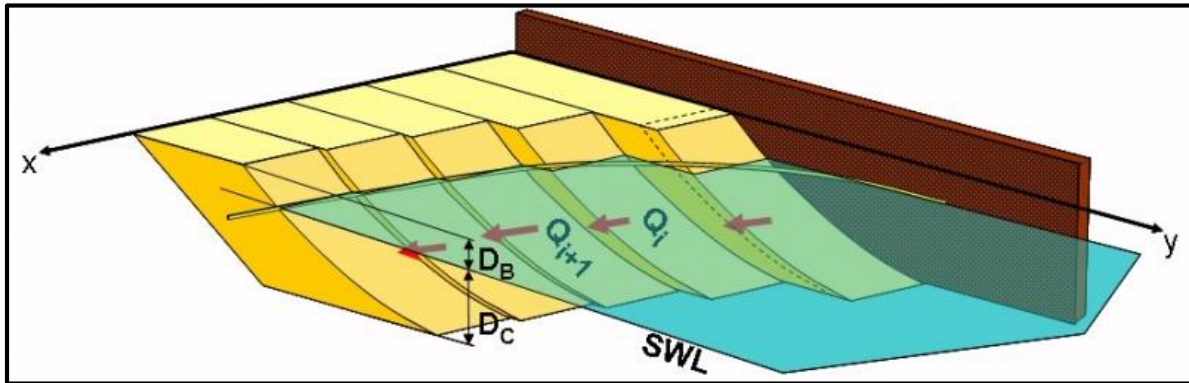
Figure 5.3. *Schematic of sediment transport rate calculation down drift of a short groin (http://www.vliz.be/wiki/Long-term_modelling_using_1-line_models_-GENESIS_and_new_extensions).*

5.2 Vagueira model spatial configuration

The spatial configuration used to setup the model for the calibration phase includes the following structures:

− a seawall placed just in front of Vagueira village houses, *Vagueira seawall* (Figure 5.4);

− a groin connect to the seawall, *Vagueira groin* (Figure 5.4);

− a groin placed immediately south of Vagueira village, *Vagueira south groin* (Figure 5.5).

Figure 5.4. *Vagueira seawall and Vagueira groin (North view). Site visit on October 2012.*

Figure 5.5. *Vagueira South groin seen from land. Site visit on October 2012.*

Figure 5.6 provides a comprehensive view of the structure positioning within the coastal stretch of interest. This is the spatial configuration used to calibrate the model.
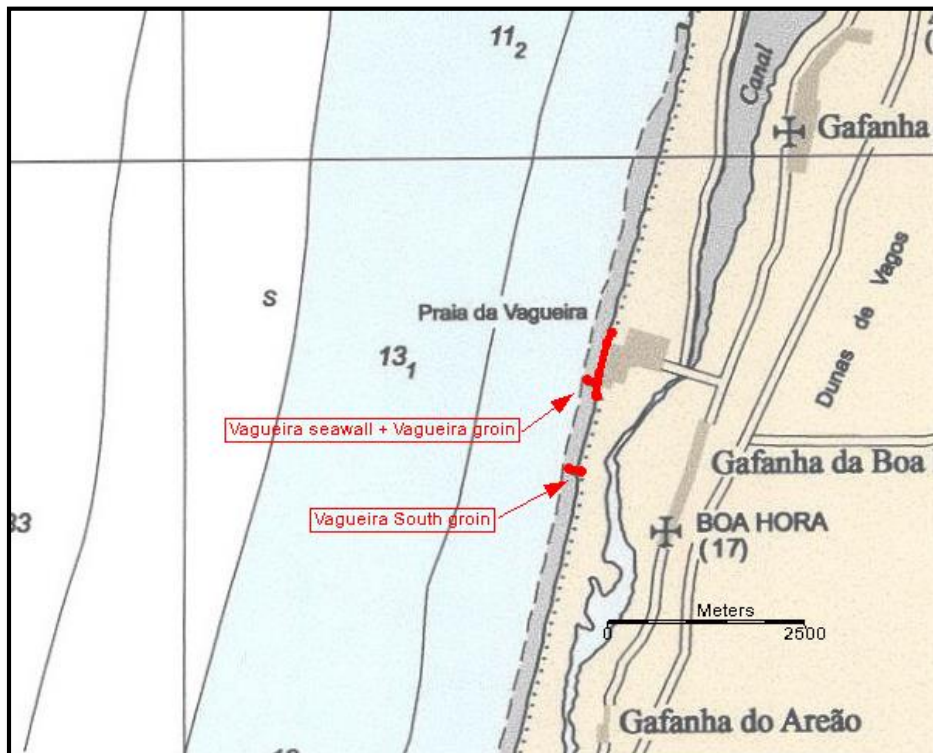
Figure 5.6. *SMS: spatial configuration used for the model calibration.*

The structures were adjusted to meet the model requirements in terms of placement, shape, and orientation. In particular the model requires the groins be located along the *Q-points* and the seawall starting and ending points to be placed at the *y-points* (see Chapter 3, § 3.2.1).

5.3 Model calibration

This section describes the model calibration. The aim is to setup the model so that the *calculated* (*final*) *shoreline position* in 2001 is close as possible to the *target* one. The model was run using a time step of 1.5h, starting from year 1996 (*initial shoreline position*) until year 2001.

The following subsections provide a detailed description of the parameters (not only the so-called *calibration parameters*) that were considered to get the best calibration result. Results are finally presented and discussed.

5.3.1 Sand and beach parameters: D_C, D_B and grain size

The *depth of closure* (D_C) and the *berm height* (D_B) define the vertical extent within sand is allowed to be transported.

These two parameters resulted to have great influence on the model results if considered

together. They were tested in two different situations. In the first case, provided that the *calibration parameters* K_1, K_2 were kept fixed, D_B and D_C were varied individually. In the second case they were varied together, with the same K_1, K_2 values. The solution in the second case resulted to vary more than in the first case.

In general the simulations proved that if K_1, K_2 are fixed and D_C and D_B are varied (both individually or together) the solution does not vary too much. On the contrary, if D_B and D_C are changed and K_1 and K_2 are re-calibrated to the new active profile extent the solution completely changes. The conclusion is straightforward: even if K_1 and K_2 are referred to as the main *calibration parameters*, they are related to the specific extent of the active profile (D_C and D_B). Only after the definition of the active profile, K_1 and K_2 can be calibrated.

The values used for this case study are D_C= 14m and D_B= 4m.

A starting indicative value for D_C was derived from Equation 5.5 (Hanson 1987).

$$D_C = 2H_{s,max}$$ (5.5)

$H_{s,max}$ represents the maximum annual significant wave height for the site of interest. The tests performed confirmed D_C= 14m to be the best choice.

The D_B value was easier to derive. The topographic inland cross sectional profiles were investigated in order to find the highest points close to the shore. D_B was derived as the average height (above MSL) of these points.

Figure 5.7 shows the resulting extension of the active profile area.
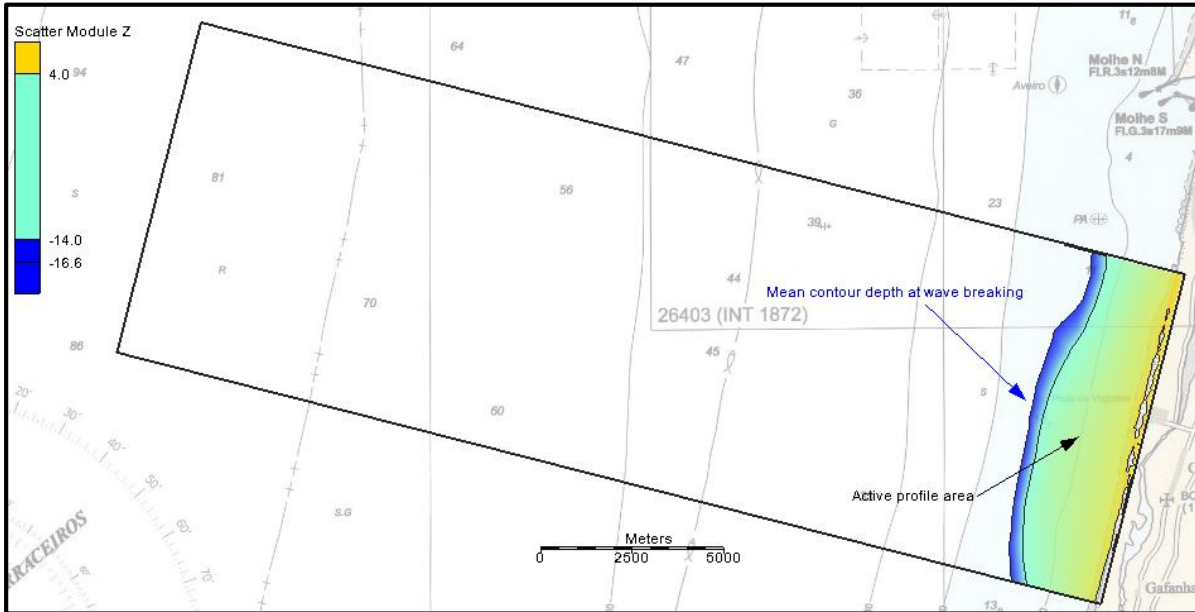
Figure 5.7. _SMS: active profile area at the shoreward side of the mean contour depth at breaking._

In Figure 5.7 the light colored contour fills represent the area of active sand transport i.e area where the long shore transport takes place. The average width is about 2km in the cross-shore direction. Of course, D_C contour must be at the shoreward side of the breaking point.

The effective _grain size_ (d_{50}) was set equal to 0.5mm. This value was derived from previous studies done in the same project area (Vaz Sena 2010). On-site visit confirmed this value as representative of the granulometric class of the sand in the coastal stretch. Figure 5.8 shows the comparison with sand samples.

Figure5.8. *Comparison of beach sand with sand samples.*

5.3.2 Long shore sand transport calibration coefficient: K_1 and K_2

K_1 and K_2 are known as *calibration parameters* and they control the sediment transport rate calculation (Equation 5.2).

K_1 (*primary calibration parameter*) is proportional to the magnitude of long shore sand transport rate and it controls the time scale of the calculation. The calculated shoreline is sensitive to this parameter especially in regions of high waves, such as at the up drift side of groins.

K_2 (*secondary calibration* parameter) is proportional to the wave height gradient alongshore. Its effects are visible in regions with strong wave height gradients alongshore, such as in the sheltered zones of diffracting jetties and detached breakwaters.

The suggested range for K_1 is [0.1; 1.0] (Hanson *et al.* 1991). The value chosen in this study is 0.8. This is the highest possible value that gives a stable solution. In fact the higher is K_1, the more enhanced is the erosion of the coast, especially at the up-drift side of the groins and in areas of high waves. Because of this, high values of K_1 give good matching between the *target* and the *calculated* shoreline, while low values of K_1 result in a less erosion, thus providing worse matching.

The suggested range of K_2 is $[0.5K_1; 1.5K_1]$ (Hanson *et al.* 1991). Simulations proved that the higher the value of K_2, the better the match of the *calculated* shoreline with the *target*. This because high values of K_2 enhance erosion in the down drift part of the groins, due to the alongshore gradient of wave height. Nevertheless, the value chosen for K_2 is not the maximum possible value giving stable solution. K_2 was fixed equal to $0.8K_1=0.64$ to account for the less importance of the alongshore wave height gradient erosion component with respect to the erosion component due to breaking wave heights with an angle to the coast. However, even for higher values of K_2 tested the shoreline profile did not vary too much.

In general, high values of both K_1 and K_2 were used, because they give the best calibration result for the whole stretch, with the exception of the two groins (*Vagueira* and *Vagueira South*). In these areas the match of the two shorelines is not good; this is due to the high values of K_1, K_2 which enhance the erosion of the sediments accumulated around the groins. Consequently, a compromise was reached between the two following solutions:

- low values of K_1,K_2 resulting in a good match of the shorelines in correspondence of the groins, but very bad match in the rest of the stretch;

- high values of K_1,K_2 providing good match of the shorelines along the whole stretch, with the only exception of the areas around the groins.

The second option was adopted, as it emphasizes the general erosion in the coastal stretch. Nevertheless, still in this solution it is possible to see how the calculated shoreline reflects the correct trend of sediments on a smaller scale i.e the zoomed image in the areas around the groins (Figure 5.9) shows a *step profile* of the *calculated* shoreline. This *step feature* represents the accumulation of sediments that occurs in reality at the up drift side of the groins, but on a smaller scale.
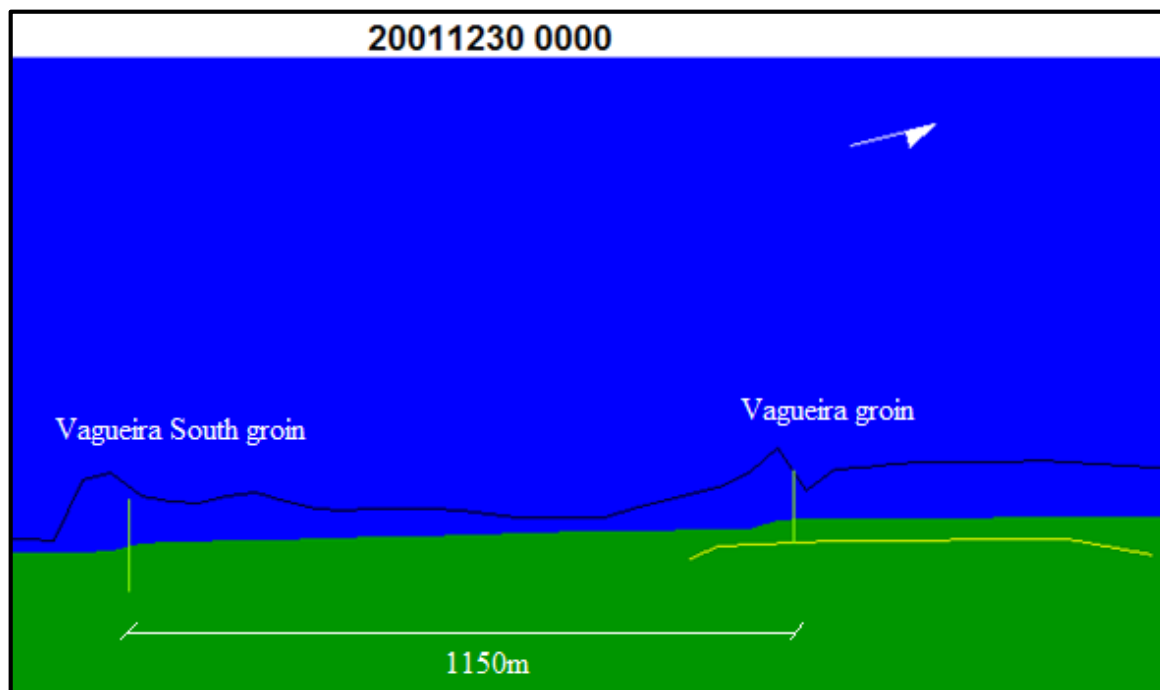
Figure 5.9. *GENESIS: zoomed image of the calculated shoreline on 30th of December 2001 (lower profile) and initial shoreline (upper profile).The area is in the groins premises: the step feature is indicative of the sediments accumulation that occurs at the up drift side of the structures, but on a smaller scale.*

5.3.3 Lateral boundary conditions

The boundary conditions are typically expressed in terms of long shore transport rate at both ends of the calculation grid, although it is possible to express boundary conditions in terms of boundary y-values (Hanson 1987).

GENESIS provides *four* different options for the description of the lateral boundary conditions.

The first option is the *pinned* lateral boundary condition. The term *pinned* refers to the shoreline position which is assumed not to move appreciably in time. In term of long shore transport rate this condition corresponds to a *free transport* condition ($dQ_l/dx=0$).

The second and third option are the *gated* boundary conditions. The model distinguishes between a *groin-gated* and a *jetty-gated* lateral boundary. Nevertheless, the underlying principle is the same: when a gated lateral boundary condition is specified, the amount of sediments that can enter the model is limited to a certain amount. This amount depends on the distance between the groin/jetty tip and the shoreline position at the external side of the model (Figure 5.10).
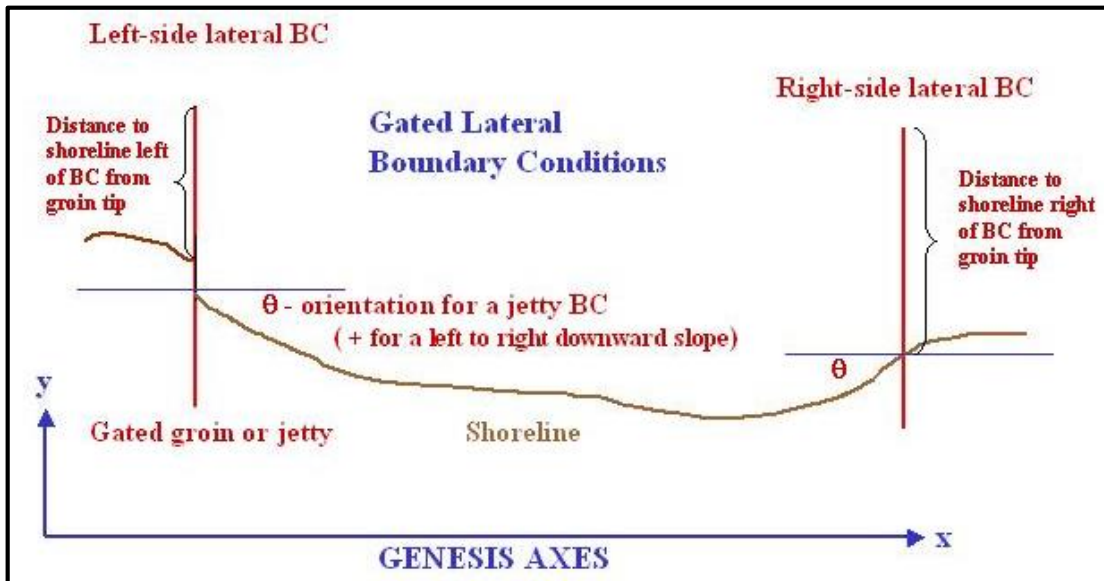
Figure 5.10. *Gated lateral boundary conditions specifications (Veri-Tech, Inc. 2004).*

The higher the distance, the less sediments can enter the model. These considerations refer to the *bypassing* mechanism. *Transmission* is allowed too, but depends on the structure permeability (see §5.3.4). In the case of a *jetty-gated* lateral boundary condition, the shoreline orientation at the boundary must be added. In terms of long shore transport rate the *gated* condition corresponds to a partial sand transport ($Q_l{\neq}0$) or a zero sand transport ($Q_l{=}0$), according to the specified distance between the groin/jetty tip and the shoreline position at the external side of the model.

The last option is the *moving* lateral boundary condition. This option is used when the shoreline is moving at a constant rate, whose value is known or can be determined.

In this study, a *moving* lateral boundary condition was specified at both sides of the model. The shoreline was assumed to move at a constant rate (-112m and -84m for left and right side respectively) over the simulation period (1996-2001). These values were derived by calculating the distance between the two shoreline positions (*initial* and *target*) at the model lateral boundaries. The minus indicates that the shoreline is receding, as known from reality. Figure 5.10 indicates the lateral boundary conditions specifications.
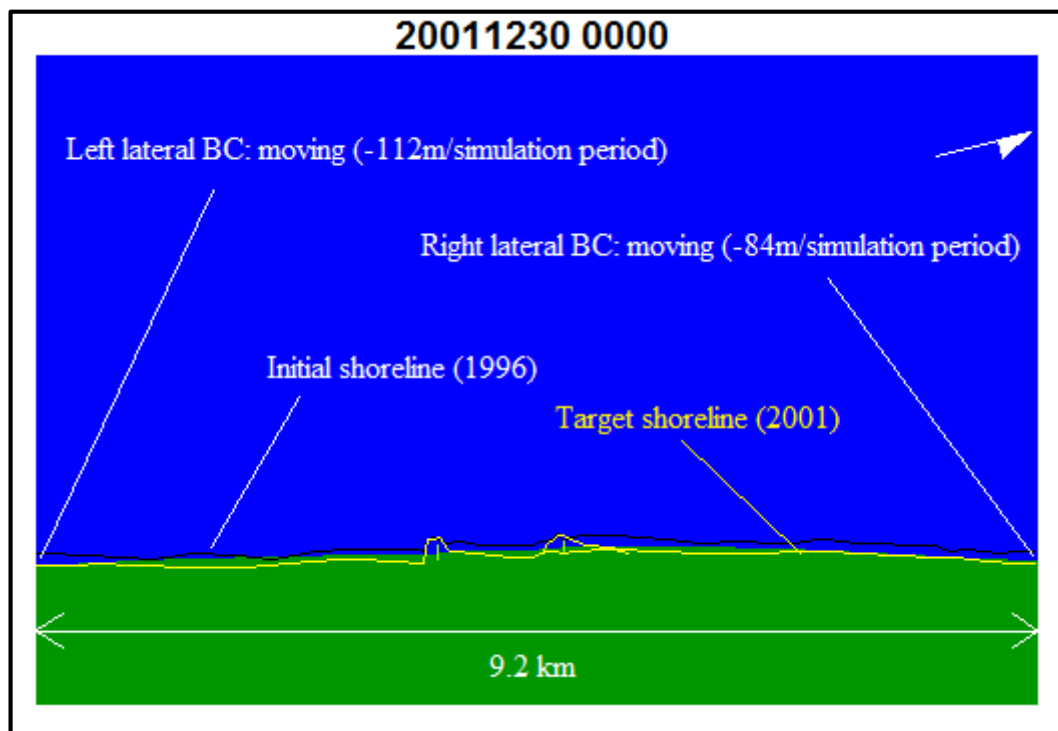
Figure 5.11.*GENESIS: lateral boundary conditions specification. The moving rates corresponds to the shift between the initial shoreline and the target shoreline. The calculated shoreline position on 30th of December 2001 (green profile) matches with the target profile (best calibration result).*

The assumption of the shoreline moving at constant rate (0.06m/day and 0.04m/day for the left and right side respectively) was a reasonable approximation of the real the asymptotic trend of the erosion velocity (the more progressed the erosion is, the slower the shoreline should move towards the equilibrium position). Nevertheless, considering that the simulation period is relatively short (5 years) the erosion rate is expected not to change so much.

5.3.4 Groin permeability

The permeability coefficient empirically accounts for *transmission* of sand through and over a groin. (Bypassing of sand around the seaward end of groins is automatically calculated by GENESIS.) (Hanson *et al.* 1991). The permeability can vary between [0; 1]. The 0 value is used for high, impermeable groin that does not allow sand to pass through or over it. A permeability value of 1.0 indicates a completely transparent groin.

In this study the permeability was assumed to be 0 for all the structures. On site visits confirm this value as a reasonable one.

5.3.5 Fine tuning and final results

The final result is presented in Figure 5.12 (a, b).
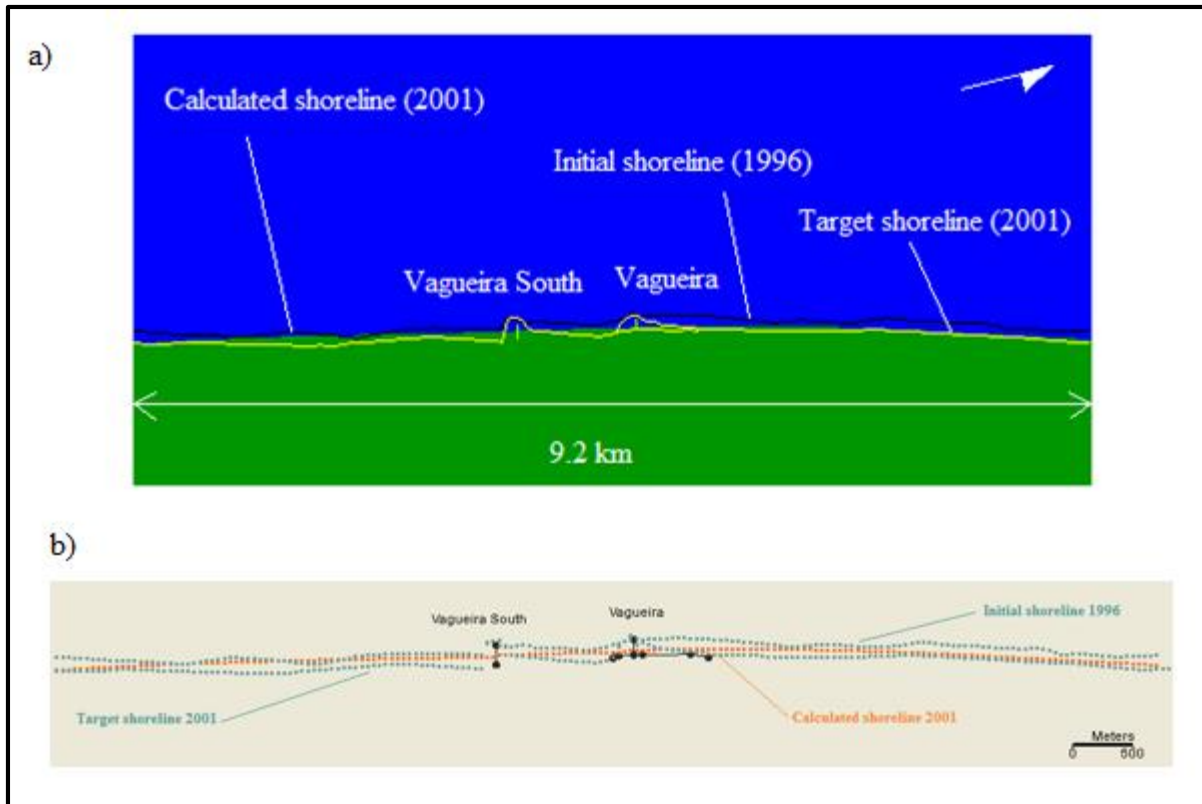
Figure 5.12. *GENESIS: final calibration result. Initial, target, and calculated shorelines are plotted on 30th of December 2001in GENESIS (a) and with more detail (b).*

The solution is close to the *target* shoreline position, with the exceptions of some anomalies in the already mentioned areas around the groins and in the stretch of coast south of *Vagueira South*. In this area, the *calculated shoreline* is further offshore than the *target shoreline*. This means that this stretch is not eroding properly. There are two possible reasons for this.

The first is related to the *offset angle* imposed as a seaward boundary condition. This value represents the wave angle amount that can be added to (or subtracted from, if negative) wave angles along the *nearshore reference line* (Hanson *et al.* 1991). This parameter allows to investigate the solution under different incoming wave direction conditions. In this study, it was used as a *fine tuning* parameter to improve calibration results. It was set equal to +5° clockwise. This small rotation was enough to improve the erosion in the in the northern stretch. It is not reasonable to use higher values, because the predominant direction of the wave climate is already contained in the wave series, as it consist of original records.

The second possible explanation is related to filling process performed to create the *continuous wave* series. The 56.6% of the missing records were of the winter maritime season and they were filled with average values (see Chapter 2, §2.2.1). Therefore, the real incoming wave heights could have been underestimated.

In order to get a sense of what would have been the calculated shoreline with higher values of wave height, the *height change factor* was used. This setting allows to multiply the wave height along the *near shore reference line* (Hanson *et al.*1991). The suggested range is [0.2-1.0] where the unit value corresponds to the unchanged wave input. The 1.5 value was chosen out of the suggested interval in order to amplify the input wave height data. The results in the southern stretch improved a lot (Figure 5.13).
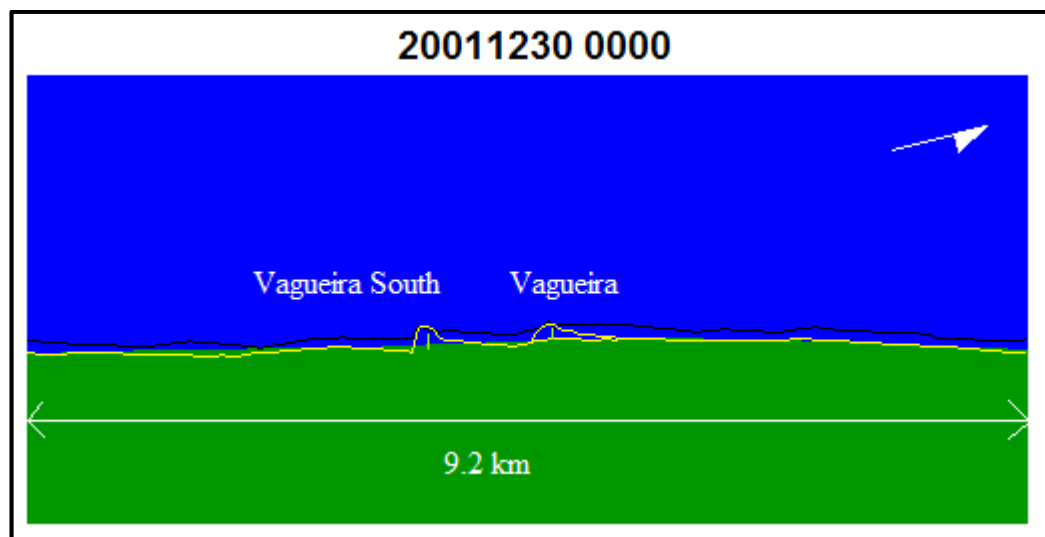
Figure 5.13. *GENESIS: amplified (1.5) wave height data at the seaward boundary improve the calibration at the southern stretch, as erosion is enhanced.*

Thought improved, the calibration of Figure 5.13 was not considered reliable because the model warnings suggested the solution could be unstable.

The best calibration results are thus the ones of Figure 5.12 (a,b). This represents the starting point for further simulations.

Chapter 6

Simulation of shoreline evolution under different scenarios

This chapter presents the simulation of shoreline evolution under different scenarios. The calibration parameters presented in Chapter 5 were used to configure GENESIS for further simulations. Starting from year 2001 the model was run up to 2011, which was assumed to be the present time reference year. Since 2011, two different future scenarios have been investigated: the *do-nothing scenario* and the *detached breakwaters protected* scenario which resulted to be the most suitable protective scheme for the project area (Chapter 1, §1.2). A detailed description of each simulation performed is presented.

6.1 Simulation up to the present time (2001-2011)

This section deals with the simulation performed in order to bring the shoreline configuration up to the present time. This was assumed to be year 2011, because the *continuous wave series* ends in this year. This was just to ensure a formal consistency with wave data, but it is not a basic requirement. In fact, the *input continuous wave series* is run in a *loop way* when the simulation period goes beyond the end of the wave series (2011). The simulation up to the present time (2001-2011) was performed in two different runs: the first run from the end of the calibration period (2001) up to 2004, and the second run from 2004 up to 2011. The reason is that in 2004 a *curved groin* was built, south of *Vagueira South* groin. The modified spatial configuration was thus considered.

6.1.1 First run: 2001-2004

This is a short time simulation (731 days); the start day is 31/12/2001 and the end date is 01/01/2004.

Spatial configuration

The spatial configuration includes three groins (*Vagueira North, Vagueira* and *Vagueira South*) and *Vagueira seawall* (Figure 6.1).
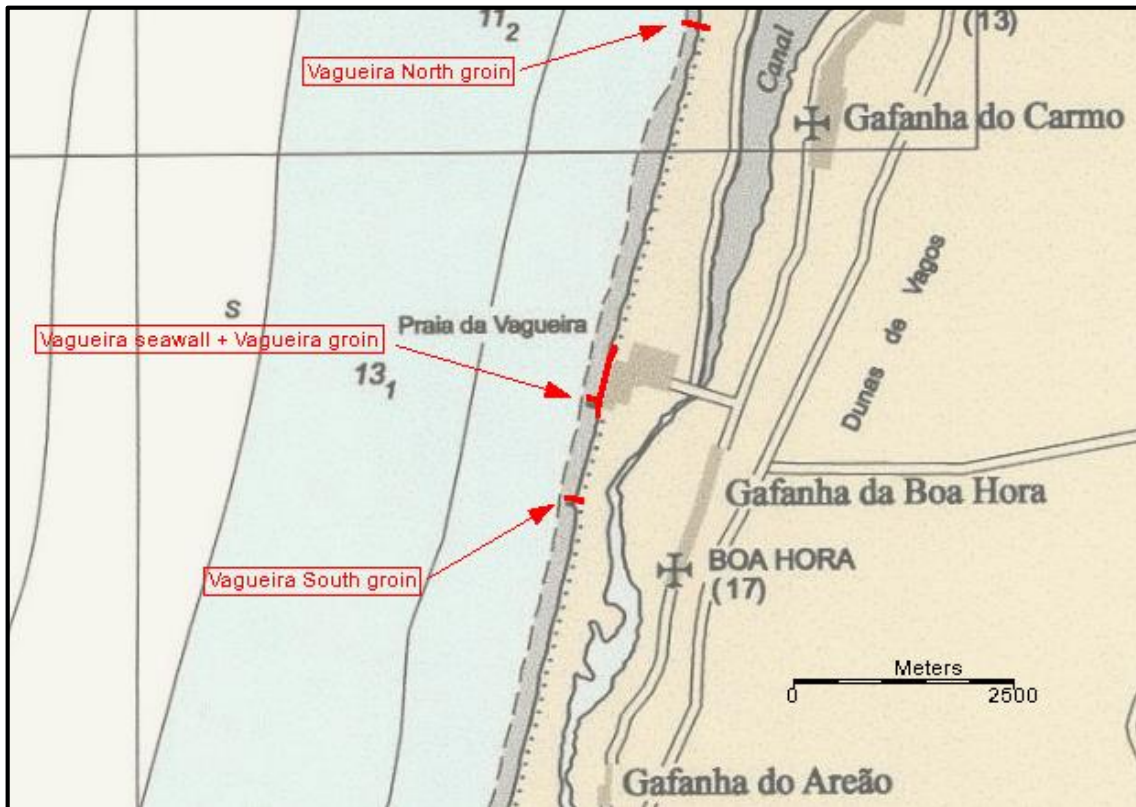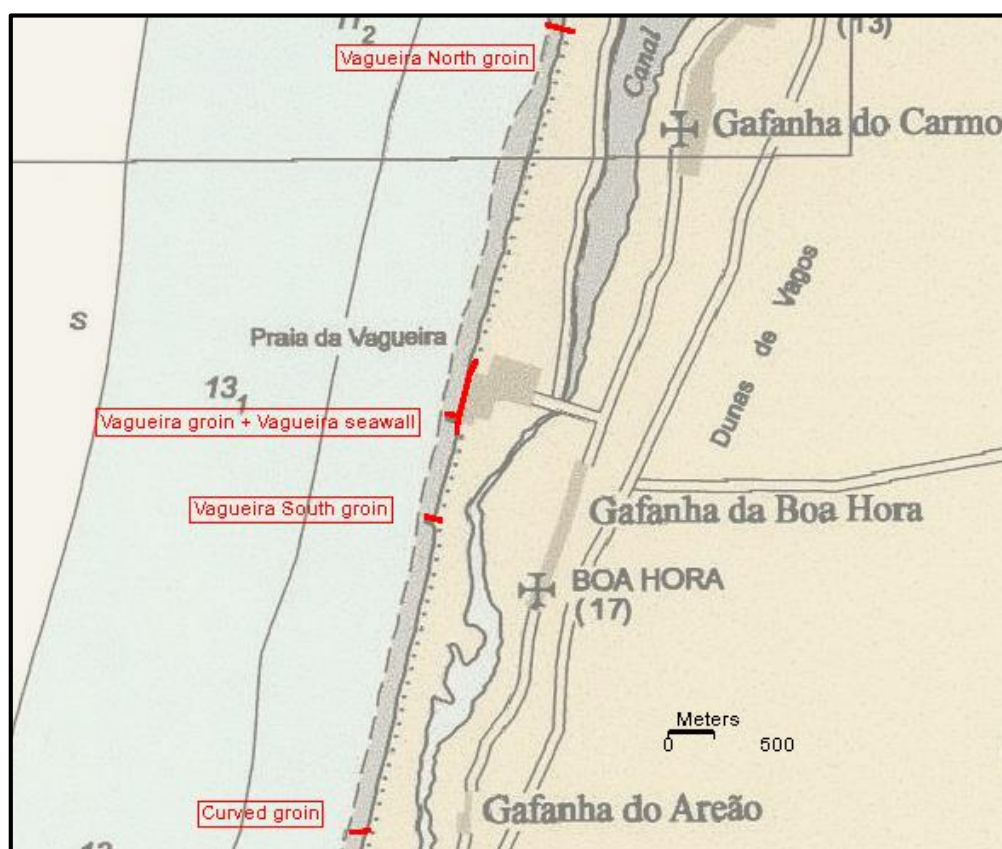
Figure 6.1. *Spatial configuration for simulation 2001-2004. The structures are placed according to the model requirements.*

Figure 6.1 shows the structures positioning according to the model requirements (groins at *Q-points*, seawall endings at *y-points*). The *Vagueira North* groin has been present at the northern boundary of the model since 1996. It was not considered during the calibration phase, due to the type of lateral boundary condition, a moving boundary with a prescribed value. Nevertheless, this groin has been hereafter considered.

Lateral boundary conditions

The lateral boundary conditions specifications were changed as shown in Figure 6.2.
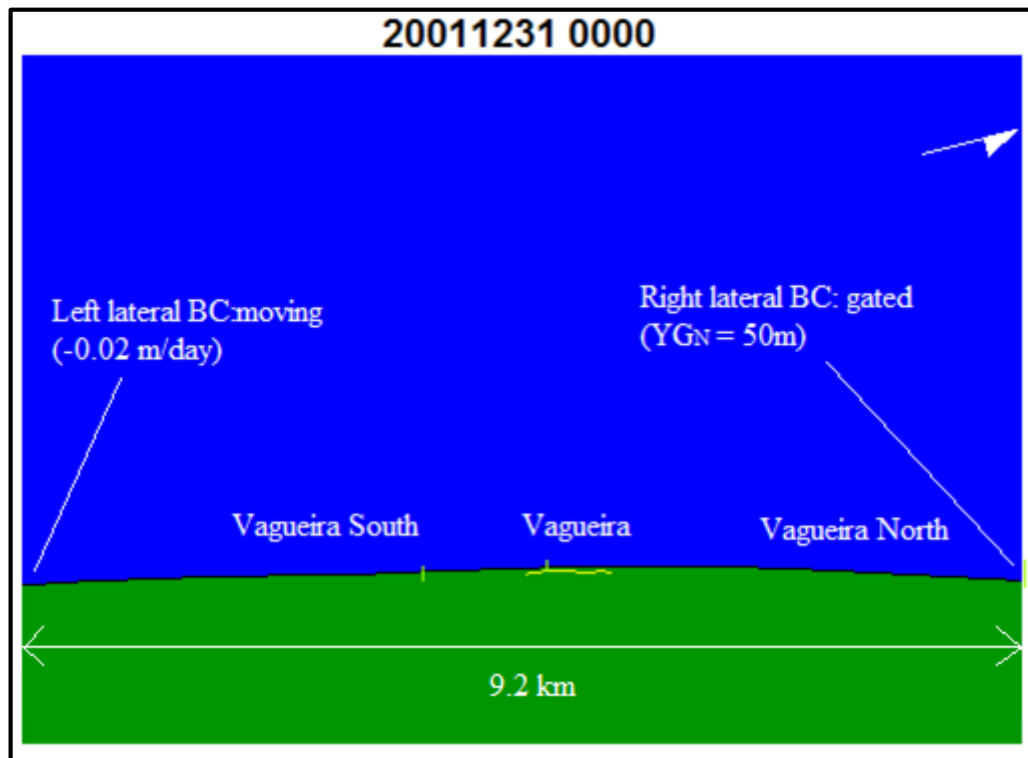
Figure 6.2. *GENESIS: lateral boundary conditions specifications, simulation 2001-2004.*

The *left* lateral boundary condition was specified as *moving* at a constant rate. In order to account for the asymptotic trend of erosion velocity, the moving rate in this simulation period was expected to be lower than the one specified in period 1996-2001, (-0.06 m/day). With reference to this, a sensitive analysis was performed on the left moving rate, to check how this parameter could influence the final result (Figure 6.3).
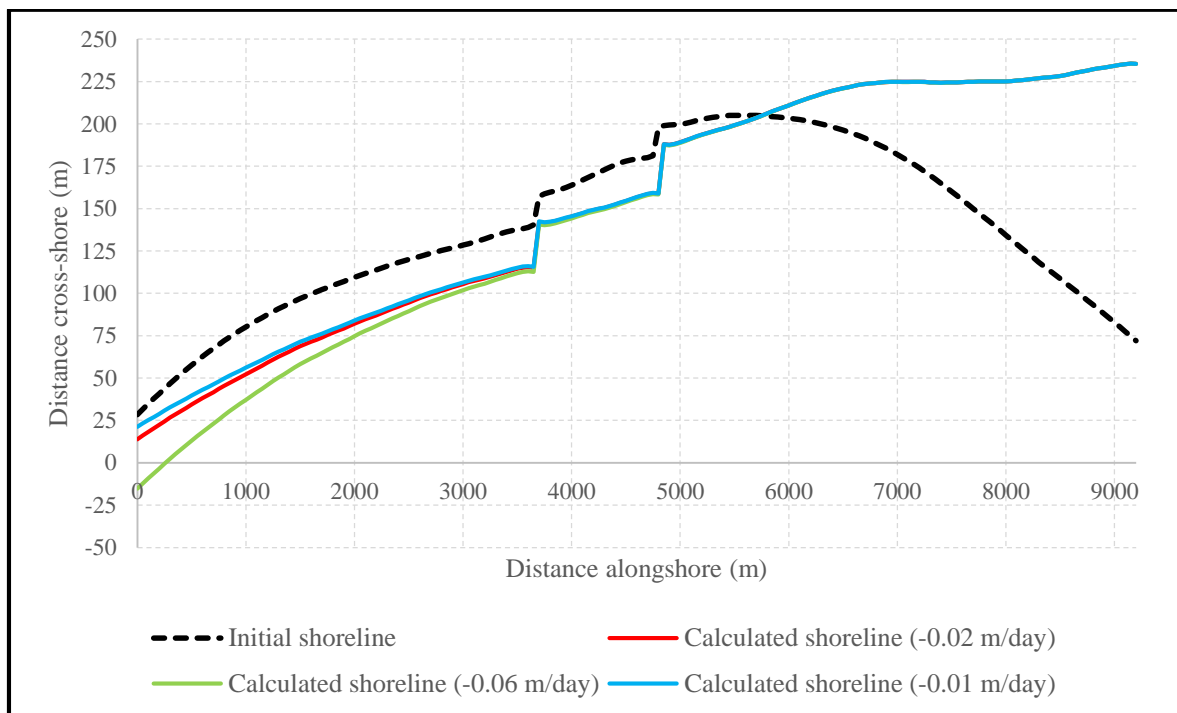
Figure 6.3. *Sensitive analysis of the moving rate at the left boundary. Starting from the initial shoreline (2001), the shoreline calculated in 2004 is plotted according to three different moving rates at the left model boundary. As the rates increases the calculated shoreline recession is enhanced. Shoreline profiles change only at the left side of the model: this is indicative of the left moving rate influence on the model.*

Figure 6.3 shows the *calculated shoreline* of 2004 resulting from three different values of the left moving rate (-0.02 m/day), -0.01 m/day and -0.06 m/day). The model resulted to be quite sensitive to this value: the three profiles are different in the left part of the grid. From the 4th km onward, the profiles coincide. The -0.01 m/day value and -0.02 m/day give very similar solution. The -0.02 m/day was definitely assumed to be a reasonable value for the simulation. Next simulation (2004-2011) will start from the *calculated shoreline* 2004.

The choice of the left moving rate (-0.02 m/day) will not affect the 2004-2011 result indeed. Irrespective of the *initial* 2004 shoreline position itself, what will change according to the *initial* shoreline, is the time needed to reach the *equilibrium position*. If the -0.06 m/day value had been used, this would have reduced the time needed to reach the *shoreline equilibrium position*. However, the *calculated shoreline position* would have been almost the same. This is related to the wave climate that is site specific. Whatever the starting point, the wave climate will drive the shoreline to the same final stable configuration i.e the *shoreline equilibrium* position.

At the extreme *right side* of the model, the *Vagueira North* groin controls the sediments entrance. A *gated* lateral boundary condition was thus specified. The amount of sediments

that can enter the model depends on the distance between the groin/jetty tip and the shoreline position at the external right side (northern) of the model (YG_{North}). Assuming that a suitable wave event (its direction is such that sediments could enter the grid from the North) occurs, the sediments are able to *bypass* the *Vagueira North* groin if YG_{North} is small compared with the groin length. This in other words means that the shoreline is very close to the groin tip. When a gated condition is specified YG must be greater than zero, so that the shoreline cannot reach the groin tip exactly, even in the extreme cases. In fact, the presence of *rip currents* prevents the up-drift shoreline position from reaching the tip of the structure.

In order to get an order of magnitude for YG_{North} historical images from *Google Earth* (Google 2011) were investigated (Figure 6.3).
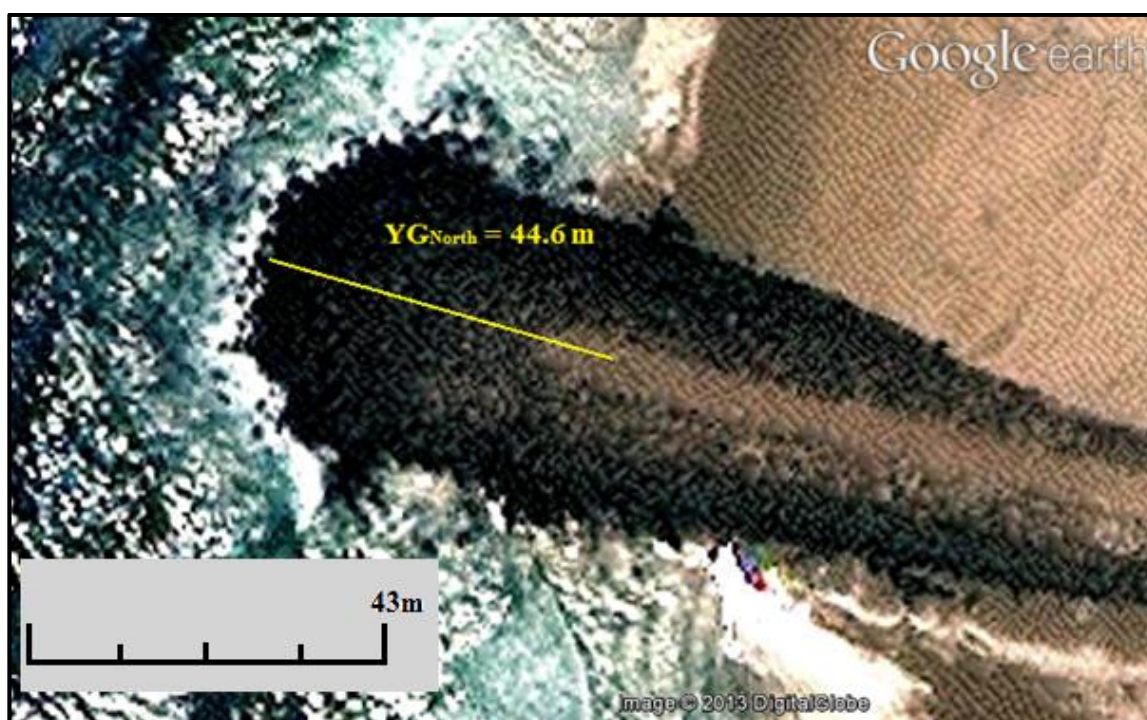
Figure 6.4. *Google Earth: YG_{North} at the Vagueira North groin on 18th of July 2010.*

Figure 6.3 refers to 18th of July 2010. The measured value is YG_{North} = 44.6m. Finally, it was approximated to YG_{North}=50m. This value resulted to be consistent with the theoretical estimation of sediments accumulation next to a groin/jetty. As a rule of thumb, it should correspond to the 20-25% of the structure length. In this case, the groin length is 290m. The resulting value is thus YG_{North}=58m, which is of the same order of magnitude of the assumed value (YG_{North}=50m).

The above considerations were done referring to year 2010, while the simulation is in 2001-

2004. This approximation is acceptable because the coastline is known not to change so much at the updrift side of *Vagueira North* groin (see Chapter 1, §1.1).

Final result

Figure 6.4 presents the final result.
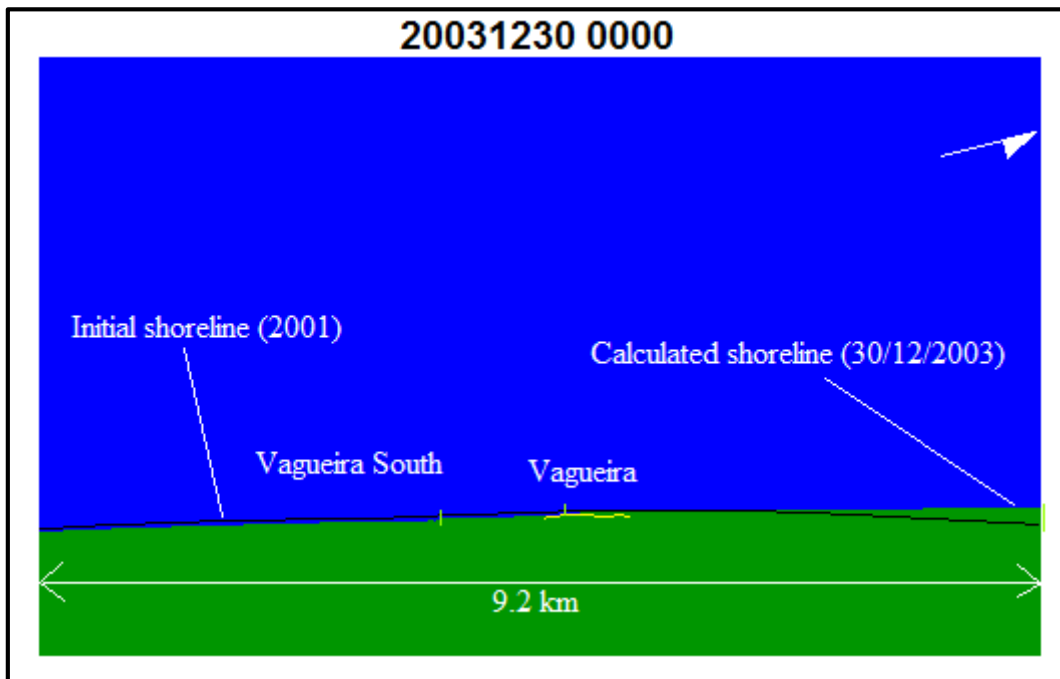
Figure 6.5. *GENESIS: final result for the simulation period (2001-2004).*

The calculated shoreline on 30th of December 2003 is indicative of the shoreline position of 2004, which will be used as *input initial* shoreline for next simulation (2004-2011).

On the right side of the model (Northern boundary), the *calculated shoreline* is further offshore than the initial one. This is consistent with the value of YG_{North} specified. As this value is small related to the groin length (290m), sediments can enter the model, driven by the north westerly wave climate, and accumulate at the down drift side of the structure. This result might be questionable as the reality confirms that the area has always been on a receding trend. Nevertheless, this simulation (2001-2004) is an *intermediate simulation* which is done only to reach the correct time for the curved groin introduction (2004). The solution will be thus adjusted in the following simulation (2004-2011) with a more suitable value for YG_{North} that is a key parameter for this model.

6.1.2 Second run: 2004-2011

This simulation is related to the time period 2004-2011. The start date is 01/01/2004 and the end date is 31/12/2011, for a total duration of 8 years (2922 days). This simulation is quite interesting because it provides the *calculated* shoreline for year 2011. On a long-term time scale, this can be assumed as present time. Besides, the *continuous wave series* ends in the same year. All these things considered it has been decided to refer to year 2011 as the present time situation. Future previsions will be made starting from the *calculated shoreline* position that results from this simulation.

Spatial configuration

In 2004 a curved groin was introduced. The spatial configuration was thus modified as shown in Figure 6.6.

Figure 6.6. *Spatial configuration for simulation 2004-2011. The structures are placed according to the model grid requirements.*

Figure 6.6 shows the adjusted structures positioning according to the model grid requirements (groins at *Q-points*, seawall endings at *y-points*). The real L-shaped curved structure was modelled with a straight line extending from the groin tip up to the groin root inland

(*Alternative n° 1,* Figure 6.7). Another possibility could have been to model the structure considering its projection on the model grid axes (*Alternative n°2*, Figure 6.7).
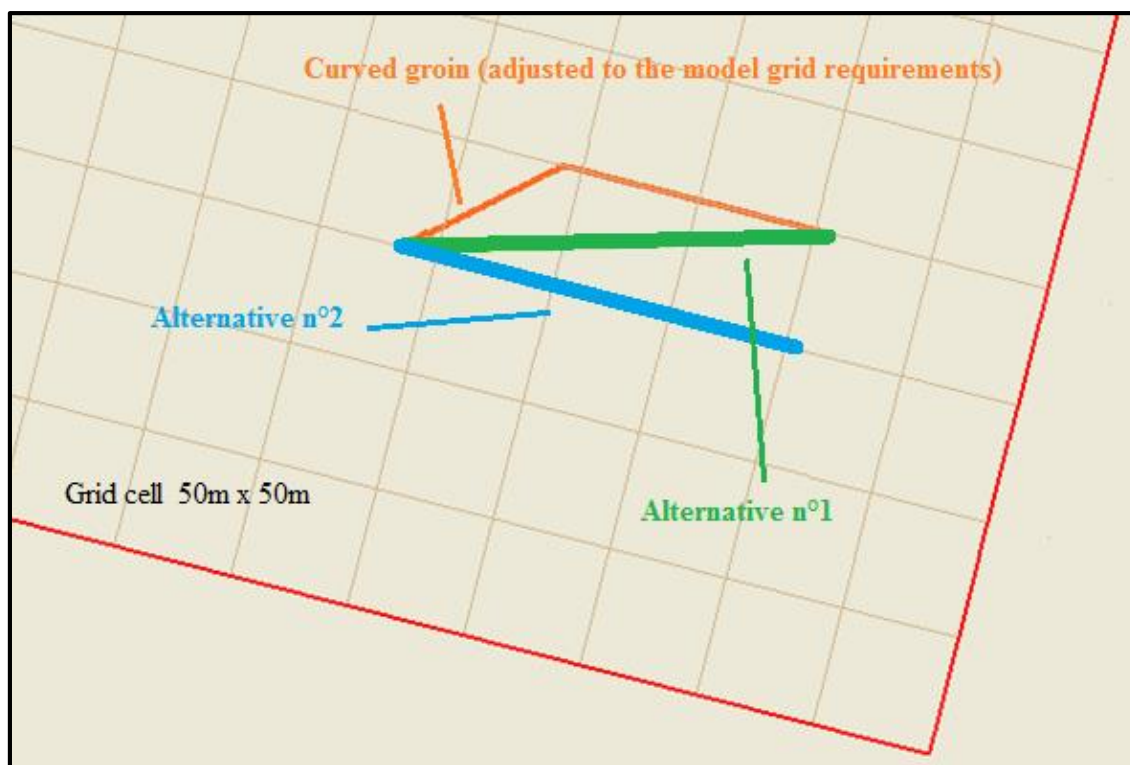
Figure 6.7. *Modelling the curved groin: comparison of alternative solutions.*

Attention was paid in reproducing the real groin tip position and the down drift sheltered area created by the structure. In these terms, the two alternatives are equivalent: they both respect the real groin tip position and they both cover the same down drift shadow area of the structure. The only difference between the two solutions is the orientation: *alternative n°1* is better than *alternative n°2*. The original structure was born as a compromise between the need of accumulating sediments updrift, and the need to ensure some bypassing along this structure from the moment it was introduced. The compromise finally resulted in a structure which is a curved groin. *Alternative n°1* was thus chosen to model the curved groin, as it is slightly inclined down drift. This models in a better way the left boundary.

Lateral boundary conditions

Figure 6.8 shows the lateral boundary conditions used for this simulation.
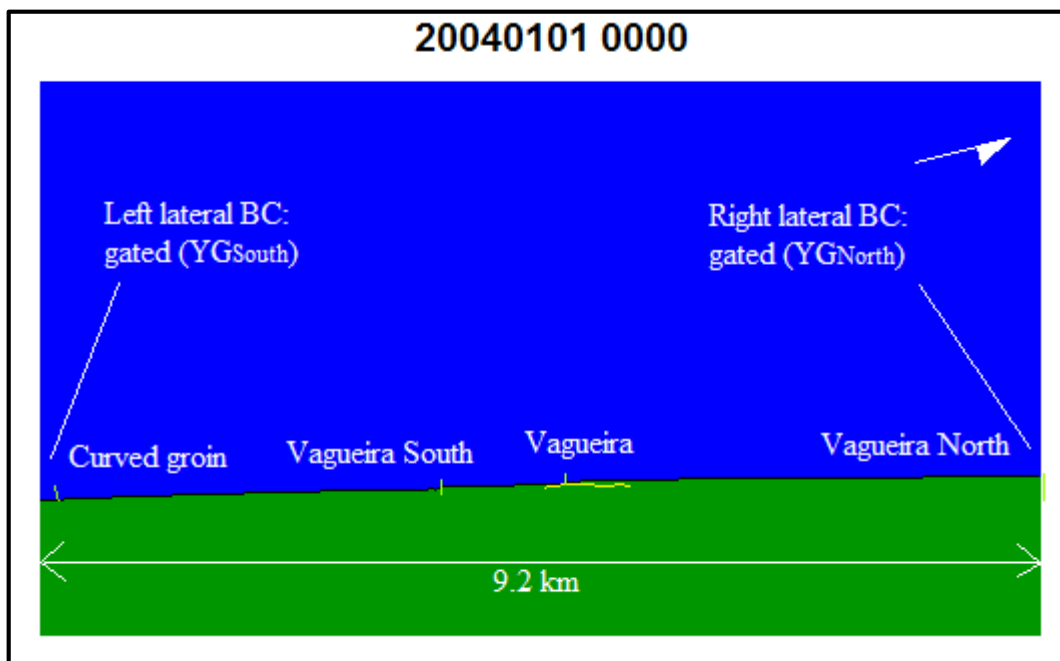
Figure 6.8. *GENESIS: lateral boundary condition specifications for simulation 2004-2011.*

As the curved groin is now present within the stretch, a *gated* boundary condition was specified also at the left boundary. The driving parameter is YG_{South}: it represents the distance between the shoreline and the groin tip outside the left model boundary. The amount of sediments that can enter/exit the model at the left boundary depends on YG_{South}. As well as YG_{North} this parameter was fundamental in the modelling. A sensitive analysis was thus performed in order to investigate how these two parameters influence the model behaviour.

Considerations on YG_{North}-

In simulation 2001-2004 the YG_{North} value was derived basing on a rough estimation done with historical images (§6.1.1). The importance of this parameter required further investigations. If the shoreline position in 2011 had been available, this parameter could have been *calibrated* and the model could have been *verified* for the present situation (2011). On the time the study was carried out, this was not the case. Nevertheless, the idea was to find a more accurate estimation for this parameter: a variation interval was derived based on the following considerations.

It was assumed that for the simulation period 2004-2011 a *moving* lateral boundary condition equal to the one set in the calibration phase (0,04 m/day) could have been used. Under this assumption the shoreline would have recede at extreme rate. The resulting recession length was calculated with expression (6.1).

$$(0.04 \, m/day)x(2922 \, days \, of \, simulation) = 117m \qquad (6.1)$$

The maximum value of YG_{North} ($YG_{North, \, MAX}$) corresponds to the value of YG_{North} that can produce a shoreline recession at the right lateral boundary equal to the one defined by the (6.1).

A similar consideration was done, to derive $YG_{North, \, MIN}$. It corresponds to the value that could produce a *calculated shoreline* in 2011, almost coincident to the *initial* one (2004) i.e many sediments could enter the model from north, preventing shoreline recession in that area.

Some tests were performed to derive $YG_{North, \, MAX}$ and $YG_{North, \, MIN}$.

$YG_{North, \, MIN}$ was found to be equal to 50m. This value complies with the abovementioned requirements, as shown in Figure 6.9.
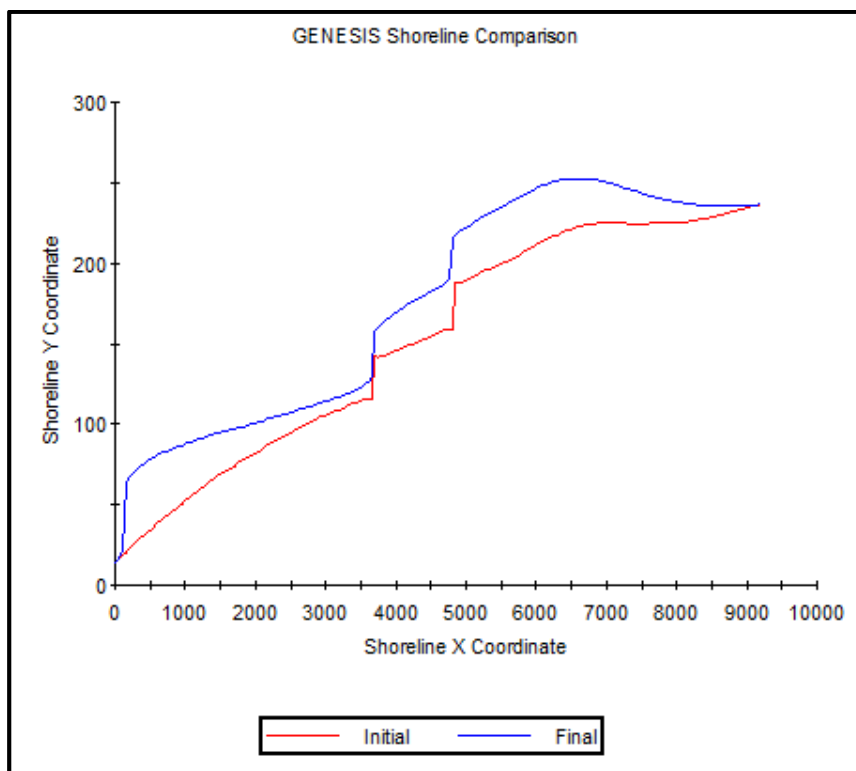
Figure 6.9. *GENESIS: Getting $YG_{North,MIN}$ value. Initial shoreline (2004) and final shoreline (2011) coincide at the right model boundary.*

Figure 6.9 refers to boundary conditions parameter, YG_{South}=150m and YG_{North}=50m. Focusing on the right model boundary (*shoreline X coordinate=9200m*), the *initial* (2004) and *final* (2011) shorelines coincide. This confirmed $YG_{North, \, MIN}$ =50m to be the correct estimate

for the minimum inferior limit of YG_{North} variation interval. In terms of sediments amount entering the grid it corresponds to the *maximum* value (the less is YG, the more sediments entering, the less the erosion).

The $YG_{North, MAX}$ value was derived after some tests. The criterion was to find a value that provides a recession length of the same order of magnitude of 117m (see expression 6.1). For the time being, the value for YG_{South} is 150m. This parameter will be discussed later.

Figure 6.10 shows the result derived with YG_{South}=150m and YG_{North}=100m,
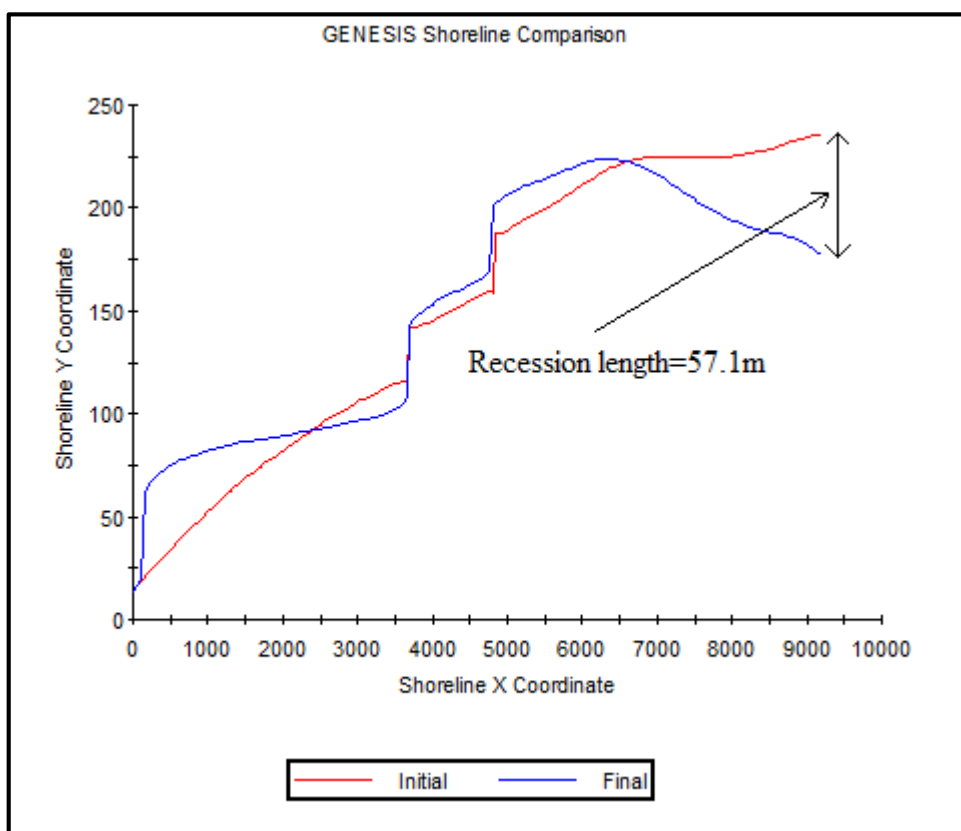
Figure 6.10. *GENESIS: initial (2004) and final (2011) shoreline calculated with YG_{South}=150m and YG_{North}=100m. The resulting recession length at the right boundary (57.1m) is not complying with the required order of magnitude (117m).*

Figure 6.10 shows the initial (2004) and final (2011) shorelines plot. The resulting recession length at the right boundary (57.1m) is not complying with the required order of magnitude (117m). The YG_{North} value must be increased in order to derive a higher recession length at the right boundary.

Figure 6.11 shows the results obtained with YG_{South}=150m and YG_{North}=140m.
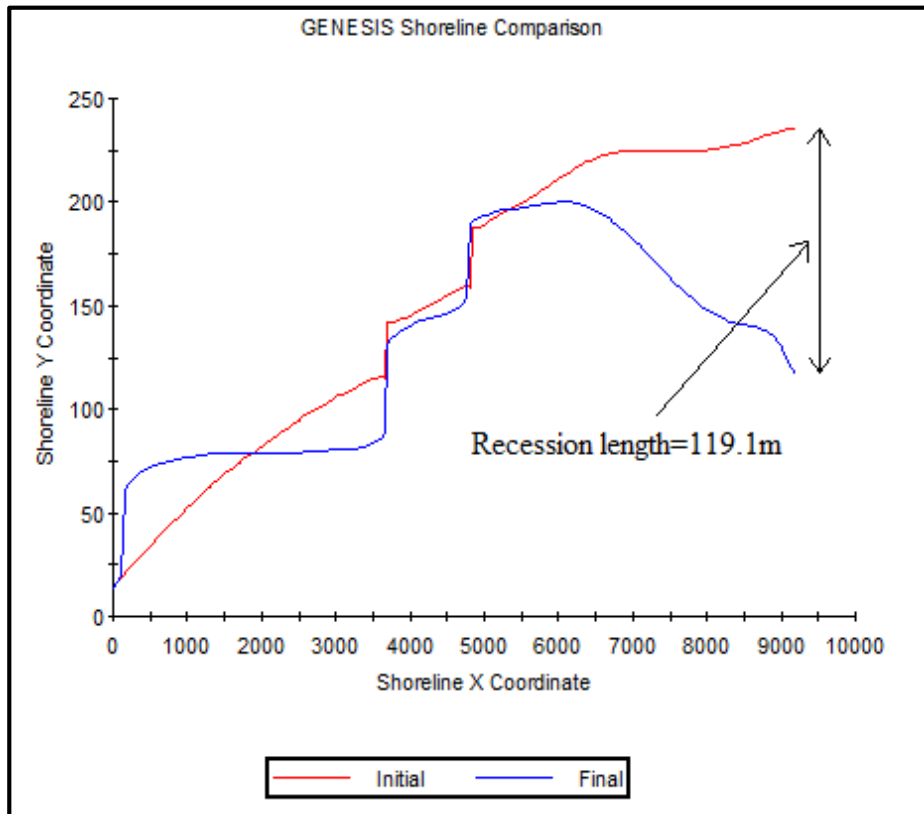
Figure 6.11. *GENESIS: initial (2004) and final (2011) shoreline calculated with YG$_{South}$=150m and YG$_{North}$=140m. The resulting recession length at the right boundary (119.1m) is of the same order of magnitude of the reference value (117m).*

Figure 6.11 confirmed that the YG$_{North}$=140m value used for this simulation is a correct estimate of YG$_{North, MAX}$. In fact the resulting recession length (119.1m) is of the same order of magnitude of the reference value (*extreme recession length*=117m).

The variation interval for YG$_{North}$ is thus:

$$50m < YG_{North} < 140m \tag{6.2}$$

The minimum and maximum limits were derived considering very extreme conditions (absent and extreme erosion at the right model boundary, respectively). However, it gives a broad orientation on the best YG$_{North}$ value that can be assumed for this simulation.

In order to definitely fix a value for YG$_{North}$, images from *Google Earth* were investigated. The acquisition date is 18/7/2010, (Figure 6.12).

Figure 6.12. *Google Earth: distance from the Vagueira North groin tip and the shoreline position at the down drift side of the structure on 18th of July 2010.*

Figure 6.12 shows the distance between *shoreline position* at the down drift side of the *Vagueira North* groin and the groin tip, on the 18th of July 2010. The measurement is just a broad estimation, as the shoreline position is affected by the tidal range variation. With reference to this, attention was paid in considering the *wet sand profile* as reliable indicator of shoreline position on that time.

The idea was to relate this distance with a value of YG_{North}, hereafter referred to as $YG_{North, Google}$. The $YG_{North,Google}$ value should be such that the distance between the groin tip and the *calculated shoreline* of 2011 is approximately of the order of magnitude of 140m. This was a reliable condition, because at present time (referred to as 2011 in the modelling) the shoreline at the down drift side of the northern groin is known to be eroding.

After some tests $YG_{North,Google}$ value was found to be equal to 120m. This value gave a *calculated shoreline* 2011, which was shifted 144 m landward from the *Vagueira North* groin tip. This is the same order of magnitude of the estimate derived from *Google Earth* (140m, see Figure 6.12). Figure 6.13 shows the details.
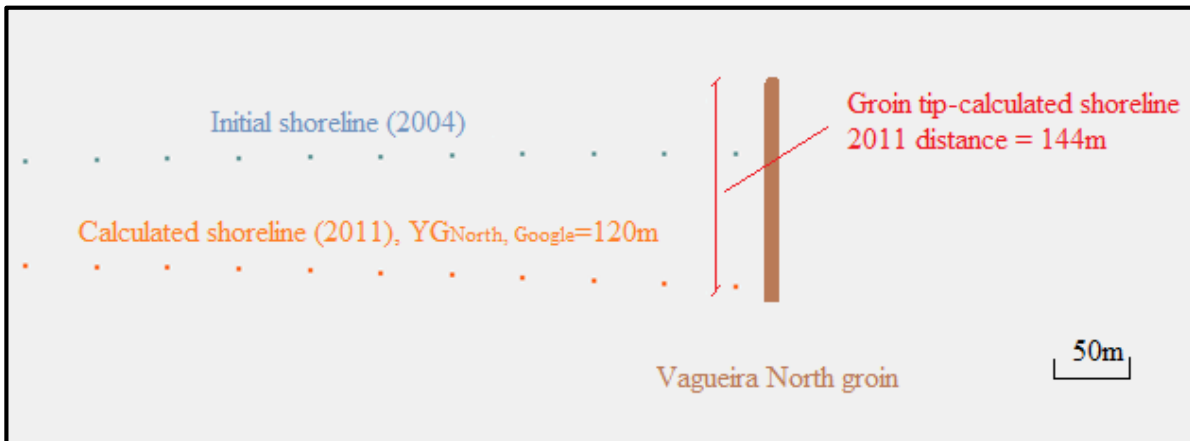
Figure 6.13. *Vagueira North groin detail: the distance between the calculate shoreline 2011(YG$_{North,Google}$ =120m) and the groin tip is 144m. The order of magnitude is the same of the estimate derived from Google Earth images (140m).*

Figure 6.13 confirms that YG$_{North, Google}$=120m is a reliable value for YG$_{North}$ parameter.

In conclusion, four simulations were performed in order to get a reliable value for YG$_{North}$. These simulations lead to the following results:

- a variation interval: 50m<YG$_{North}$<140m derived under extreme assumptions (the less and the most receded scenario, respectively);

- a reference value: YG$_{North,Google}$= 120m thought being affected by many approximations (estimation shifted in time, adjusted position for the north groin, influence of the tidal range in *Google Earth* images);

All these things considered it was assumed YG$_{North}$= 100m. This value corresponds to the mid-range value of the variation interval and it is close to the *Google Earth* estimation (YG$_{North, Google}$= 120m).

YG$_{North}$ was confirmed to be a key parameter, as it controls the sediments entrance within the model domain.

Considerations on YG$_{South}$

YG$_{South}$ resulted to be of secondary importance respect to YG$_{North}$ The reason is that sediments are driven by the input wave climate, north-westerly directed. Consequently, sediments are more likely to *leave* from the southern boundary, rather than *enter* the model there.

Several tests were performed in order to test the influence of YG$_{South}$ on the model results.

The simulations refer to the already set value for YG_{North} (100m).

Figure 6.14 shows the results of the *calculated shoreline position* in 2011, according to different values of YG_{South}.
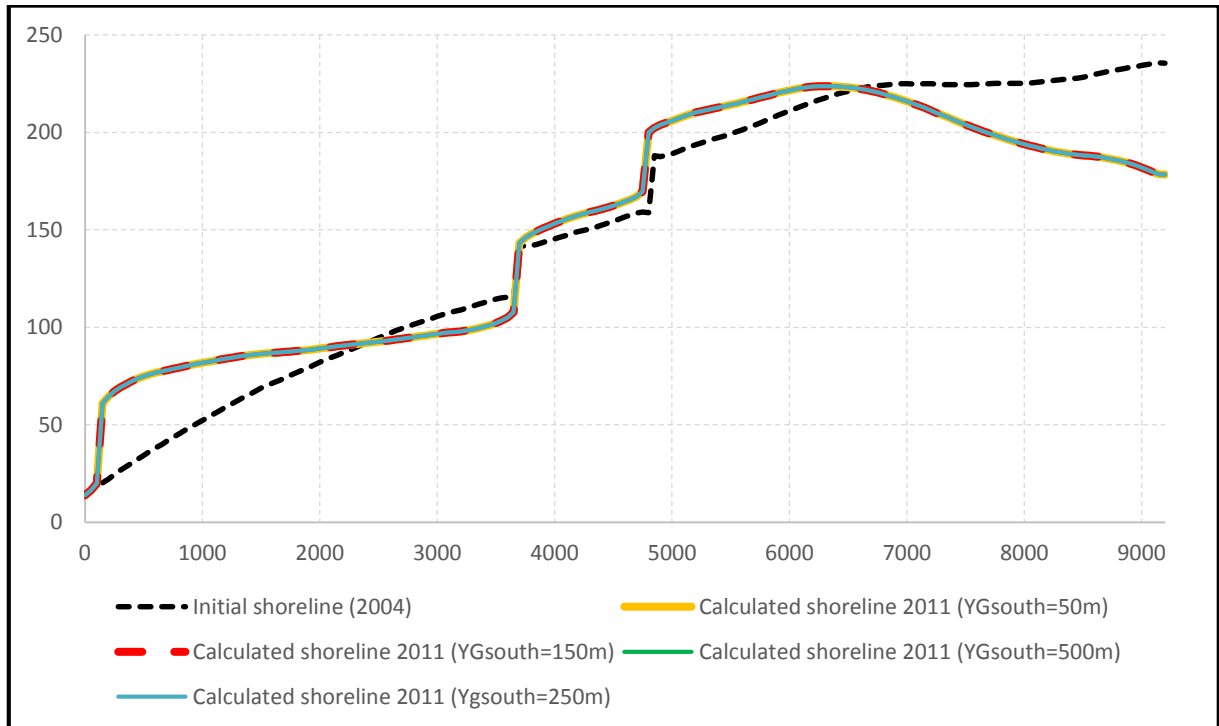
Figure 6.14. *Calculated shoreline in 2011, according to different values of YG_{South}. As the YG_{South} value changes, the profiles remain the same; this indicates the zero influence that this parameter has on the model.*

Figure 6.14 presents the *ccalculated shoreline* in 2011, according to different values of YG_{South}. Although YG_{South} value changes, the profiles remain the same (even for very high and low values, YG_{South}=500m, YG_{South}=50m respectively). This confirms that this parameter is not influencing the model results. That being so, whatever value could be assumed as reasonable. The YG_{South}=150m was definitely chosen. This value was derived from *Google Earth* images on the 18th of July 2010. Figure 6.15 shows a broad estimation of YG_{South} at the *curved groin* location.
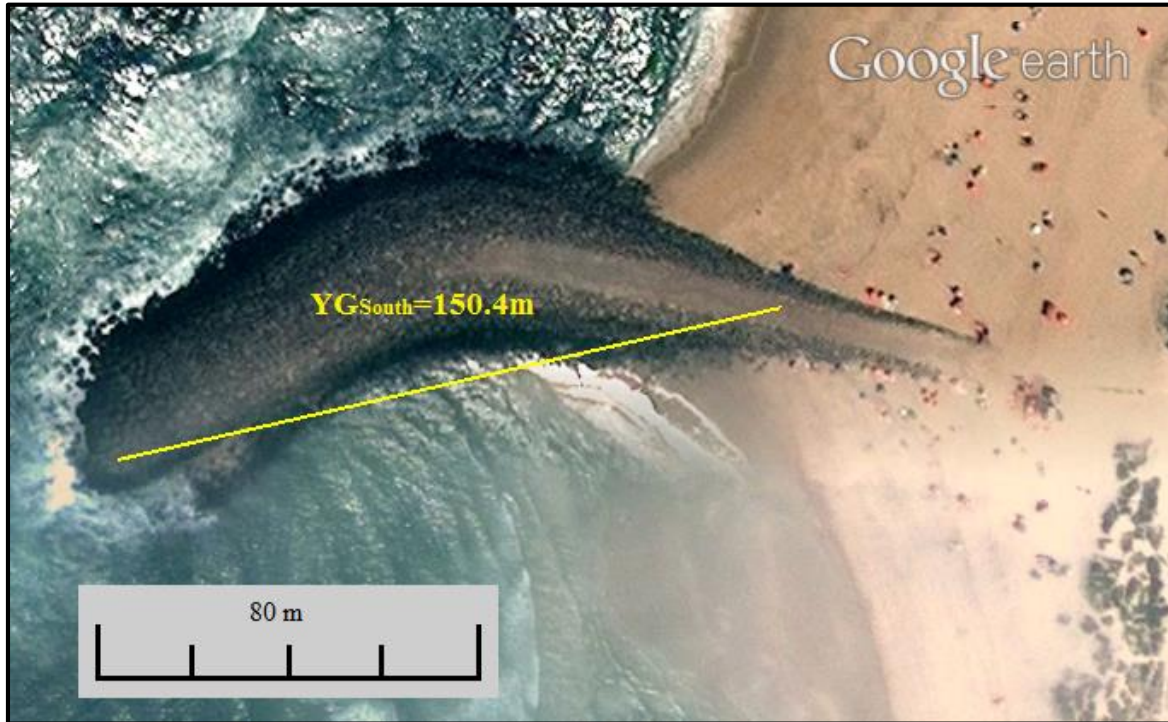
Figure 6.15. *YG$_{South}$ value broad estimation, from Google Earth images. Acquisition date is 18th of July 2010.*

Figure 6.15 shows an indicative value for YG$_{South}$. This estimate is affected by the tidal range variation, shift in time (acquisition time does not refer to year 2011). Thought being affected by these approximations, this value was chosen for the simulation without any restrictions, as it was proved not to influence the model result at all.

Final result

Figures 6.16 (a,b) show the final result (YG_{North}= 100m, YG_{South}=150m).
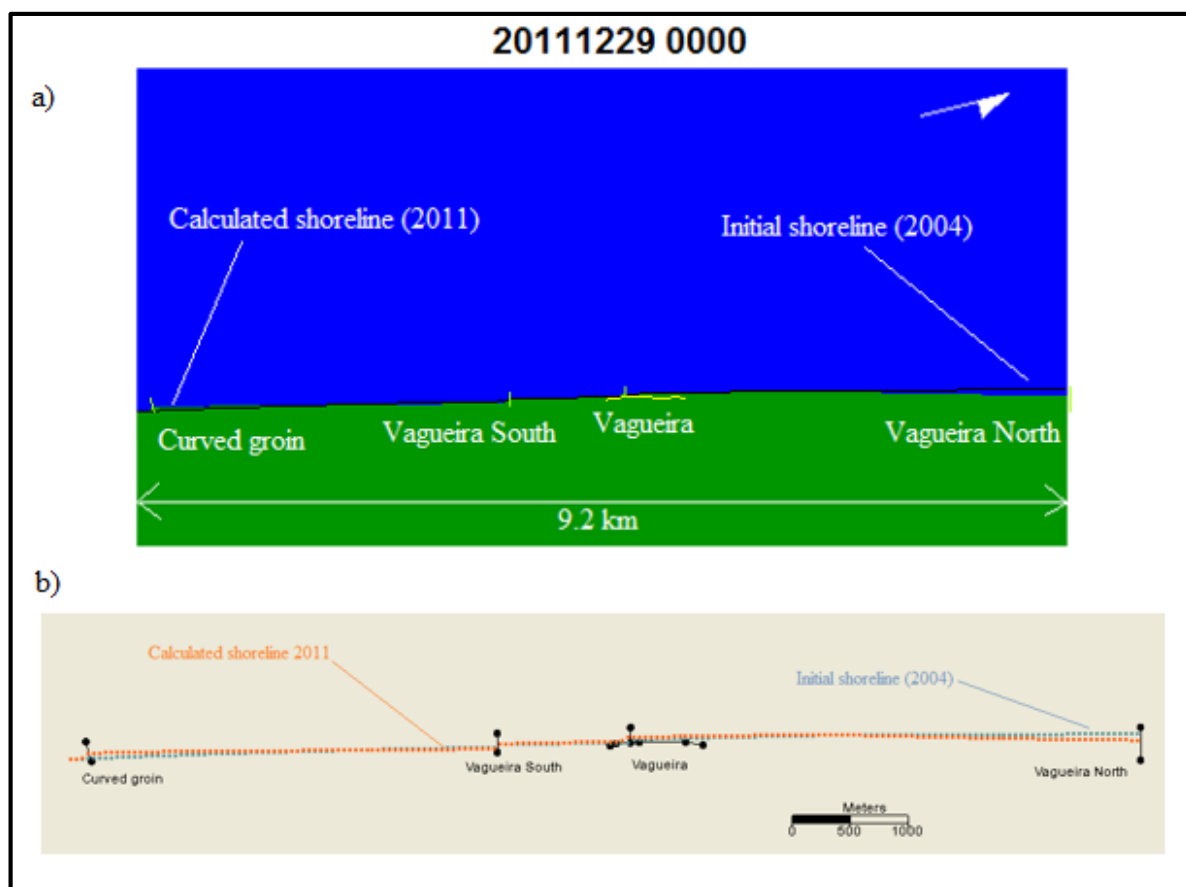
Figure 6.16. *Final result: the calculated shoreline in 2011 already indicates an erosion trend in the northern stretch (a), this recession is of the order of 30m near to the Vagueira North groin (b).*

Figures 6.16 (a,b) show the model result for the reference time situation (2011). The results were consistent with what is known to be the present time situation in this coastal stretch. The coastal stretch inspection with site visits confirms that in the northern stretch, in Costa Nova beach, erosion is a visible process. In the southern stretch, the *curved groin* is still accumulating sediments in the updrift side. However, simulations show that those structures will not be enough to protect the coast in the future.

LIDAR data were available only after. The *calculated shoreline* 2011 was compared with the shoreline position resulting from a LIDAR survey. Figure 6.17 shows the comparison.
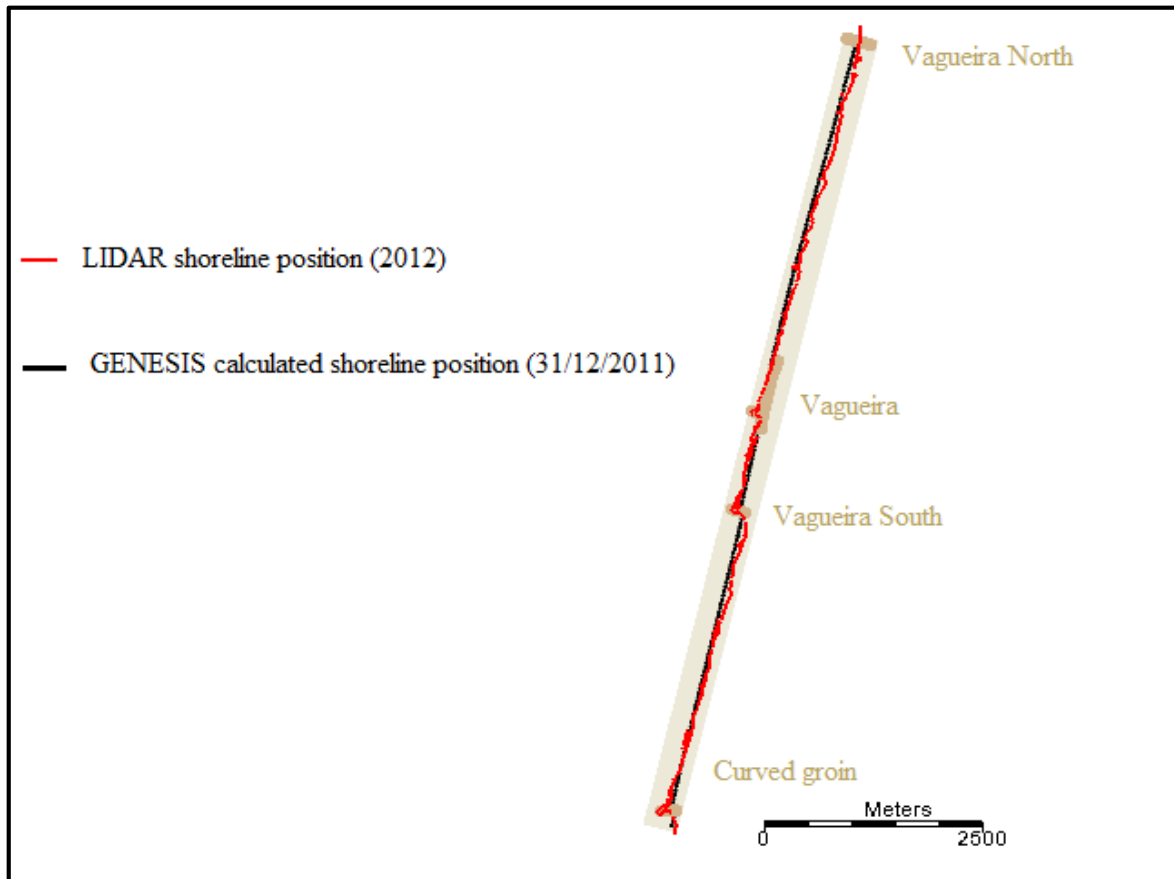
Figure 6.17. *Comparison between GENESIS calculated shoreline position on 31/12/2011 and the LIDAR shoreline position in 2012. The two profiles are very close to each other, this is indicative of the reliability of the present simulation and the future investigations that will start from the calculated shoreline 2011.*

Figure 6.17 definitely proved that the very final *calculated shoreline* (end date of simulation is 31/12/2011) is consistent with the shoreline position of 2012 derived from LIDAR survey.

This is an important result because the future scenarios will be investigated starting from the *calculated shoreline* 2011, which was proved to be very close to the real shoreline position, as shown in the very detailed LIDAR survey. It must be said that LIDAR data were given on a 2m square grid and the data are continuous from the offshore into dry land (no interpolation is needed). This confirms the shoreline starting position, important for the future scenarios (see §6.2, §6.3).

6.2 Do-nothing scenario

This section presents future simulation, from 2011 onward, assuming that *no interventions* will be carried out in the coast (*do-nothing* scenario). The purpose of this simulation is to find out the coastline will evolve, the *equilibrium shoreline position* and the time needed to reach it. The entire input wave series (from 17/07/1996 to 31/12/2011) was used to cover the longest simulation period. When the simulation period is longer than the input wave data (15 years series) the model runs the wave data in a loop way. The start date of simulation is 31/12/2011, the *initial shoreline* for simulation is the *calculated 2011 shoreline* (see §6.1.2). The end date of simulation is the unknown (*equilibrium shoreline position*). The idea was to follow a step-by-step procedure: starting from 31/12/2011 future shoreline positions were calculated with a time variation of five years.

Spatial configuration

The *do-nothing* scenario implies no change in the coastal defence scheme. The spatial configuration is thus equal to the present time configuration of the costal stretch. The structures positioning is the same of simulation 2004-2011 (§6.1.2). Figure 6.18 shows the spatial configuration for completeness.
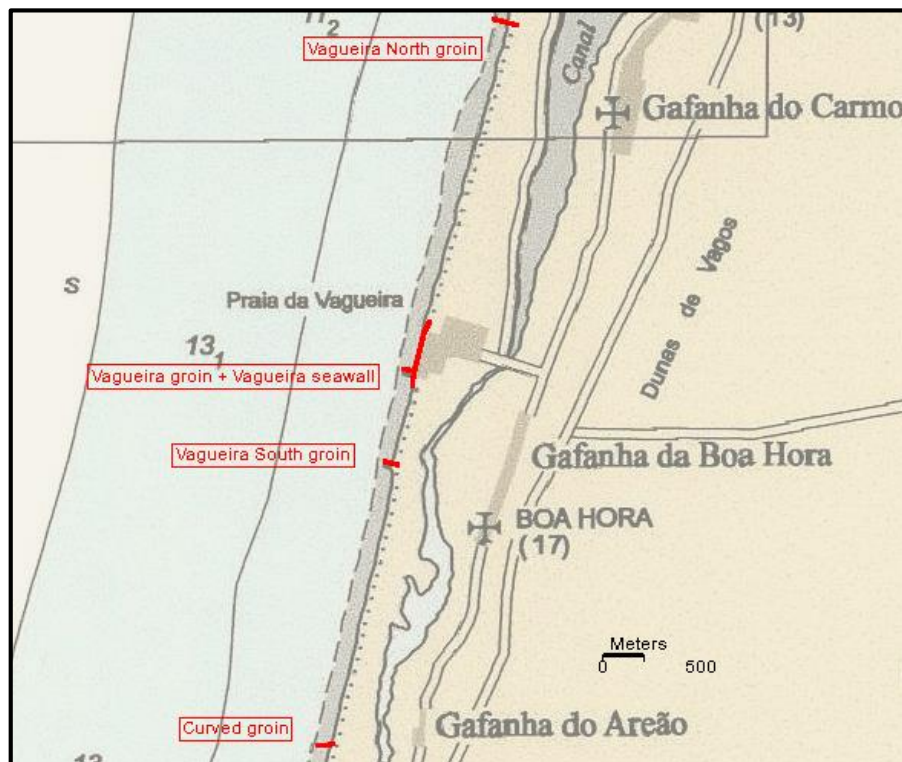
Figure 6.18. *Spatial configuration for the do-nothing scenario simulation. The structures are placed according to the present time situation on the stretch; their positions coincide with the ones of simulation 2004-2011.*

<u>Lateral boundary conditions</u>

The lateral boundary conditions are the same of simulation 2004-2011 (see §6.1.2), as shown in Figure 6.19.
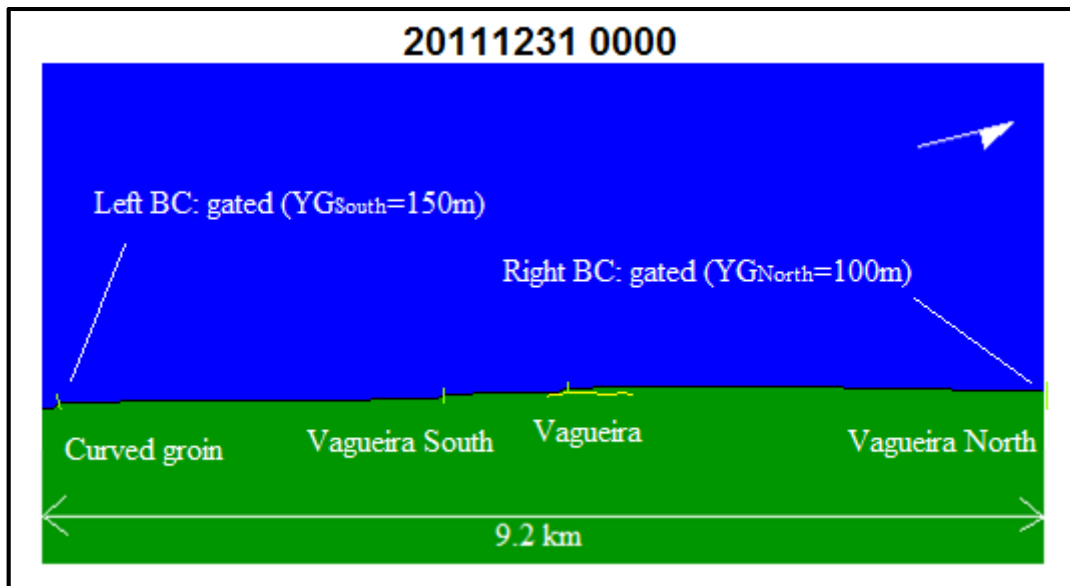
Figure 6.19. *Lateral boundary condition specifications for the do-nothing scenario simulation. Conditions refer to the present time situation along the coast. The YG values at both sides are indicative of the present time sediments amount, which is entering (right side), and leaving (left side) the coastal stretch.*

Figure 6.19 show unchanged lateral boundary conditions respect to simulation 2004-2011. These YG values resulted to be consistent with the present time amount of sediments, which is entering (right side) and leaving (left side) the coastal stretch. YG_{South} has no influence on the model behaviour. On the other hand, YG_{North} was confirmed to be the key parameter of the model, as it regulates the flux of sediments into the coastal stretch. Due to this uncertainty, the model was run with more than one value of YG_{North}. Two different types of simulation were performed. The *first type* uses the value for YG_{North} (100m). These simulations are hereafter called *calibrated simulations*. The term *calibrated* indicates that the amount of sediments entering from North (right boundary) is equal to the present time situation (see §6.1.2). The *second type* of simulations, hereafter referred to as *extreme simulations*, uses a very high value for YG_{North} ($YG_{North}=200m >> YG_{North, MAX}=140m$). This high value was assumed to be enough, in order to ensure *no sediments entering* the model, from the northern (right) boundary. These two types of simulations provide a more detailed knowledge of what could be this stretch of coast in the future if no further interventions are carried out.

<u>Calibrated simulations (YG$_{North}$=100m)</u>

The *calculated shorelines* indicate the coastal stretch evolution under the assumption that the amount of sediments arriving from north will remain the same as at present time. Figure 6.20 shows the *calculated shoreline* into the future at intervals of five years.
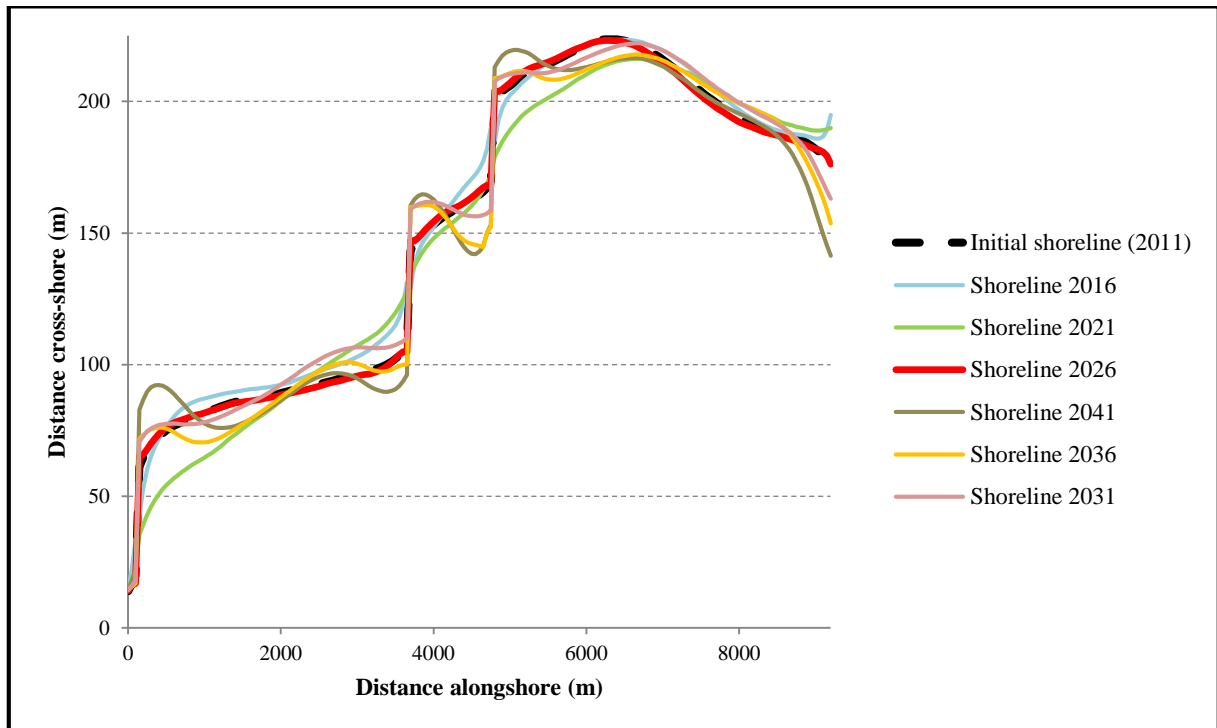
Figure 6.20. *Do-nothing scenario. Calibrated simulations results. The equilibrium shoreline position is reached in 2026. This profile coincides with the initial shoreline (2011). This is related to YG$_{North,}$ which controls the sediments entrance at the northern boundary.*

The *initial* (2011) and the *calculated* 2026 shoreline almost coincide. At present time, it is known that the coastline is eroding, but: after 15 years (2026), the shoreline returns to the *initial* position. This is explained by the YG$_{North}$ value used for this simulation (YG$_{North}$=100m). As shown before, this value controls the amount of sediments entering from north. In the present simulation, the flux of sediments is enough to feed (compensate) the potential long shore transport. The compensation is such that after 15 years the shoreline is almost in the *initial* position.

The key point is that, the future behaviour of this coastal stretch depends directly on the amount of sediments that can enter at the northern boundary. If this value is high enough, the coastline will not face severe problems, but in case of sediments shortage at north, the consequences will be drastic. *Extreme simulations* consider this possibility.

<u>Extreme simulations (YG$_{North}$=200m)</u>

These simulations were done considering a very high value of YG$_{North}$ (YG$_{North}$=200m $\gg$ YG$_{North, MAX}$=140m). This value was considered high enough so that no sediments could enter the model from the northern boundary. The aim of these tests is to investigate what could be the coastal stretch in case of sediments shortage. The limit is that the shortage of sediments cannot be exactly estimated i.e there was no control on the relation between YG$_{North}$ and the sediments rate entering the model. However, considering that the *Vagueira North groin* length is of 285m and considering that YG$_{North}$=200m it can be reasonably assumed that *no sediments* are entering the stretch. The YG$_{North}$ is very close to the groin length; consequently, the shoreline at the up drift side of the structure is so far from the groin tip that *any bypassing* process would be prevented. This is the *extreme* condition assumed for these simulations. Figure 6.21 shows the results.
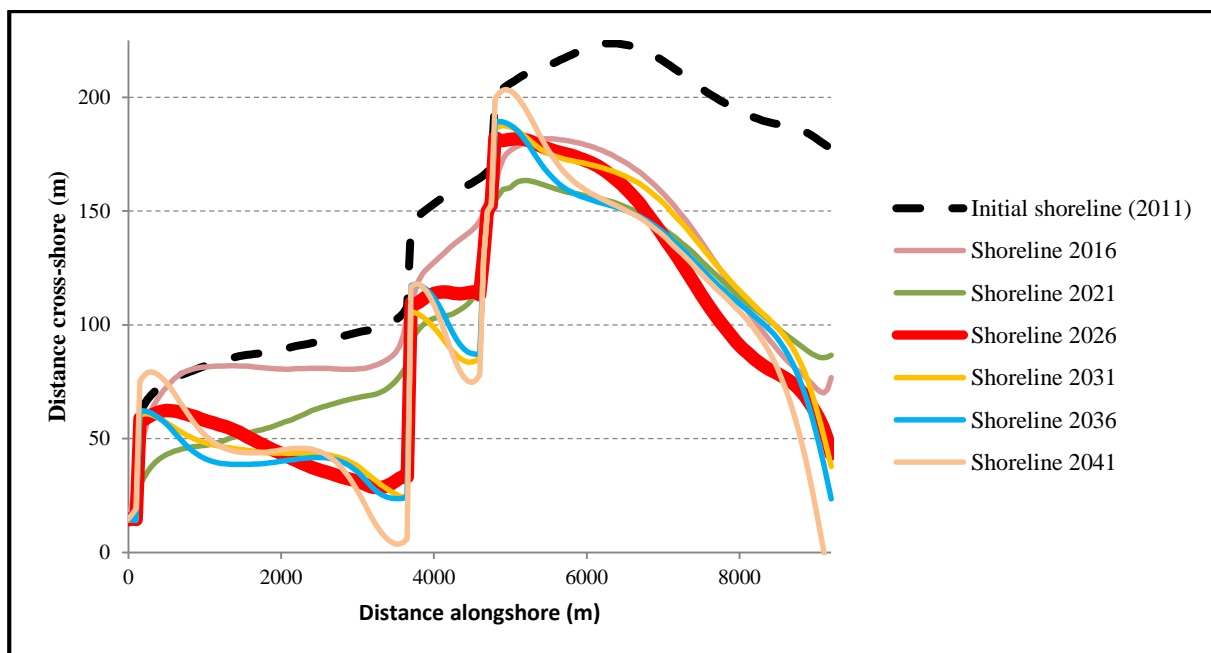
Figure 6.21. Do-nothing scenario: *calculated shoreline profiles in the extreme simulations. Starting from 2011 the shoreline reaches its equilibrium position in 2026.*

Figure 6.21 shows that from 2011 up to 2026 the shoreline profile changes considerably. After 2026, they are quite similar. The 2026 shoreline position can be thus assumed to be the *equilibrium shoreline position* for the *extreme* situation. The equilibrium position represents the convergence point for the shoreline profiles. The solutions after 2026 are quite unstable and show some fluctuation.

Conclusions

The most significant simulations were the *extreme* ones, the situation where there is an acute shortage of sediments entering from the northern boundary. In fact, in this case, it could be reasonably assumed that no sediments were entering the model at the northern boundary. Figure 6.22 shows the model result, in the *extreme* case, for year 2026 (reach of the *equilibrium position*).
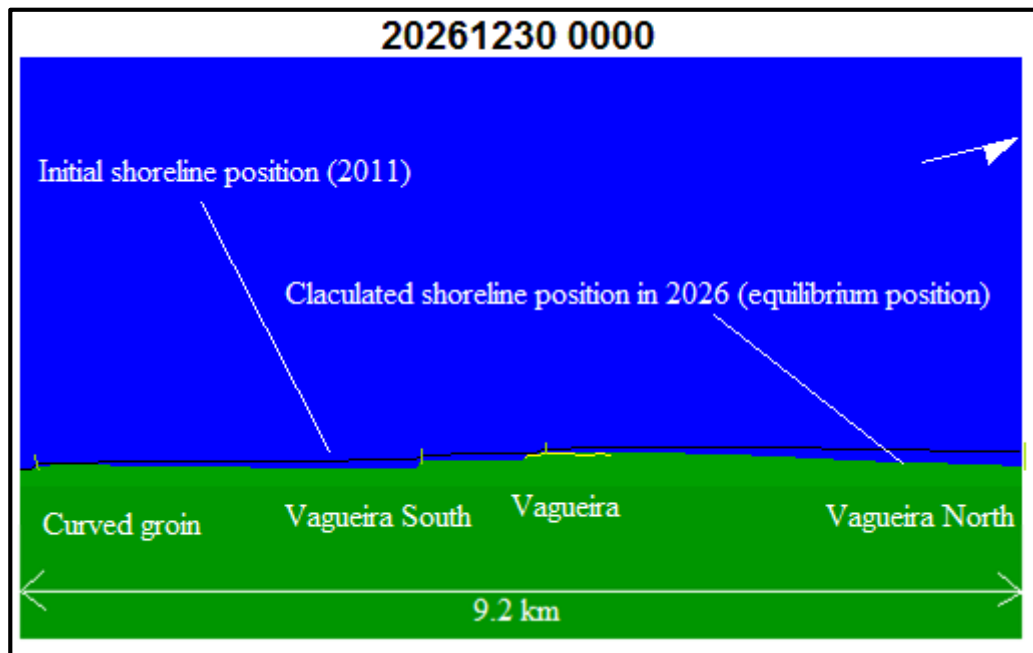
Figure 6.22. *Do-nothing scenario:the coastal stretch in the 2026, when the shoreline equilibrium position will be reached. The extreme condition (no-sediments arriving from north) will cause a severe erosion along the entire stretch. Vagueira curved groin and Vagueira groin are the hinge point for the shoreline rotation in the southern and northern stretch respectively.*

When the *equilibrium position* will be reached (2026), there will be a severe erosion along the entire stretch. In the Northern part the coastline will rotate around the *Vagueira groin* which will serve as an *hinge* point. Between *Vagueira* and *Vaguira South,* the shoreline will rotate around the *Vagueira South* groin, which will be almost disconnected from land. In the southern stretch, even if the *curved groin* will be still effective in stopping sediments at the up drift side, it will be also the *hinge* point for the shoreline rotation in this area. The shoreline rotation in all these sub stretches will cause the shoreline to be oriented parallel to the wave crests of the incoming wave climate. Figure 6.23 shows the orientation angles.
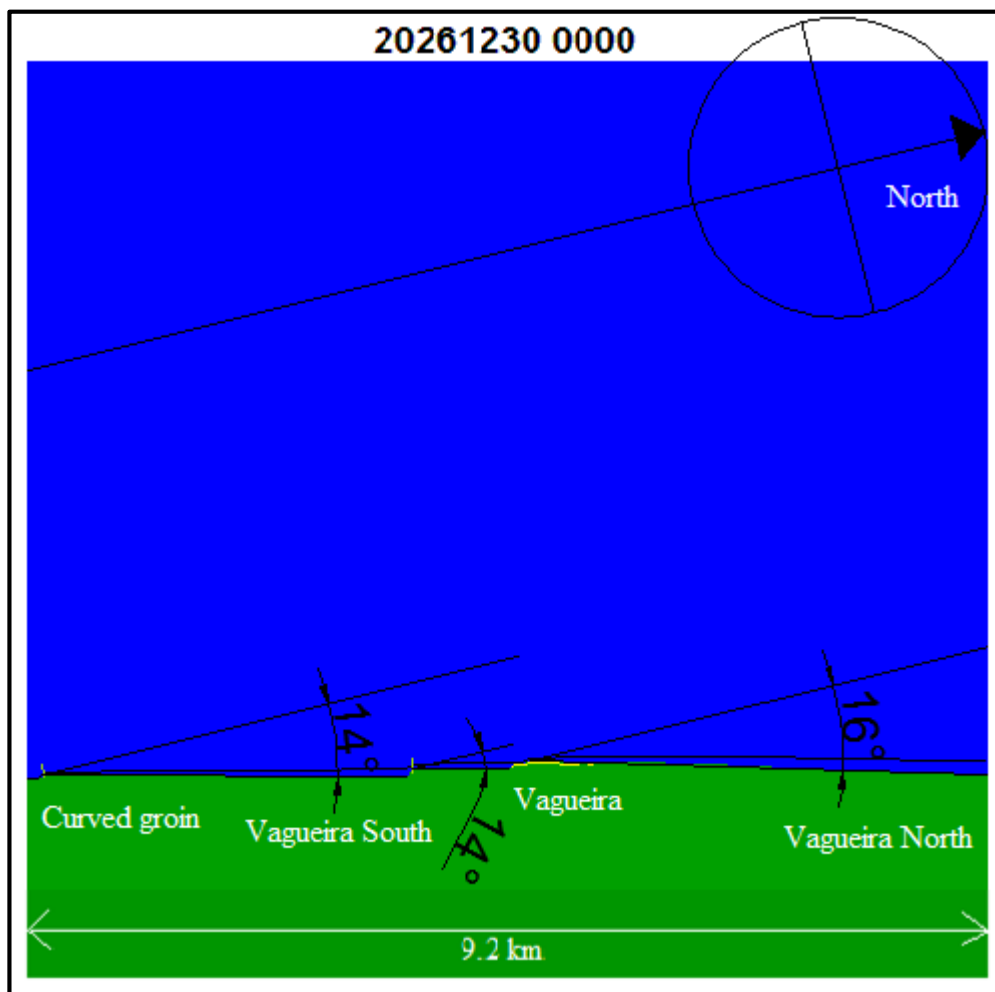
Figure 6.23. *Do-nothing scenario: rotation angle estimation for all the sub stretches. In the southern stretch the shoreline will be rotated of 14°t respect to the north. The rotation will occur around the curved groin. In the middle stretch, the shoreline will be rotated of 14° respect to the North. The rotation will occur around Vagueira South groin. In the Northern stretch the shoreline will be rotated of 16° respect to the North and the rotation will be around Vagueira groin.*

Figure 6.23 provides angle orientation estimation for all the sub stretches. These values were compared with orientation angles derived in the "*Carta de Risco do Litoral*" study (CEHIDRO & ICIST 1999) based on aerial photographs of the area. The angle values were consistent with values derived from aerial photographs analysis: 21° and 20° oriented shoreline, respect to North, in the northern stretch (*Vaguiera-Vagueira North*) and in the southern stretch (*curved groin-Vagueira South*), respectively.

The main problem with this evolution scenario is that the amount of erosion expected (calculated) immediately south of *Vagueira south groin*, to reach the so called equilibrium position, is enough to breach the sand spit barrier. This will have tremendous consequences on the hydrodynamics of the lagoon since a new inlet will be opened.

These results were derived from an *extreme* scenario. However, real events like the breaching opened at *Labrego* beach (immediately south of the *Vagueira south groin*) on the 3rd of November 2011 (Chapter 1, §1.1, Figure 1.5), confirm that the extreme scenario is not so far from reality.

6.3 Detached breakwaters protected scenario

The aim of this section is to investigate what could be the coastal stretch of interest in the future if detached breakwaters structures were designed and introduced to protect the project area. This protective solution was considered among the other the most feasible and effective for the project site (Chapter 1, §1.2). The aim of these simulations is to find the *equilibrium position* and the time needed to reach it. Besides, as design criteria, the *tombolo* formation is required: this will ensure a new effective accreting trend on the entire stretch. The GENESIS-T version was used because *tombolo* formations are present in the simulation. The detached breakwater structures were tested in different positions and orientations, in order to meet this requirement. The following subsections illustrate, in order, the different tests that were performed to obtain the best position for the detached breakwaters.

6.3.1 Scenario A: three detached breakwaters parallel to the present shoreline (2011)

The start date of simulation was 31/12/2011. Simulations were run step by step advancing in intervals of ten years.

Spatial configuration

Figure 6.24 illustrates the spatial configuration.
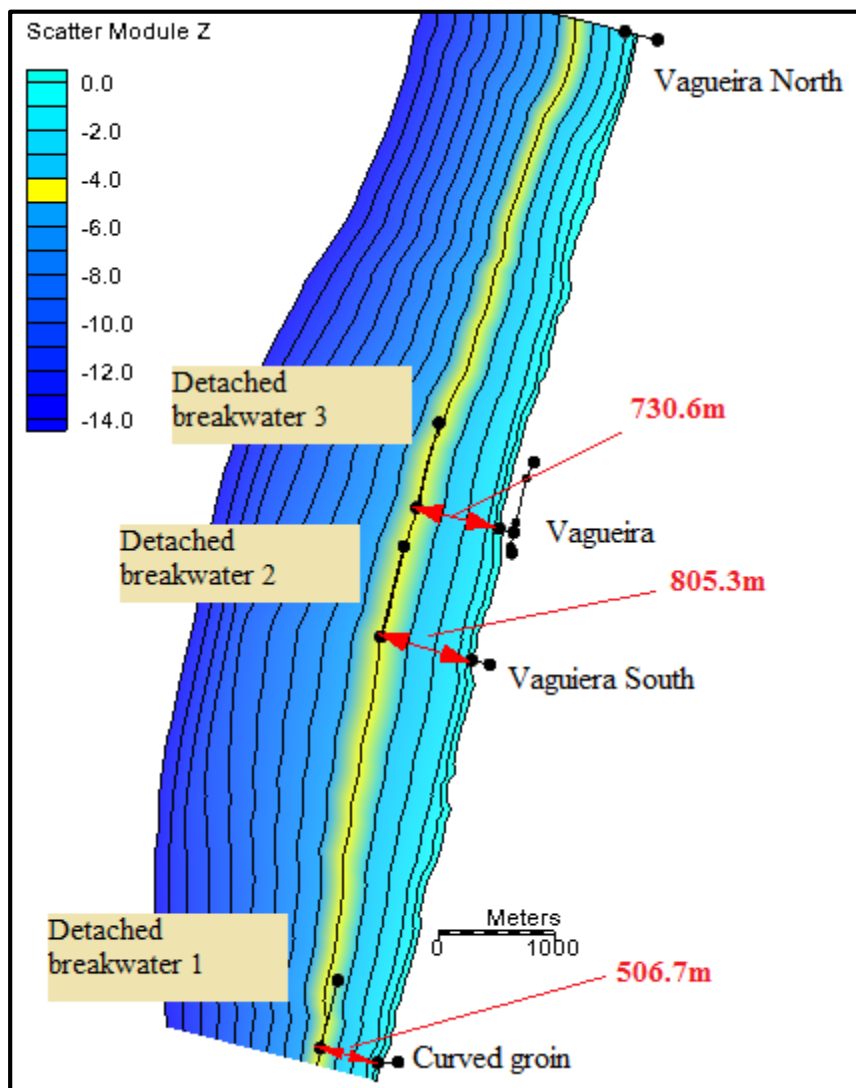
Figure 6.24. *Detached breakwaters protected scenario A: three detached breakwaters are placed along the stretch in correspondence to the already existing structures. Their orientation is parallel to the shoreline in 2011. They are positioned at the 5m contour depth. The distance from the nearest existing structure tip is specified.*

The detached breakwaters were placed along the 5m water depth contour line and were oriented approximately parallel to the position of the coastline in 2011. Table 6.1 summarizes the structures length.

Structure	Length (m)
Detached breakwater 1	600
Detached breakwater 2	800
Detached breakwater 3	750

Table 6.1 *Detached breakwater protected scenario A: structures length specifications.*

The length of the detached breakwaters was chosen to be of the same order of magnitude to the distance to the shoreline to promote tombolo formation (US Army Corps of Engineers 2008).

To describe wave transmission at the detached breakwater, the model requires the *transmission coefficient* specification (K_T). The transmission coefficient, defined as the ratio of the height of the incident waves directly shoreward of the breakwater to the height directly seaward of the breakwater, has the range of [0;1]*,* for which a value of 0 implies no transmission and 1 implies complete transmission(Hanson *et al.*1991). In this study, a zero value was assumed for all detached breakwater.

Lateral boundary conditions

Lateral boundary conditions are set equal to the values derived in the simulation 2004-2011 (§6.1.2) as shown in Figure 6.25.
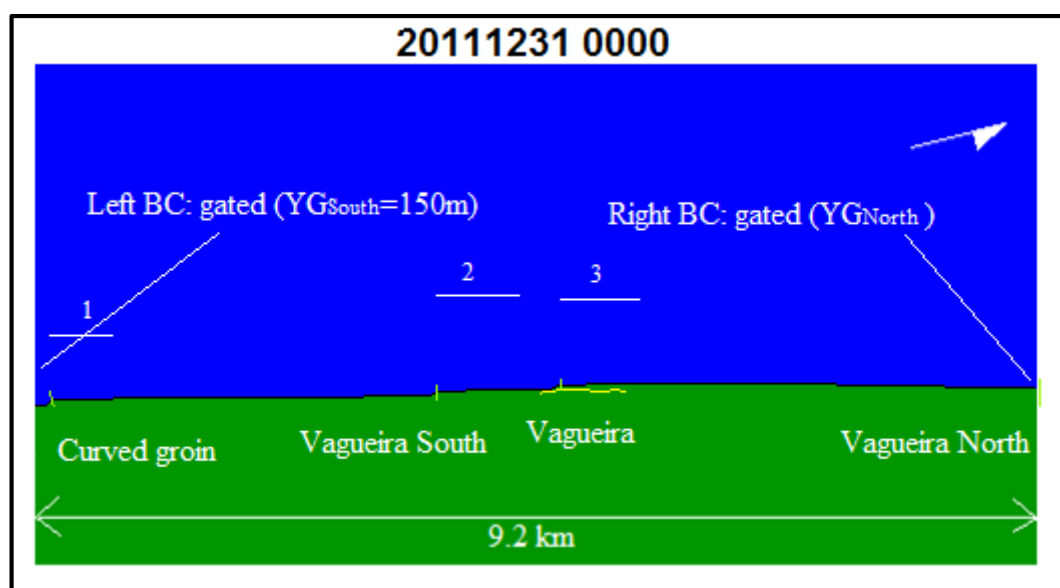
Figure 6.25. *Detached breakwaters protected scenario A: gated boundary conditions are specified at both sides of the model. On the left side, YG$_{South}$ is set equal to 150m. At the northern boundary, YG$_{North}$ will be varied to investigate the extreme and calibrated situation.*

The value of YG$_{North}$ is not specified in Figure 6.25. In fact, two different values were tested: the *calibrated* value (YG$_{North}$ =100m) and the *extreme* value (YG$_{North}$ =200m). This was to test the influence of sediments entrance at the northern boundary on the *tombolo* formation. YG$_{South}$ was kept equal to 150m.

<u>YG$_{North}$ =200m: extreme condition (no sediments entering the model)</u>

Figure 6.26 shows the coastline evolution in *extreme* conditions i.e no sediments entering the model at the northern boundary.
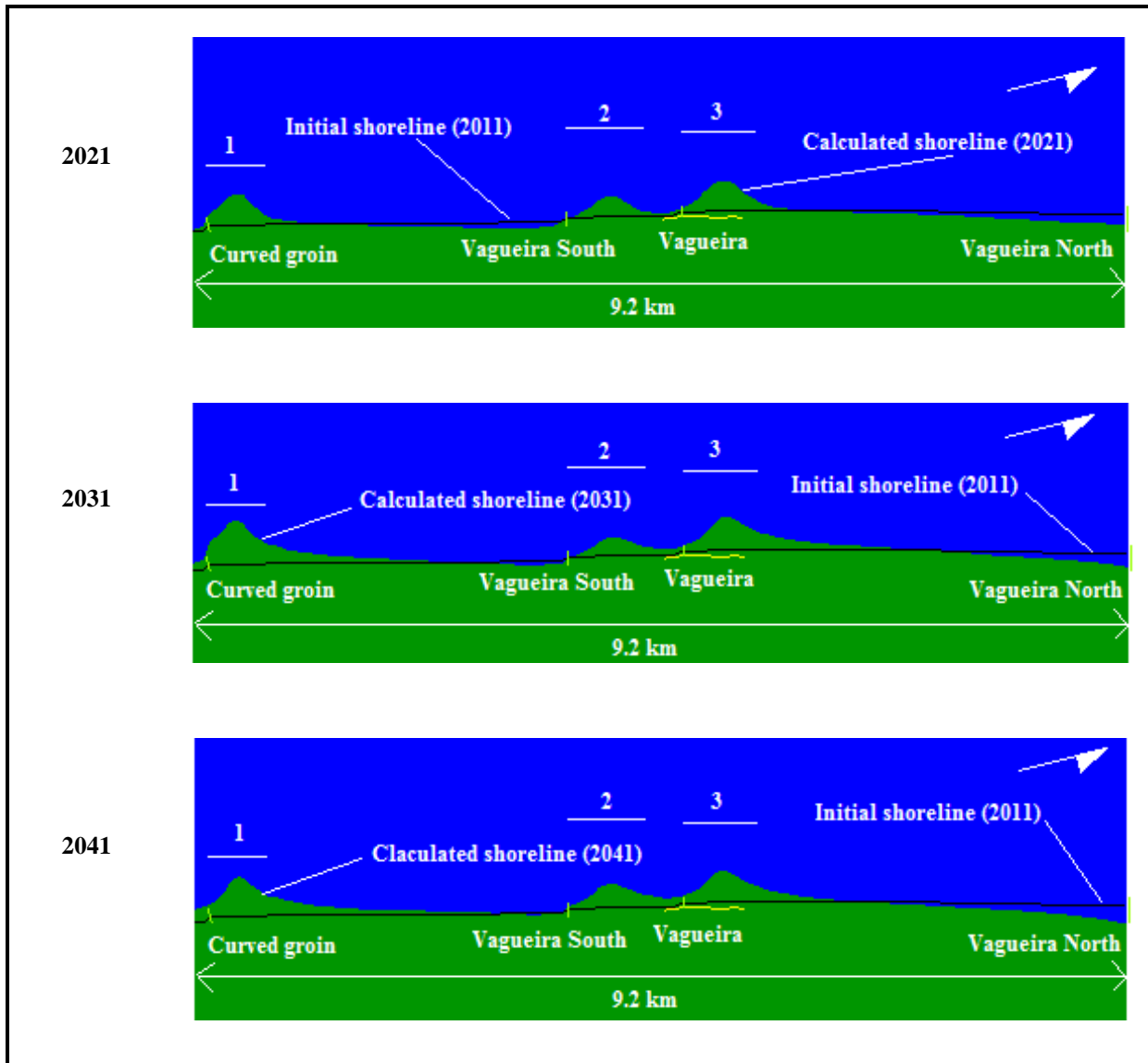
Figure 6.26. *Detached breakwaters protected scenario A, extreme conditions: shoreline evolution calculated with a time step variation of 10 years. After 30 years, the tombolo formation has still to be reached. The shortage of sediments entering the model (extreme conditions, YG$_{North}$=200m) has visible effect on the northern stretch. This part is progressively eroding and the sediments are transported down drift to feed the tombolo formation.*

The calculated shoreline position progressively extends seaward (*salient*), influenced by the presence of the detached breakwaters structures. Meanwhile, the northern stretch is facing severe erosion. The sediments eroded in the northern part are transported down drift to feed the *salient* in the southern stretch. Nevertheless, the volume of sediments is not enough to allow the *tombolo* formation, not even in 30 years' time. This is due to the shortage of sediments imposed at the right boundary (YG$_{North}$ =200m). The *calibrated* condition was thus

considered to investigate how the shoreline profile would change if sediments were available at the northern boundary.

The farthest into the future, the more the *shoreline* away from the *salient*, tend to be parallel to the incoming wave crests (and thus to the *equilibrium shoreline position*) at the up drift side of the detached structure. This is the due to the northwesterly wave climate.

YG North =100m: calibrated condition (sediments entering the model)

Figure 6.27 shows the coastline evolution in *calibrated* conditions where some volume of sediments is entering the model at the northern boundary.
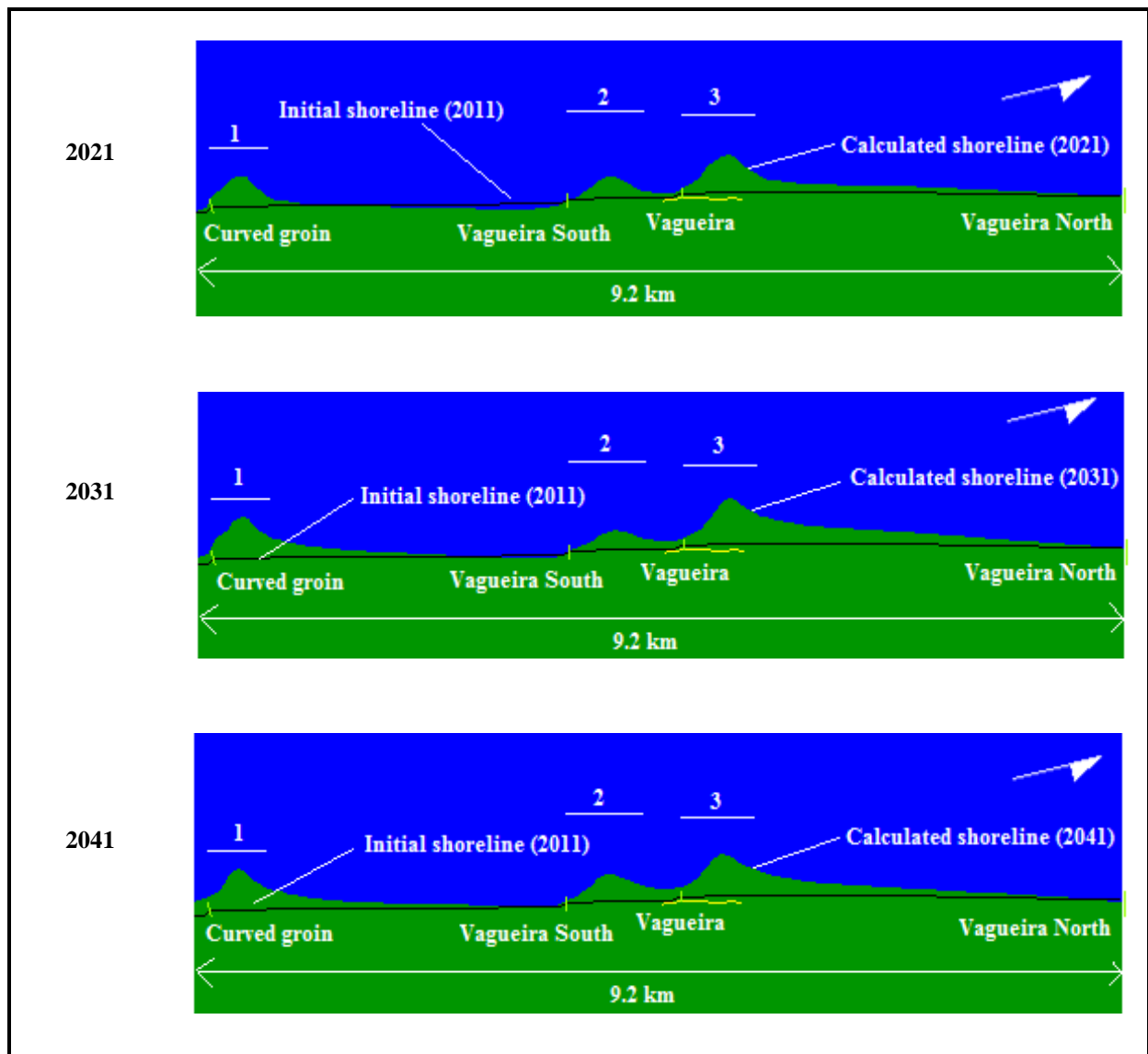
Figure 6.27. *Detached breakwaters protected scenario A, calibrated conditions: shoreline evolution calculated every 10 years since 2011. The tombolo formation is still not occurring (even after 30 years). Nevertheless, the sediments entering from north prevent the northern stretch from eroding i.e this amount of sediments is enough to feed the present salient extension, but is not suitable to reach the tombolo formation.*

The detached breakwaters influence the shoreline evolution: *salients* form in correspondence of each structure. The sediments entering from north provides material for the *salient* accretion in front of *detached breakwater 3*. This has good effects in the northern stretch, as it prevents erosion in the northern part. The erosion in 2021, south of *Vagueira South* groin is evidently related to the *salient* formation in front of the *detached breakwater 2*. It is evident in 2021, at the very initial stage of *salient* formation. It is progressively compensated later (2031, 2041) when sediments are better redistributed along the stretch. Also in this case, *tombolo* formation is still not occurring, even after 30 years. Yet, the farthest into the future, the more the *shoreline* tend to be parallel to the incoming wave crests (and thus to the *equilibrium shoreline position*) at the up drift side of the detached structure. The northwesterly wave climate is the constant driving force of sediments.

Conclusions

In both the *calibrated* and *extreme* simulations the *tombolo* formation is not occurring. Therefore, another configuration for the detached breakwaters was investigated. Nevertheless, these tests provided important information about the conditions that could help the *tombolo* formation:

– sediments entering from the northern boundary should be enough to provide material for the *salients* accretion. Otherwise, the *salients* will be formed using the sediments already within the coastal stretch. This will cause severe erosion in same spots;

– the detached breakwaters structures should be placed closer to the shoreline; this will help the *tombolo* formation and reduce the time to reach it;

– the orientation of the detached breakwaters could be set parallel to the incoming wave direction crest (or *equilibrium shoreline position*). This will maximize the sheltering effect of the detached breakwater and will also help with tombolo formation.

6.3.2 Scenario B: finding the best position for detached breakwater 1

Considering the results of the previous tests (§6.3.1), the detached breakwaters positioning was changed. The idea was to investigate the detached breakwater introduction (construction) at different instants in time. Results from *scenario A* (§6.3.2) showed that even if sediments are entering the stretch (*calibrated* condition) s*alients* will not form without some erosion along the coast. Therefore, it was decided to first introduce the *detached breakwater 1* (Figure 6.28).
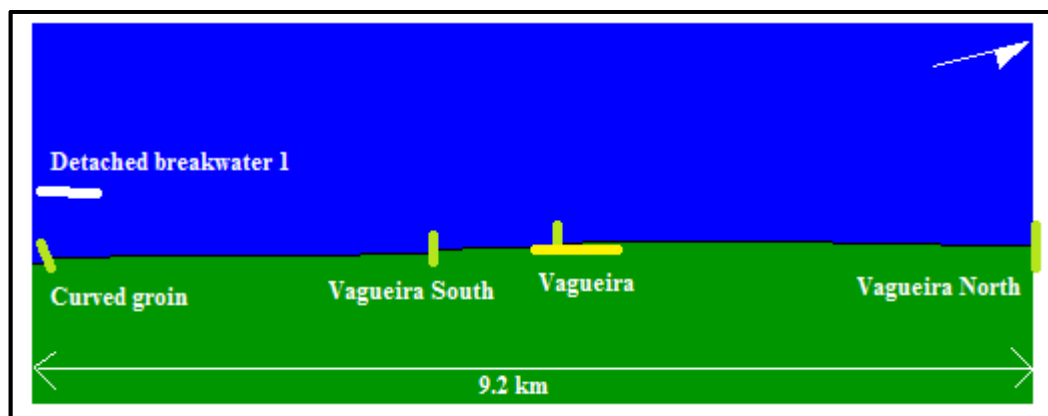
Figure 6.28. *Detached breakwater protected scenario B: definition sketch of the model configuration. Detached breakwater 1 is considered individually at first stage.*

The final result must comply with the following requirements:

- *tombolo* formation occurring at the *detached breakwater 1*;

- no erosion within the costal stretch, especially in the southern part which has been proved to be the most sensitive area (remember *Labrego* beach breaching on 3rd of November, 2011);

To comply with this second requirement a minimum accretion distance (d_1) between the *calculated shoreline equilibrium position* and the *initial shoreline* (2011) immediately south of *Vagueira South* was fixed to be in the range [50m;100m]. This widening distance (d_1) is considered to be enough, to prevent breaching in the area.

The *detached breakwater 1* length was set equal to 500m. The orientation to the north was fixed equal to 18°. This value is within the [14°;20°] interval, which represents the interval between the *equilibrium shoreline orientation* found in the *do-nothing* scenario (§6.2) and the *equilibrium shoreline orientation* derived by the aerial photographs survey (CEHIDRO &

ICIST 1999). The rotation was performed by rotating the structure around its southern tip (hereafter called *hinge tip*).

The start date of simulation is 31/12/2011. The *detached breakwater 1* length and orientation were kept fixed, while the *position of its southern tip* was varied in the cross-shore direction, in order to meet the abovementioned requirements. The following sections illustrate the results for three different configurations. At the model boundaries the *calibrated* boundary condition were specified (gated, YG_{North} =100m, YG_{South} =150m).

Hinge tip at -2.5m contour line

Figure 6.29 shows the *detached breakwater 1* positioned right in front of the *curved groin*. The *hinge tip* of the detached structure is place at the -2.5m contour line. The distance from this point up to the *curved groin* southern tip is 137.8m.
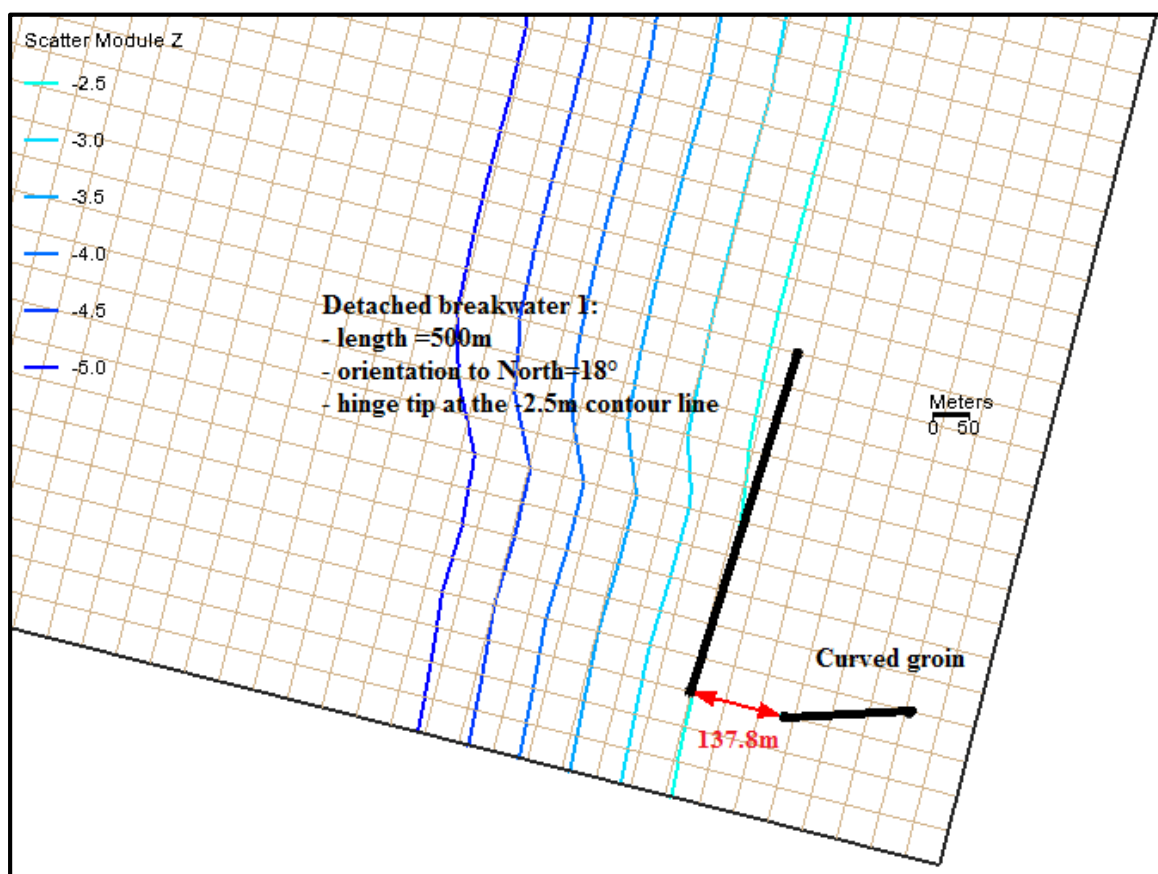
Figure 6.29. *Detached breakwater protected scenario B: the detached breakwater is positioned right in front of the curved groin. The southern tip (hinge tip) is aligned with the curved groin tip and the distance is of 137.8m.*

The resulting *shoreline equilibrium position* occurs in 2026. Figure 6.30 shows the *calculated shoreline* profile in 2026.
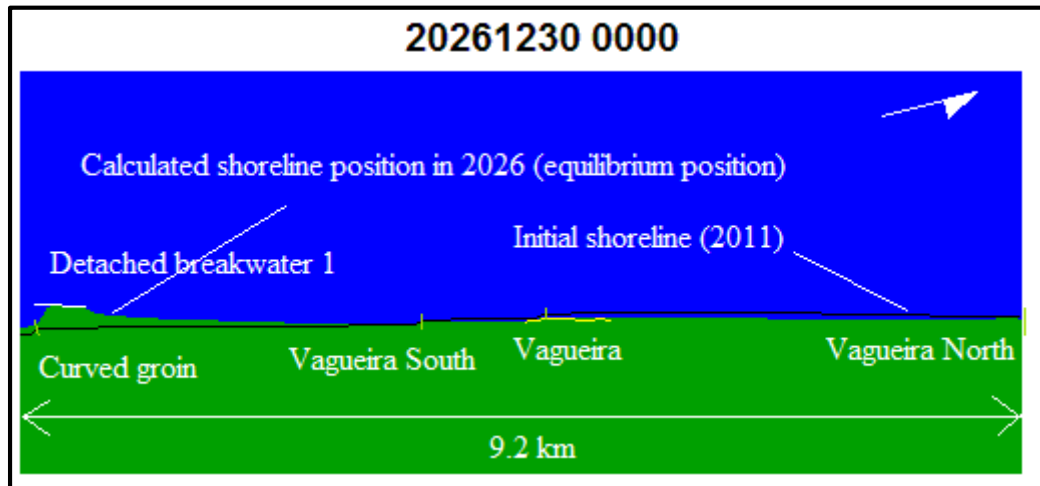
Figure 6.30. *Detached breakwater protected scenario B: the equilibrium shoreline position is reached in 2026. The tombolo formation requirement is met, but there is no sediments accumulation in correspondence of Vagueira South.*

This spatial configuration complies with the *tombolo* formation requirement, but there is no sediments accumulation in the south of *Vagueira South* i.e the *initial* (2011) and the *calculated shoreline* (2026) are almost coincident at the down drift side of the structure. Therefore, the criteria for d_1 is not met. The detached breakwater should be moved further offshore in order to widen the southern stretch.

<u>Hinge tip at -3.5m contour line</u>

Figure 6.31 shows the *detached breakwater 1* positioned further offshore: the *hinge tip* is at the -3.5m contour. The distance from the *curved groin southern tip* is 281.8m.
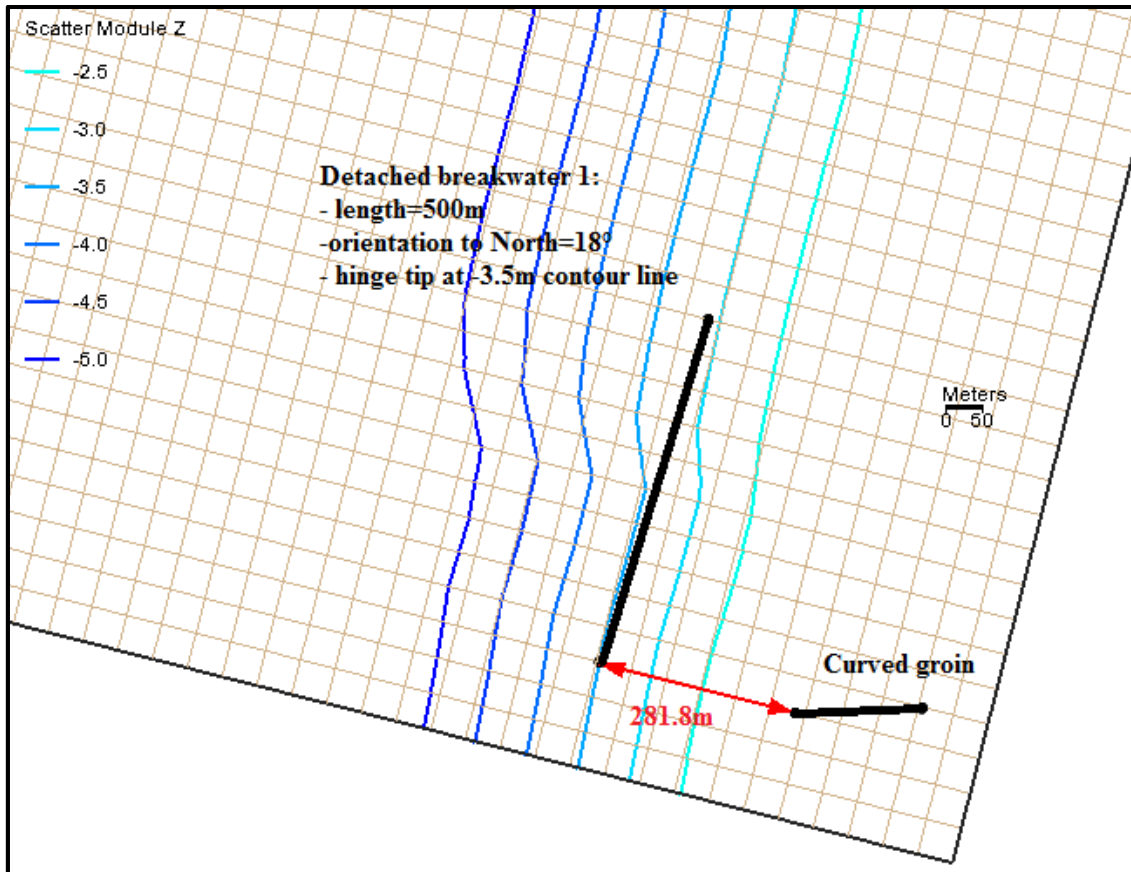
Figure 6.31. *Detached breakwater protected scenario B: the detached breakwater is positioned right in front of the curved groin. The southern tip (hinge tip) is aligned with the curved groin tip and the distance is of 281.8m.*

The *equilibrium position* will be reached in 2026, with a *tombolo* formation, as shown in Figure 6.32.
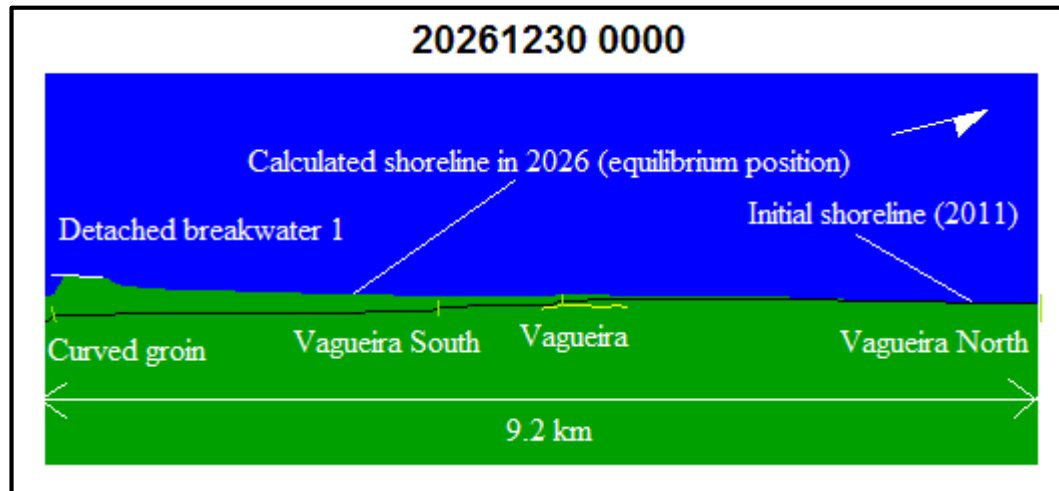
Figure 6.32. *Detached breakwater protected scenario B: the equilibrium shoreline position is reached in 2026. The tombolo formation requirement is met, and there is sediments accumulation in correspondence of Vagueira South.*

Figure 6.32 shows sediments accumulating in correspondence of *Vagueira South*. The accumulation width was checked with more detail, in order to verify the requirement on d_1 (50m< d_1 <100m). Figure 6.33 shows the results.
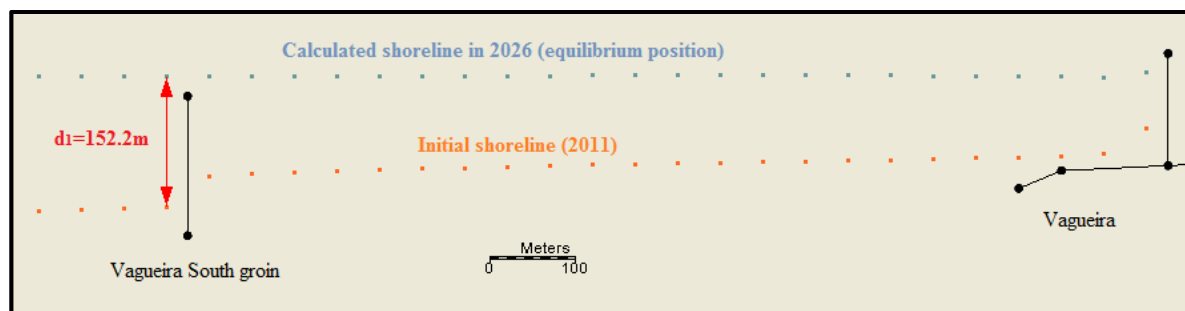
Figure 6.33. *Detached breakwater protected scenario B: verification of d₁ value at the down drift part of the Vagueira South groin. The value is out of the required interval (50m< d₁<100m).*

The detached structure was shifted further offshore. This caused the shoreline in the southern stretch to widen. The d_1 value is out of the required interval [50m; 100m]. The correct position should be somewhere between the -2.5m and the –3.5m contours.

Hinge tip at -3.0m contour line

Figure 6.34 shows the *detached breakwater 1* positioned between the -2.5m and the –3.5m contours. The *hinge tip* is at the -3.0m contour. The distance from the *curved groin southern tip* is 207.2m.
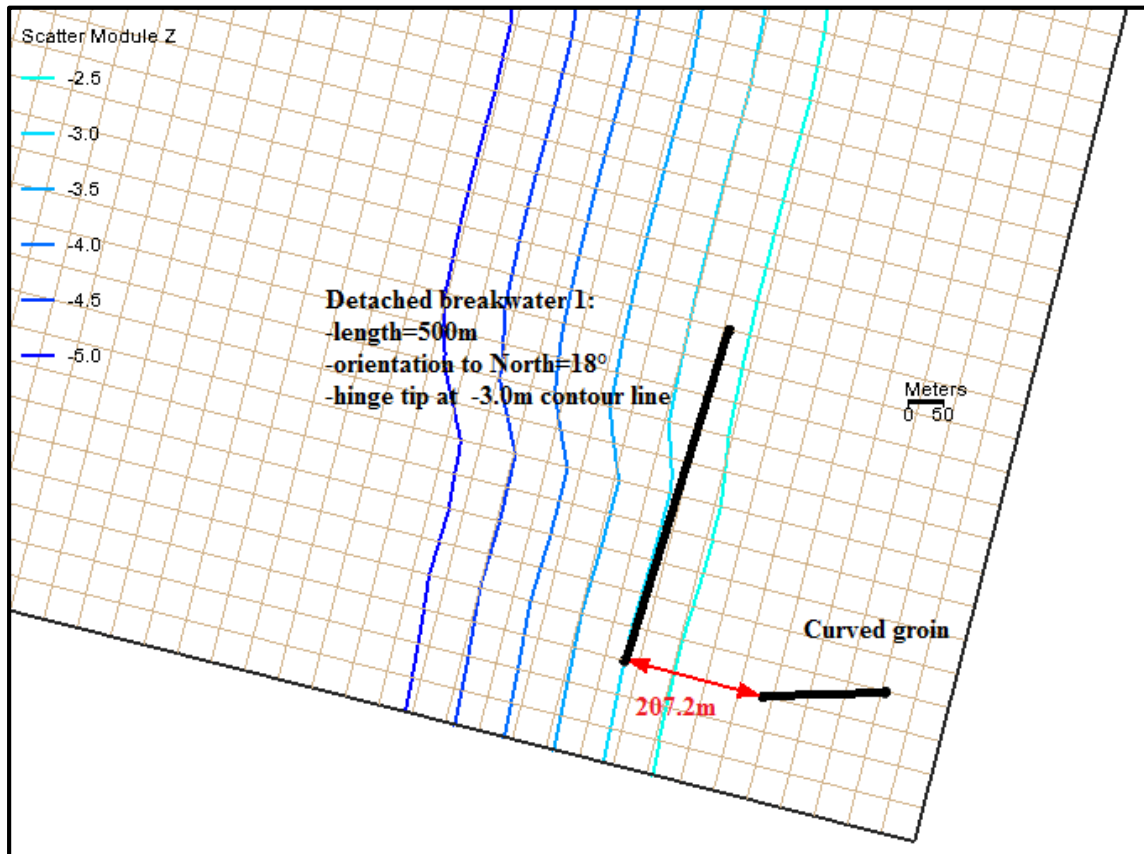
Figure 6.34. *Detached breakwater protected scenario B: the detached breakwater is positioned right in front of the curved groin. The southern tip (hinge tip) is aligned with the curved groin tip and the distance is of 207.2m.*

With this spatial configuration the *shoreline equilibrium position* will be reached in 2026, with the *tombolo* formation, as shown in Figure 6.35.
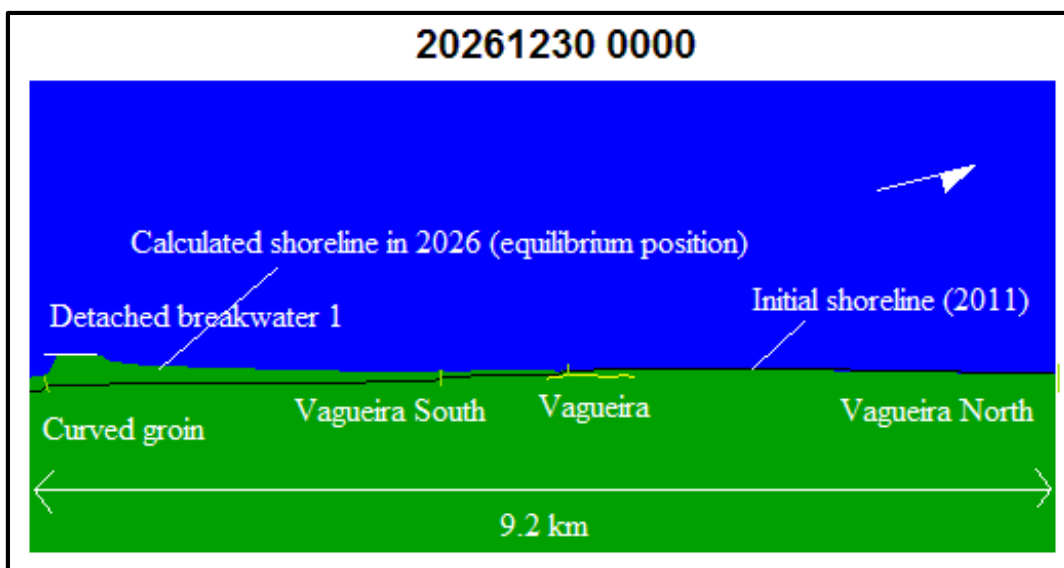
Figure 6.35. *Detached breakwater protected scenario B: the equilibrium shoreline position occurs in 2026. The tombolo formation requirement is met. Sediments accumulate in correspondence of Vagueira South.*

Figure 6.35 shows sediments accumulation near *Vagueira South groin*, which is expected to meet the requirements ($50m< d_1 <100m$). In Figure 6.36, the shoreline accretion is measured.
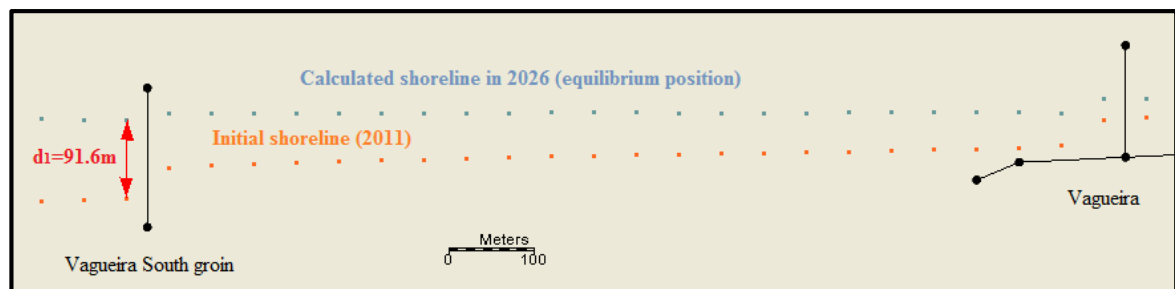
Figure 6.36. *Detached breakwater protected scenario B: verification of d1 value at the down drift part of the Vagueira South groin. The shoreline accretion value complies with the required interval (50m< d1<100m).*

Figure 6.36 shows that the d_1 parameter is within the required interval ($50m< d_1 <100m$).

<u>Conclusions</u>

The tests performed show how the *detached breakwater 1* influence the accumulation of sediments, especially in the southern part. The further offshore the structure, the greater is the quantity of sediments accumulating in *Vagueira south*. As the detached structure is placed close to the coast, the d_1 value decreases. This has a good effect in preventing erosion in the southern stretch, which is the most sensitive. Besides, the vicinity with the already existing *curved groin* could help the detached breakwater construction. The best position of the *detached breakwater 1* is definitely set to be the one with the hinge tip at the -3.0m contour. The resulting *equilibrium configuration* (2026) will be used in the next scenario to find out the best position for a second detached breakwater (*detached breakwater 2*) which will protect the northern stretch. In fact, even if the northern stretch is not facing a significant erosion (Figure 6.35) the sand spit must be widen also in that part. The simulations (6.3.3) will demonstrate that the *detached breakwater 2* is sufficient for the protection of the remaining coastal stretch.

6.3.3 Scenario C: getting the best position for detached breakwater 2

This section presents the model behaviour when a second detached breakwater (*detached breakwater 2*) is introduced in the model to widen the sand spit in the northern stretch. Figure 6.37 provides a sketch of the spatial configuration used in this scenario.
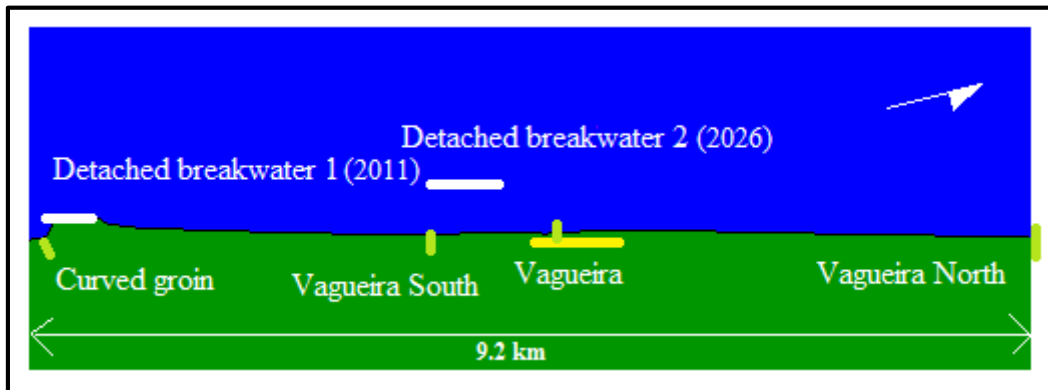
Figure 6.37. *Detached breakwaters protected scenario C: definition sketch of the model configuration. Detached breakwater 2 is inserted in 2026, when the detached breakwater 1 equilibrium position is reached.*

The simulations start from year 2026 (start date is 31/12/2026), which represents the *equilibrium configuration* for the stretch when only *detached breakwater 1* is present.

The aim is to find the *shoreline equilibrium position* (hereafter referred to as *final equilibrium position*) when both structures are present in the model. Simulations will demonstrate that the insertion of *detached breakwater 2* is enough to secure the entire stretch from future erosion. The *final equilibrium position* must comply with the following requirements:

- *tombolo* formation must be reached in correspondence of *detached breakwater 2*;

- the previously accretion width d_1 must be ensured in correspondence of *Vagueira south* i.e the *tombolo formation* at the *detached breakwater 2* must not influence the southern stretch;

- in the northern stretch the *final shoreline equilibrium position* must be such that the sand spit will be widen of a certain amount (d_2) in correspondence of *Vagueira North groin;*

The last requirement is similar to the d_1 used for the southern part. d_2 represents the distance between the *final calculated shoreline equilibrium position* and the *present shoreline position* (2011) in correspondence of *Vagueira North groin.* This value must be in the range of [100m; 200m]. The interval is much larger than the one fixed for d_1. The reason is that the northern stretch (*Vagueira-Vagueira North*) is longer than the southern stretch (*Curevd groin-Vagueira South*).

The *detached breakwater 2* length was set equal to 700m. Its orientation to the north was

fixed equal to 18°. The lateral boundary conditions were *gated*-type conditions at both side of the model under *calibrated* conditions (YG$_{North}$ =100m, YG$_{South}$ =150m).

Two different spatial configurations were tested for detached breakwater 2. The structure was moved from its southern tip (*hinge tip*) and place at different contour lines (-4.0m and -3.5m).

Hinge tip at -4.0m contour line

Figure 6.38 shows the *detached breakwater 2* positioned right in front of the *Vagueira south groin*. The *hinge tip* of the detached structure is place at the -4.0m contour line. The distance from this point up to the *Vagueira south groin* southern tip is 565.1m.
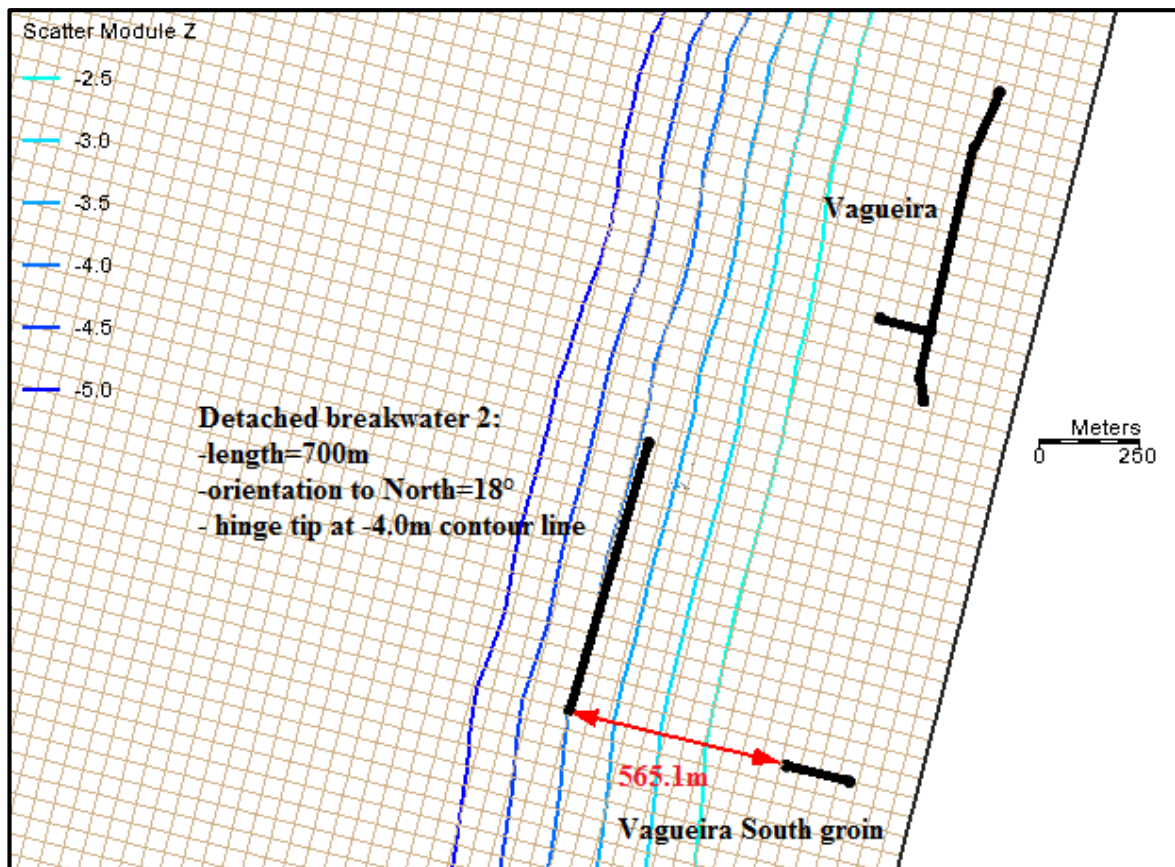
Figure6.38. *Detached breakwater protected scenario C: the detached breakwater 2 is positioned right in front of the Vagueira south groin. The hinge tip is aligned with the Vagueira south groin tip and the distance is of 565.1m.*

With this spatial configuration, *tombolo* formation at *detached breakwater 2* resulted to be impossible to reach. In fact, in 2086 it will not be reached yet. Figure 6.39 shows the shoreline evolution in 2086.
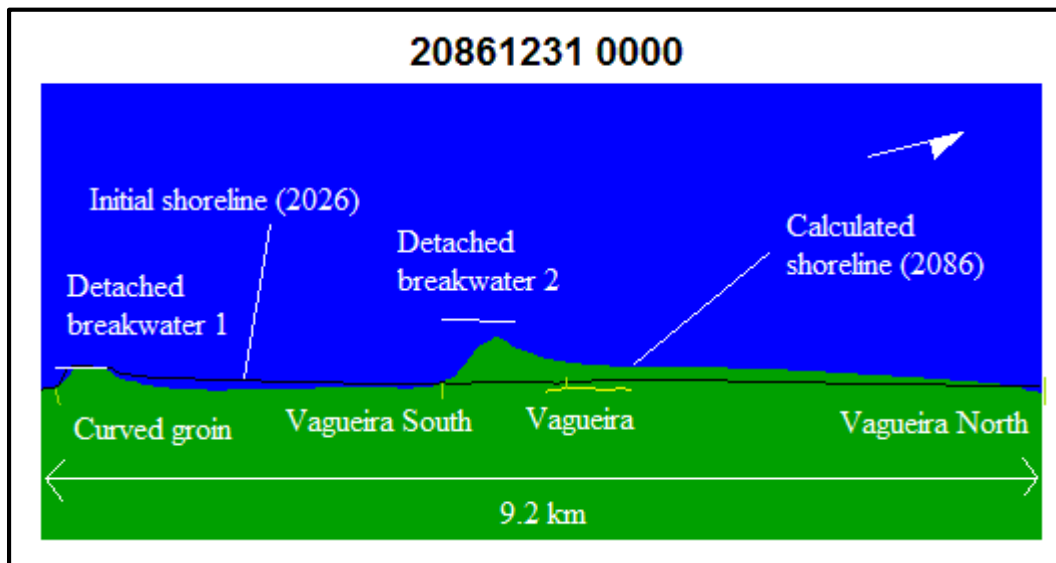
Figure 6.39. *Detached breakwater protected scenario C: the tombolo formation at detached breakwater 2 is unfeasible. After 60 years (2086) the calculated shoreline does not reach the detached structure.*

The *detached breakwater 2* position is too much offshore, and this causes the *tombolo* formation to be unfeasible. From 2026 up to 2086 the southern stretch will lose the previously gained width as it will recede behind the initial shoreline position. This is not consistent with the d_1 requirement. The northern stretch will erode too, as sediments are used for the *salient* formation behind the *detached breakwater 2*. None of the requirements is met, thus this is not a feasible position for the *detached breakwater 2*. This structure should be moved closer to the coast.

<u>Hinge tip at -3.5m contour line</u>

Figure 6.40 shows the *detached breakwater 2* positioned closer to the coast. The *hinge tip* is at the -3.5m contour line. The distance from the *Vagueira south groin* southern tip is 446.9m.
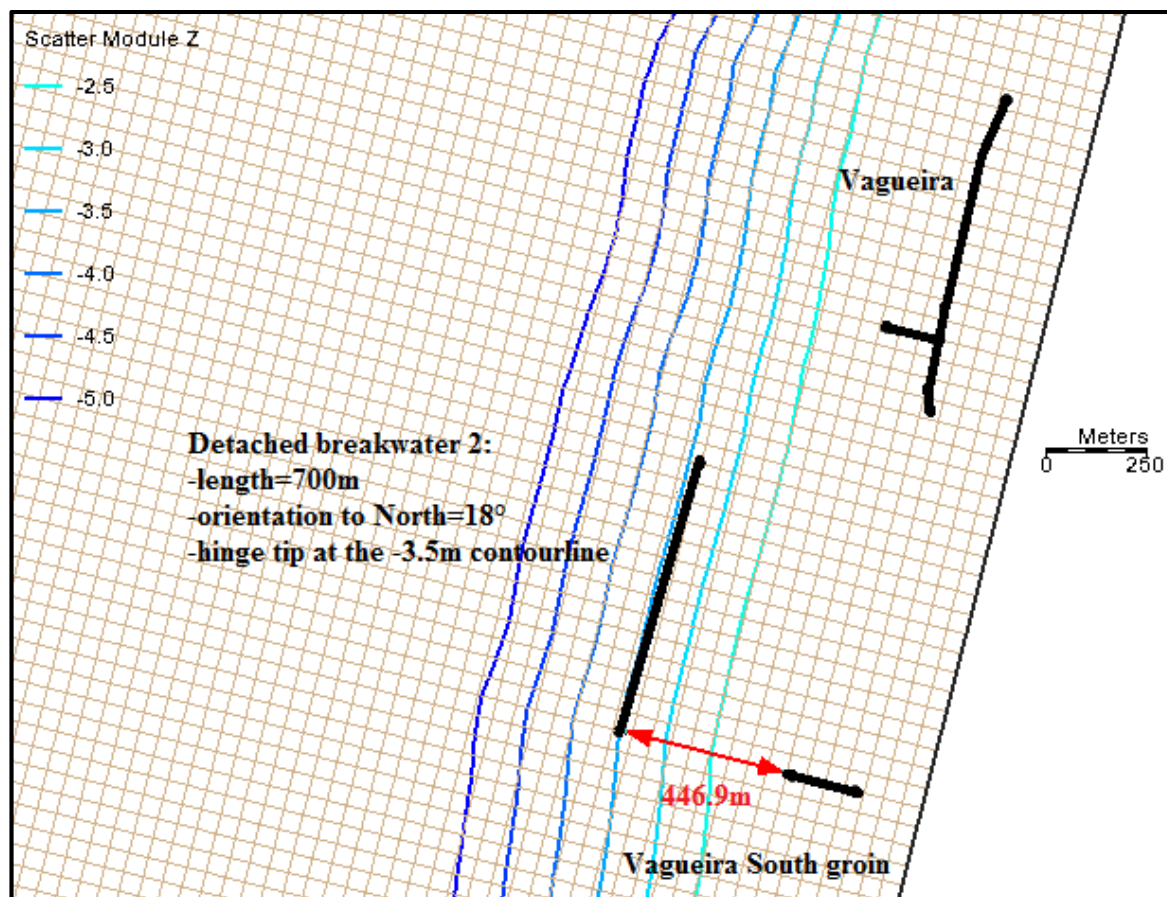
Figure 6.40. *Detached breakwater protected scenario C: the detached breakwater 2 is positioned closer to the coastline. The hinge tip is aligned with the Vagueira south groin tip and the distance is 446.9m.*

With this spatial configuration the *final equilibrium shoreline* almost complies with all the requirements. The *calculated shoreline* profile is shown in Figure 6.41 for year 2056, which is the year when the *final equilibrium position* will be reached.
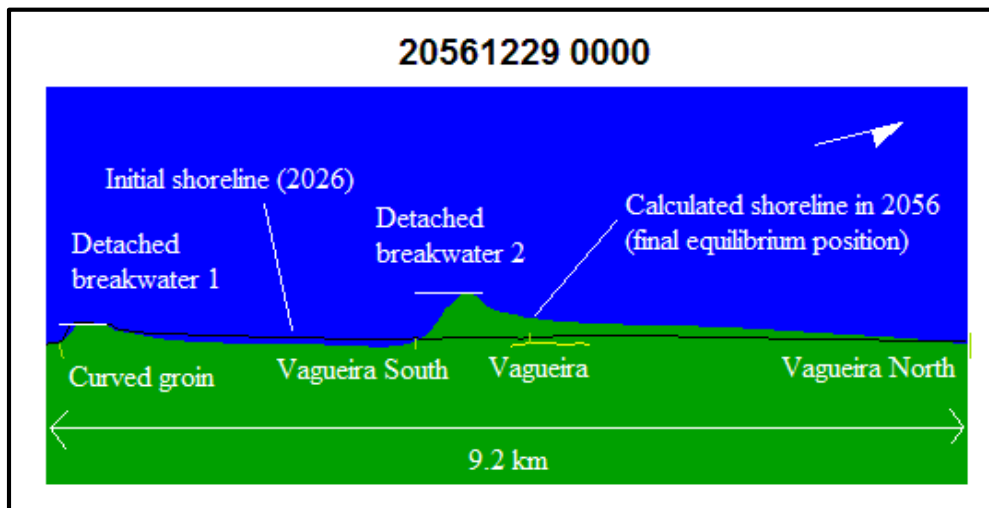
Figure 6.40. *Detached breakwater protected scenario C: the tombolo formation at detached breakwater 2 is reached after 30 years. In the northern stretch the tombolo behind detached breakwater 2 makes the shoreline to be further offshore than the initial one. The gained width progressively reduces approaching north. In the southern stretch, the calculated shoreline is shifted landward respect to the initial position. This recession reaches its maximum at the down drift side of Vagueira South groin.*

The requirement on *tombolo* formation is met. In the southern stretch the d_1 valued must be checked with more detail. In the northern stretch the *tombolo* formation will make the shoreline to be further offshore than the initial one. Nevertheless, this accreted width progressively reduces northwards. The requirement on d_2 must thus be checked. Figure 6.41 provides estimation of d_1 and d_2.
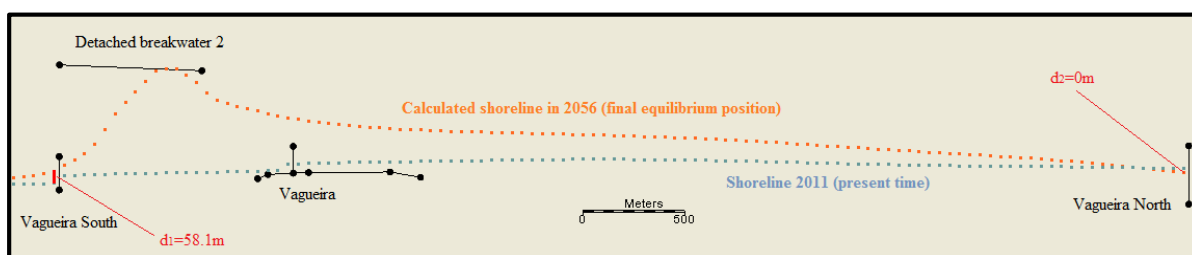
Figure 6.41. *Detached breakwater protected scenario C: verification of d_1 and d_2 values. d_1 is 58.1m and d_2 is 0m.*

The d_1 is equal to 58.1m. This is very close to the minimum possible value (50m), but still acceptable. On the other hand, d_2 is zero; this is not consistent with the required interval [100m; 200m]. However, the northern stretch will not face erosion: the sand spit width decreases as reaching the northern boundary, but it will be at minimum zero. This means that in *Vagueira North* the shoreline will maintain the present time position at the very down drift part of the groin.

Conclusions

Even if not all the requirements were met ($d_2=0$), the last spatial configuration (*detached breakwater 2* hinge tip at -3.5m contour line) resulted to be very good in compensate the erosion and start a new accreting trend on the entire stretch. This is an important result as it lays the foundation for further studies and the fine-tuning of the detached breakwaters design. The knowledge gained at this point is enough for a feasibility study. In particular, the simulations provided important information about the influence that the detached breakwaters structures could have in this coastal stretch. Here a list follows.

a) The distance between the detached structure and the initial coastline has great influence on the time needed to reach the *tombolo* formation i.e the smaller the distance, the earlier and more feasible the *tombolo* formation. In addition, this distance has significant effects also on the possible width that can be gained i.e the greater the distance, the wider the sand spit.

b) The orientation of the detached breakwater can increase/decrease the time needed for the *tombolo* to be reached. In particular, the more the structure is rotated parallel to the incoming wave crests (*equilibrium position* at present time), the earlier the *tombolo* formation.

c) The *tombolo* formation depends on sediments availability within the stretch. If no sediment are available the *tombolo formation* will trigger an eroding trend in the entire stretch from the early stage (*salient* accretion).

d) The number of detached structures required to protect the entire stretch is related to the structure length. Few longer structures can serve the same function of shorter structures; in this case two structures of 500m and 700m resulted to be enough.

e) The detached breakwaters (1 and 2) were placed just in front of already existing coastal protections (*curved groin* and *Vagueira South groin,* respectively). This could be considered as an advantage if the detached protections would be constructed. The access from land is also a possibility.

f) Due to the very flat bathymetry of the project area, the detached breakwaters are placed in relatively shallow water (around -3.5m). This could reduce the constructions costs.

Conclusions

The aim of this study is to provide an important contribution to the design of a shore protection works for the Vagueira region on the Portuguese west coast using mathematical modelling of coastal evolution.

Before entering the model setup phase, much work was done in the input data preparation. The model requires topographic and bathymetric input data, wave climate information and the shoreline position in two different years for the model calibration. The Hydrographic Institute of Portugal provided original wave data, derived from the Leixões recording buoy. Though valued, these data were not meeting the model requirements, as the wave series was not continuous and regular in time. A very detailed statistical analysis was performed in order to check the wave series composition. Finally, a filling method was devised in order to create a proper format for the wave climate information to be input in the model. The two shoreline positions required for the model calibration (calibration period 1996-2001) were not available. This proved to be a very time consuming task, to devised a method for the shoreline position derivation on both dates. The final solution was to perform a linear interpolation between the bathymetric data set and the topographic datasets in 1996 and 2001, respectively. LIDAR data, available only afterwards (2012), confirm the reliability of the method devised. The model was then calibrated. Shoreline evolution was simulated starting from the initial shoreline (1996) up to year 2001, when the target shoreline was available. Model parameters and lateral boundary conditions were adjusted in order get the best match between the calculated shoreline and the target shoreline in 2001. The same parameters were then used to simulate coastline evolution from 2001 to 2011, considered as reference year for the present situation. New structures built since 2001 onward were introduced to get the present configuration. Lateral boundary conditions were accordingly adjusted to make simulations as closest as possible to the reality. On that time there was no shoreline position datum available in 2011 for the model verification. Only afterwards, when LIDAR data were available the calculated shoreline in 2011 was verified. It resulted to be close to the real shoreline position indicated by the very detailed LIDAR survey. This lead to the conclusion that, despite the calibration period being relatively short (5 years), the model is reliable and can be used as predictive tool.

The final results consist of investigation of two different scenarios: the do-nothing scenario and the detached breakwaters protected scenario.

The do-nothing scenario definitely confirms what the present situation and recent breaching events along the coast are showing. If no further interventions were carried out in the Vagueira region, the coastal stretch will continue eroding. Results proved that in case of zero sediments supplied at the northern boundary (extreme), the shoreline will recede until 2026. At this time, the shoreline equilibrium position will be reached and will be oriented 14-16° clockwise to North. The entire stretch will be affected by severe erosion as the shoreline will rotate around hinge points to be parallel to the incoming wave crests. If some sediments were available at the northern boundary, the present shoreline position is closer to the equilibrium position and erosion will be limited. However, the uncertainties on the amount of sediments which is entering the coastal stretch, make this scenario not reliable. The extreme result finally resulted to be closer to reality (breaching on the 3rd of November 2011). The detached breakwaters protected scenario was investigated following a trial and error procedure. The idea was to look for equilibrium positions with tombolo formation. The introduction of two detached breakwaters in two different instants in time resulted to be the best solution. A first detached breakwater, placed right in front of the curved groin, will widen the sand spit in the southern part during time period 2011-2026. At this time (2026) the equilibrium shoreline position will be reached. In the same year, the introduction of a second detached breakwater will definitely solve the future erosion problem. This structure placed right in front of Vagueira South groin, will control the northern stretch evolution. The equilibrium position will be reached in 2056. At this time the sand spit will be widen also in the northern part. This detached breakwater protected scenario will thus reverse the present eroding phase: the structures will start a new accreting trend. Besides, the structures length is enough to accommodate for the installation of windmills which could provide energy nearshore. The flat bathymetric pattern of the project area could reduce costs of both detached structures constructions and wind mills installation. In addition, the already existing protruding groins could provide direct access from land for construction.

This study lays the foundations for the fine tuning of these defence coastal structures, as a serious option to protect the Vagueira coast in the near future. Structure length, orientation and design criteria might be further investigated. The impact of this coastal defence scheme on the downdrift coast, up to cape Mondego should be further investigated. One option to

minimize the impact of the coastal defence scheme is to promote tombolo formation using material from the maintenance dredging of the Port of Aveiro navigation channel. Maintenance dredging is estimated to be of the order of 400000 m3/yr. Besides a wider computational grid could be used to test the boundary effect on wave propagation from the offshore boundary up to the near shore location. A more site-specific wave climate could then be used to test the model response.

References

Aquaveo LLC. (2013) STWAVE Analysis. *Tutorial*, Provo, Utah, USA.

CEHIDRO & ICIST. (1999). Carta de risco do Litoral, versao digital, I ed. Lisboa, September.

Gomes, N.A., Mota Oliveira, I., Pinto Simoes, J., Pires Castanho, J. (1981). "Coastal erosion caused by harbour works on the Portuguese coast and corrective measures." *25th PIANC Congress*. Edimburgh, pp.877-898.

Hanson, H, M.B Gravens, and N.C Kraus. (1991). GENESIS: Generalized model for simulating shoreline change. Report n°2 - *Workbook and system user's manual*. U.S. Army Corps of Engineers, Coastal Engineering Research Centre, Vicksburg, Mississippi, USA.

Hanson, H. (1987). GENESIS - A generalized shoreline change numerical model for engineering use. *Doctoral thesis*, Lund Institute of Technology, Report No. 1007, Department of Water Resources Engineering, Lund, Sweden.

Holthuijsen, L.H. (2007). Waves in oceanic and coastal waters. Cambridge University Press. New York, USA.

ICCE, International Conference on Coastal Engineering (1993). "Design and reliability of coastal structures – Proceedings of the short course on design and reliability of coastal structures". *23rd International Conference on Coastal Engineering*. Scuola di S.Giovanni Evangelista, 1-3 October 1992, Venice.

McKee Smith, J., A.R Sherlock, and D.T. Resio. (2001). User's Manual for STWAVE, Version 3.0. *User's manual*. Coastal and Hydraulics Laboratory, Vicksburg, Mississippi, USA.

Talbi, O., Moussa, M., Trigo Teixeira, A. (2008). "Coastline change. Simulation in the Maceda-Torreira region." *1st Seminar on Coastal Research*, Porto.

US Army Corps of Engineers. (2002). Longshore sediment transport. *Coastal Engineering Manual*, Part III, Chapter III-2, Engineer Manual 1110-2-1100, U.S. Army Corps of Engineers. Washington DC, USA.

US Army Corps of Engineers (2008). Shore protection projects. *Coastal Engineering Manual*, Part V, Chapter V-3, Engineer Manual 1110-2-1100, US Army Corps of Engineers, Washington DC, USA.

US Army Corps of Engineers. (2003). Surf zone hydrodynamics. *Coastal Engineering Manual*, Part II, Chapter II-4,Engineer Manual 1110-2-1100, U.S. Army Corps of Engineers. Washington DC, USA.

US Army Corps of Engineers. (2008). Water wave mechanics. *Coastal Engineering Manual*, Part II, Chapter II-1, Engineering Manual 1110-2-1100. Washington DC, USA.

Vaz Sena, M. (2010). "Modelação de Evolução da Linha de Costa, Influência do Uso de Séries Sintéticas de Agitação.". *Master thesis*, Instituto Superior Tecnico, Lisboa.

Veri-Tech, Inc. (2004). "NEMOS System Components & Typical procedures." *Tutorial*, Summit, Mississippi, USA.

Web sites

http://www.aquaveo.com/sms (last accessed 13/06/2013)

http://www.vliz.be/wiki/Long-term_modelling_using_1-line_models_-_GENESIS_and_new_extensions (last accessed 25/06/2013)

http://www.veritechinc.com/products/cedas/CEDASmanuals.php (last accessed 29/005/2013)

List of figures and tables

List of symbols

H_{m0} = Significant wave height estimated from the wave spectrum (m).

T_P = Wave peak period (s).

θ = Mean direction associated to the peak period, respect to the True North (°).

H_b = Significant wave height at breaking (m).

y = Shoreline position (m).

D_B = Average berm height (m).

D_C = Depth of closure (m).

Q = Long shore transport rate (m^3/s).

q = Line sources/sinks along the coast (m^3/s/m shoreline).

C_g = Wave group speed (m/s).

a_1 = GENESIS first non-dimensional parameter for long shore transport rate calculation.

a_2 = GENESIS second non-dimensional parameter for long shore transport rate calculation.

H_b = Wave height at breaking (m).

θ_{bs} = Wave angle at breaking, respect to the local shoreline (°).

K_1 = GENESIS primary calibration parameter.

K_2 = GENESIS secondary calibration parameter.

ρ_S = Density of sand (kg/m^3).

ρ = Density of water (kg/m^3).

p = Porosity of sand.

$\tan\beta$ = Average bottom slope.

H_{rms} = Root-mean-square wave height (m).

H_{max} = Maximum annual significant wave height (m).

YG_{North} = Distance between the groin tip and the shoreline position at the external right side (northern) of the model (m).

YG_{South} = Distance between the groin tip and the shoreline position at the external left side (southern) of the model (m).

$YG_{North,MAX}$ = Maximum limiting value for the YG_{North} variation interval (m).

$YG_{North,MIN}$ = Minimum limiting value for the YG_{North} variation interval (m).

$YG_{North,Google}$ = Google Earth derived estimate of YG_{North} (m).

K_T =Detached breakwater transmission coefficient.

d_1 =Distance between the best equilibrium shoreline position of scenario B and the present time shoreline position (2011) in correspondence of *Vagueira South groin* (m).

d_2 =Distance between the best equilibrium shoreline position of scenario C and the present time shoreline position (2011) in correspondence of *Vagueira North groin* (m).

Acknowledgements

First of all I want to express my gratitude to Prof. Trigo Teixeira, of Instituto Superior Técnico, who first introduce me to the field of numerical shoreline evolution modelling in Padua (during the course of *Coastal Management and Protection*) and then gave me the possibility to do the master thesis in the same field in Lisbon. For the entire period of my master thesis experience, he has always been a constant presence providing technical and moral support. He gave me the possibility to experience different ways of working and living.

I wish also to direct my thanks to his team at Instituto Superior Tecnico in Lisbon. Amélia Araújo who has been a valid technical support and source of inspiration. Ana Paula, the very kind ArcGis expert. Dulce Fernandes, who has always welcomed me with an encouraging and sweet smile.

My gratitude is also directed toward Prof. Ruol who has been my supervisor in Padua. Without his help, the experience in Lisbon would have not been possible neither would have started.

To my family, boyfriend, teammates and friends: thank you for being understanding, patient and encouraging me anytime, anywhere.